1-1-2013

Characteristics Of Cold Start Of A Diesel Engine Using Jp8 And Ulsd Fuels

Madhushankar Palanisamy
Wayne State University,

Characteristics of Cold Start of a Diesel Engine using JP8 and ULSD Fuels

by

Madhushankar Palanisamy

Master's Thesis

Submitted to the Graduate School

of Wayne State University,

Detroit, Michigan

in partial fulfillment of the requirements

for the degree of

Masters of Science

2013

MAJOR: MECHANICAL ENGINEERING

Approved by

____

Advisor **Date**

ACKNOWLEDGMENTS

First and foremost I would like to express my sincere gratitude for my graduate advisor Professor Dr. Dinu Taraza. His guidance and support has helped me get through tough times during the period of this work and it has been my privilege to work for him as his student in the Center for Automotive Research at Wayne State University. The director of CAR, Dr. Naeim Henein has been very helpful in answering all of my questions regarding engines and combustion whenever I was in doubt. I have learnt a lot from his professionally and personally. I am also thankful to Dr. Marcis Jansons for his valuable help and suggestions whenever I needed it.

I am also sincerely thankful for all the efforts and help provided by my friends and colleagues at the Center for Automotive Research (CAR), Amrinder Singh, Chandrasekaran jeyakumar, Tamer badawy, Florin Mocanu, Anshul sharma and other members for their assistance and support throughout the period of this work.

TABLE OF CONTENTS

LIST OF FIGURES

NOMENCLATURE

BTDC	Before Top Dead Center
EVO	Exhaust Valve Opening
TDC	Top Dead Center
IMEP	Indicated Mean Effective Pressure
CPC	Common Powertrain Controller
MCM	Motor Control Module
EGR	Exhaust Gas Recirculation
EPA	Environmental Protection Agency
ECU	Engine Control Unit
SV	Spill Valve
NCV	Needle Control Valve
NOP	Nozzle Opening Pressure
SOI	Start of Injection
ULSD	Ultra Low Sulfur Diesel
JP8	Jet Propellant 8

CHAPTER 1

LITERATURE REVIEW

1.1 Introduction

Diesel engines are becoming increasingly popular in USA because of the fact that it gives better fuel economy and along with significantly higher low end torque, in comparison with the gasoline engine. Despite its advantages, diesel engines possess significant challenges as well. One of the major challenges in diesel engine is the cold start .In gasoline engines, a well-mixed fuel and air is inducted into the cylinder followed by the compression and then followed by the combustion, which is initiated through spark. Unlike gasoline engines, diesel engine uses fuel injectors to inject the diesel fuel directly into the engine combustion chamber which leads to the fuel combustion process. Diesel engine works in the principle of auto ignition. Hence the in cylinder temperature and pressure before the fuel injection is an important parameter in the diesel engine cold start.

A successful cold starting involves minimum assistance from the starter motor and less number of cranking cycles to reach the idling speed and continue to run without any misfires. Misfires are a major contributor of unburnt hydrocarbon emissions during the cold start. During the cold start of the diesel engine, heat transfer and blow by losses increase significantly, which leads to a reduction in the in cylinder compression temperature and pressure, which contributes to the engine misfire .Engine misfires when the Engine oil viscosity is a very strong function of temperature, which means that, the lower the ambient temperature, the higher the engine oil friction which means the starter motor has to work hard to maintain a constant cranking speed.

1.2 Important factors affecting the Diesel Engine cold start

Henein [1], Zahdeh *et al* [24], Biddulph *et al* [13], Austen *et al* [12] extensively studied the cold start phenomena and described the following factors as having a significant effect on the startability characteristics of a diesel engine cold start

- Ambient Temperature
- Fuel Injection
- Fuel Properties
- Cranking Speed
- Accumulated Fuel

1.2.1 Ambient Temperature

Nakamura *et al* [25], Henein [1], Zahdeh *et al* [24], described ambient temperature as one of the most important factors affecting the diesel engine cold startability. They concluded that the Lower the ambient temperature the higher the heat losses to the engine coolant, higher will be engine oil frictional losses because of the increased oil viscosity. It has to be noted that the oil viscosity is an exponential function of temperature. Figure 1.1 illustrates a simple model developed by Henein [1] to show the effect of ambient temperature on cranking speed, gas torque, ignition delay and starter torque in an engine which was assumed to be frictionless.

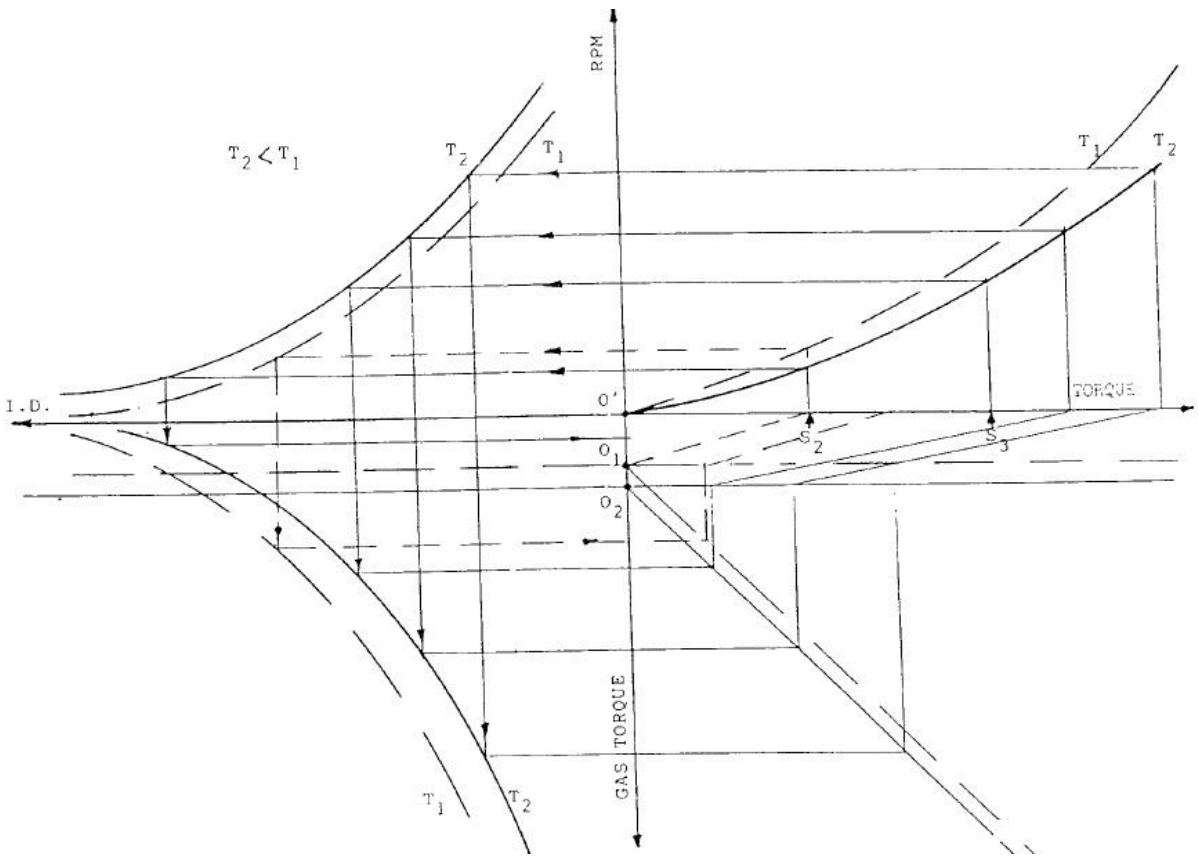

Figure 1.1 – Effect of Ambient Temperature on Cold Starting [1]

Henein [1] assumed that the engine was frictionless; hence lowering the ambient temperature affects only the ID and indicated work done. The dotted lines are for temperature T_1 and solid lines are for temperature T_2 .T_2 is less than T_1. He showed that for the same starter torque (torque supplied by the starter motor through the power supplied by the battery), T_1 results in higher cranking speed than T_2 and for the same cranking speed, T1 results in less ignition delay than T2. This demonstrates the basic relationship between the starter torque, ignition delay, cranking speed and the gas torque.

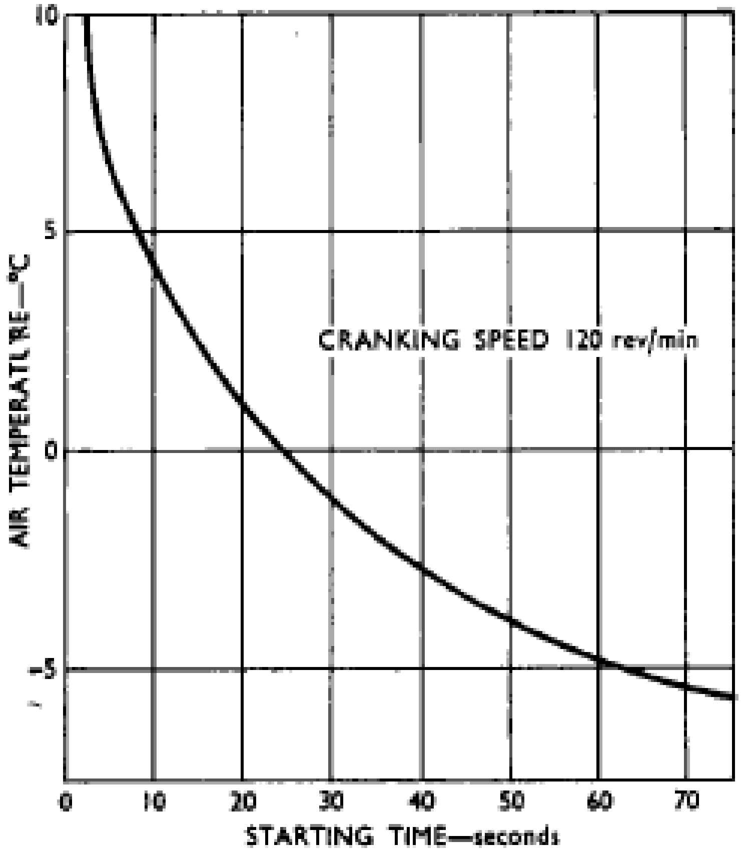

Figure 1.2 – Effect of Ambient Temperature on Starting Time [12]

Austin *et al* [12] used two automotive type 4-cylinder diesel engines of about 2-1 capacity to observe the relationship between the starting time and the ambient air temperature. They described the results (figure 1.2) of the engine starting time as observed on a diesel engine cold start at a cranking speed of about 120 rpm. They noted that a drop of ambient temperature of 10°C (+8°C to -2°C) resulted in an increase of about 32 s in starting time (3 to 35 s). They also concluded that the lower the ambient temperature the longer the engine starting time. This indicated the significance of the ambient temperature on the engine starting time.

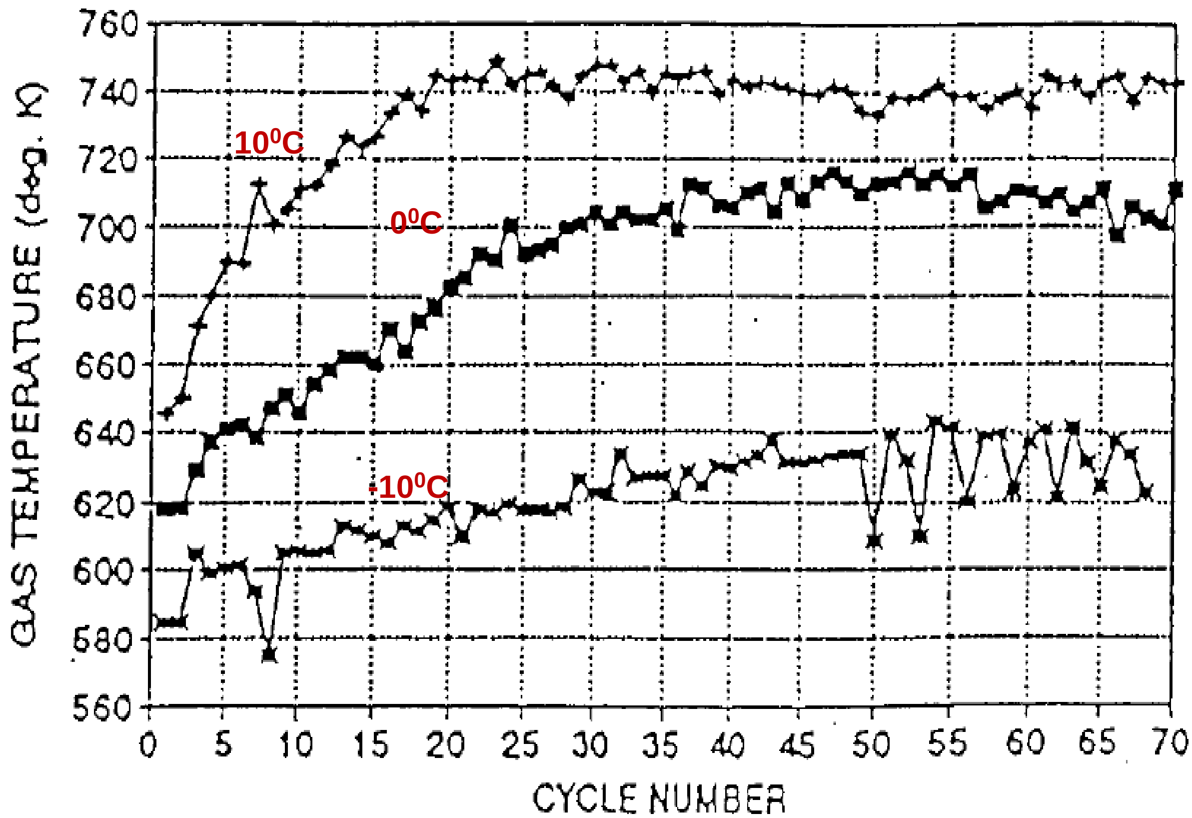

Figure 1.3 - Effect of Ambient Temperature on in cylinder gas temperature [25]

Bryzik *et al* [25] studied the variation of the in cylinder gas temperatures with the change in ambient temperature (10 ºC, 0 ºC and -10ºC) and they observed that the lower the ambient temperature the lower the in cylinder gas temperature as a result of high heat losses coupled with the low engine cranking speeds.

Kobayashi *et al* [6], Henein [1] stated that lowering the ambient temperature affects the engine startability characteristics as stated in the following ways.

1.1 Reduced cranking speeds because of the low battery discharge rates along with the higher engine oil viscosity

1.2 Reduced ignition delays in comparison with the warmed up operation because of the lower in-cylinder compression temperatures

1.3 Low gas torques as a result of increased heat losses accompanied with slower fuel evaporation rates and the combustion chemical reaction rates

1.2.2 Fuel Injection Characteristics

Kobayashi *et al* [6]. Zahdeh *et al* [7], Henein [1] identified the possibility of misfire in the later cycles when the engine is accelerated to high speeds by the earlier firing cycle, leaving inadequate time around the TDC for the successful fuel autoignition and combustion. Austen *et al* [12] discovered that the optimum injection timing for warmed up engine operation is generally too advanced for optimum cold start which lies between 10° and 20° BTDC by static timing. At very low engine speeds such as cranking speed, heat loss and blow-by losses increase, hence cylinder air temperature is lower than that at high speed. Hence, the required ignition delay time becomes longer at starting, but the required timing in crank angle degrees becomes much less.

Generally in diesel engines, injection timing is configured in such a way that maximum amount of heat released occurs shortly after the TDC of the cylinder, in order to get maximum thermal efficiency. In cold start however thermal efficiency is not a constraint, hence the timing needs to be adjusted based of the ignition delay period of the fuel and its characteristics.

Lyn *et al* [8] compared the injection timing and the ignition delay for two fuels and concluded that fuel injections before TDC always resulted in minimum ignition delays.

They also observed that under specific engine speeds, away from the injection timing which gives the shortest ignition delay before TDC, ignition delay will increase until to an injection timing at which the ignition will fail. Curvature of ignition delay versus timing may be useful to identify how wide the injection timing can vary without leading to a misfire.

1.2.3 Fuel Properties

Fuel properties such as cetane number and volatility are the most important properties affecting the cold start characteristics of the diesel engine. Rofail [10] described that the effect of cetane number is highly significant at the minimum starting temperature because below this temperature the engine will be non-operable. Han [5], Zahdeh [7] and Henein [1] indicated that the instability in combustion during the diesel engine cold start was not specific to a particular fuel. It is understood that a fuel with higher cetane number will provide better cold start performance than the fuels with low cetane number. The lower activation energy present in the higher cetane number fuels result in reduced ignition delay when compared with lower cetane number fuels. Other reports from Yassine *et al* [9] a fuel with low cetane number and higher volatility showed better cold start characteristics. Higher volatility fuels tend to vaporize quickly and form the combustible mixture in order to initiate the combustion process. A clear effect of volatility is not defined in the literature because different fuel blends result in varied volatilities. According to Clerc [11] a decrease in a cetane number of the diesel fuel from 45 to 40 would increase the minimum cold starting temperature of the engine by less than 3^{o}C. Hara *et al* [15] conducted cold start investigations at different ambient temperatures with fuels of different cetane numbers with and without cetane improver additives.

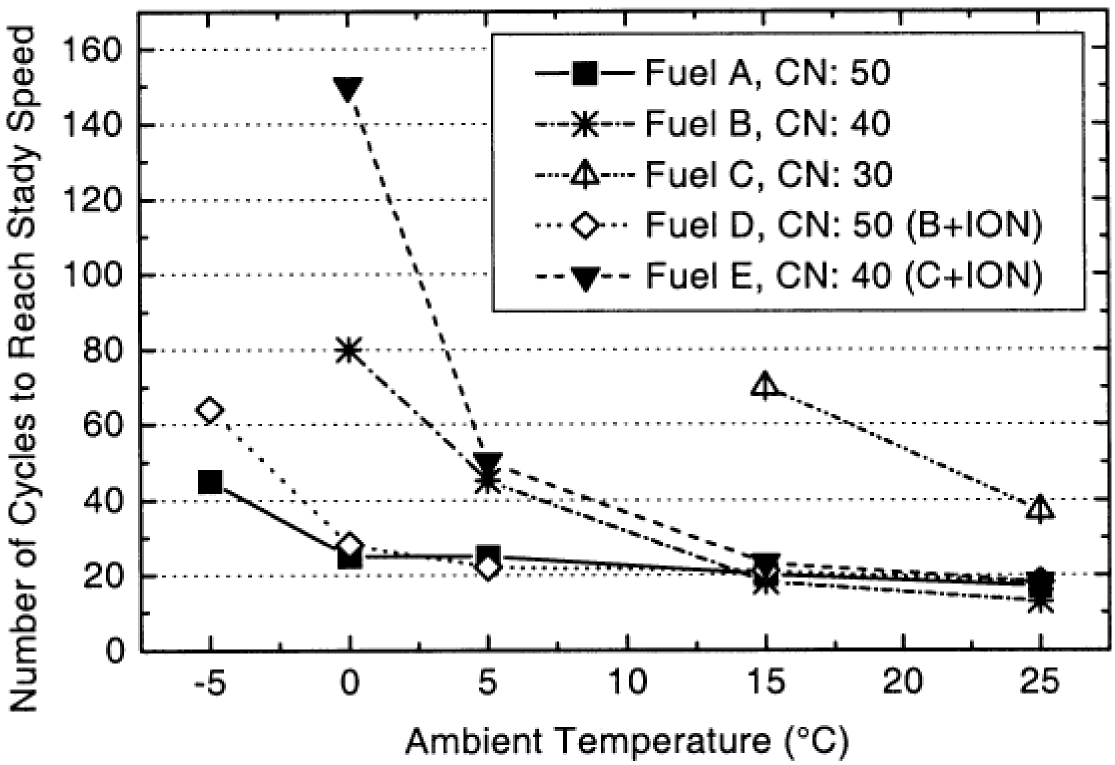

Figure 1.4 – Effect of cetane number on engine startability [15]

They observed that the fuels with higher cetane numbers reached the steady speed comparatively earlier than the fuels with less cetane number (Figure 1.4). Fuel with a very low cetane number of 30 failed to start below the ambient temperature of 15^{o}C. A difference of 58 cycles was observed regarding the time taken to reach steady speed as a result of a cetane number change of 10 between 50 and 40 at 0^{O}C ambient temperature which is a very significant in terms of the white smoke emissions perspective. In general higher cetane number results in lower overall activation energy and hence results in better cold starting capability. They also observed that low cetane fuels with additives shows similar characteristics as the high cetane number fuels.

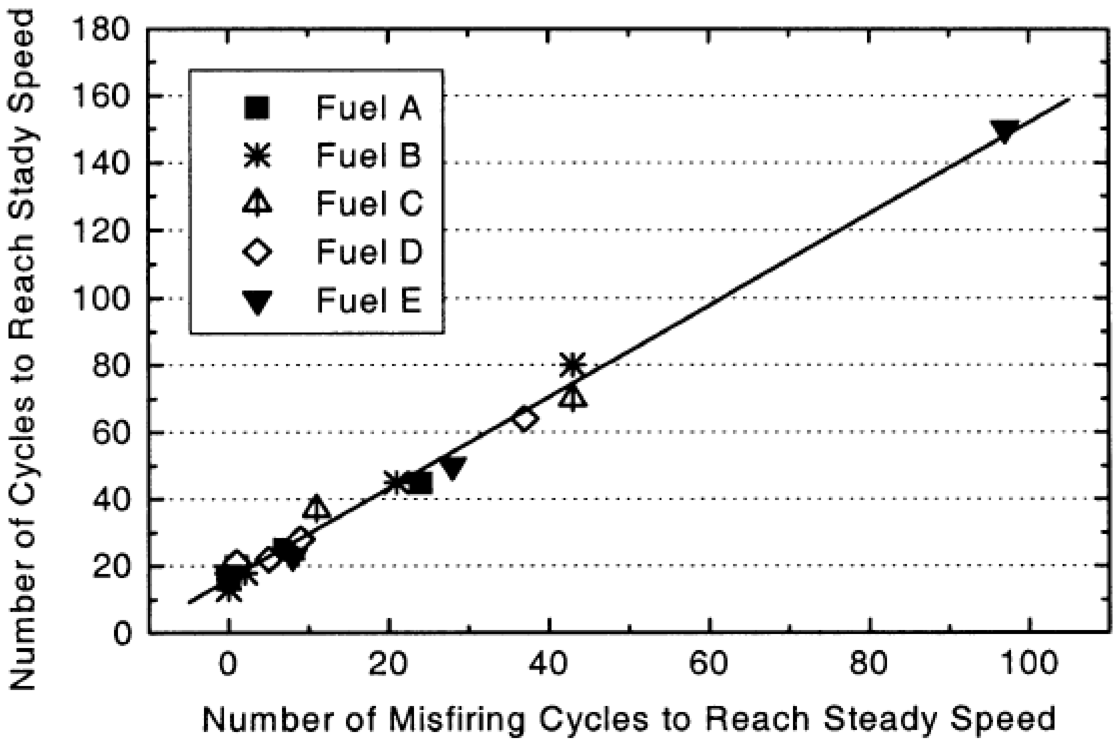

Figure 1.5 – Effect of Ambient temperature on the number of misfires [15]

Hara *et al* [15] also investigated the effects of ambient temperature on the total number of misfires before reaching a steady engine speed. They found that the use of higher cetane number fuel (Fuel A – 50) resulted in less number of misfires as well as less number of cycles to reach the steady speed in comparison with the fuel of low cetane number (fuel C - 30). These results highly emphasize the importance of higher cetane numbered fuels especially at low ambient temperatures.

1.2.4 Cranking Speed

The cranking speed is one of the most important parameters in the cold start. Zahdeh *et al* [24] explained that the cranking speed, without fuel injection, was dependent on the ambient temperature, while all the other starter parameters were kept constant. Lowering the ambient temperature caused an increase in frictional torque and a drop in cranking speed. Gonzalez *et al* [28], Henein [1] described that cranking speeds are important in the sense that it should provide enough high pressure and temperature inside the combustion chamber for the fuel to auto ignite. Low cranking speeds provide ample time for the fuel to mix and reach the autoignition temperature, but results in increased blow by and heat losses. They pointed out that another important effect of the cranking speed is the time period of the piston around the TDC. Higher cranking speeds result in higher in cylinder temperatures, reduced blow by and heat transfer losses, but reduces the time period in which piston is around the TDC, this means that the fuel has less time to auto ignite and result in successful combustion. Lyn *et al* [12] mentioned that in their cold start study at low cranking speeds, increase in cranking speed of 100 rpm resulted in an increase in the in cylinder compression temperature of 70^{o}C, which is highly significant for a successful cold start.

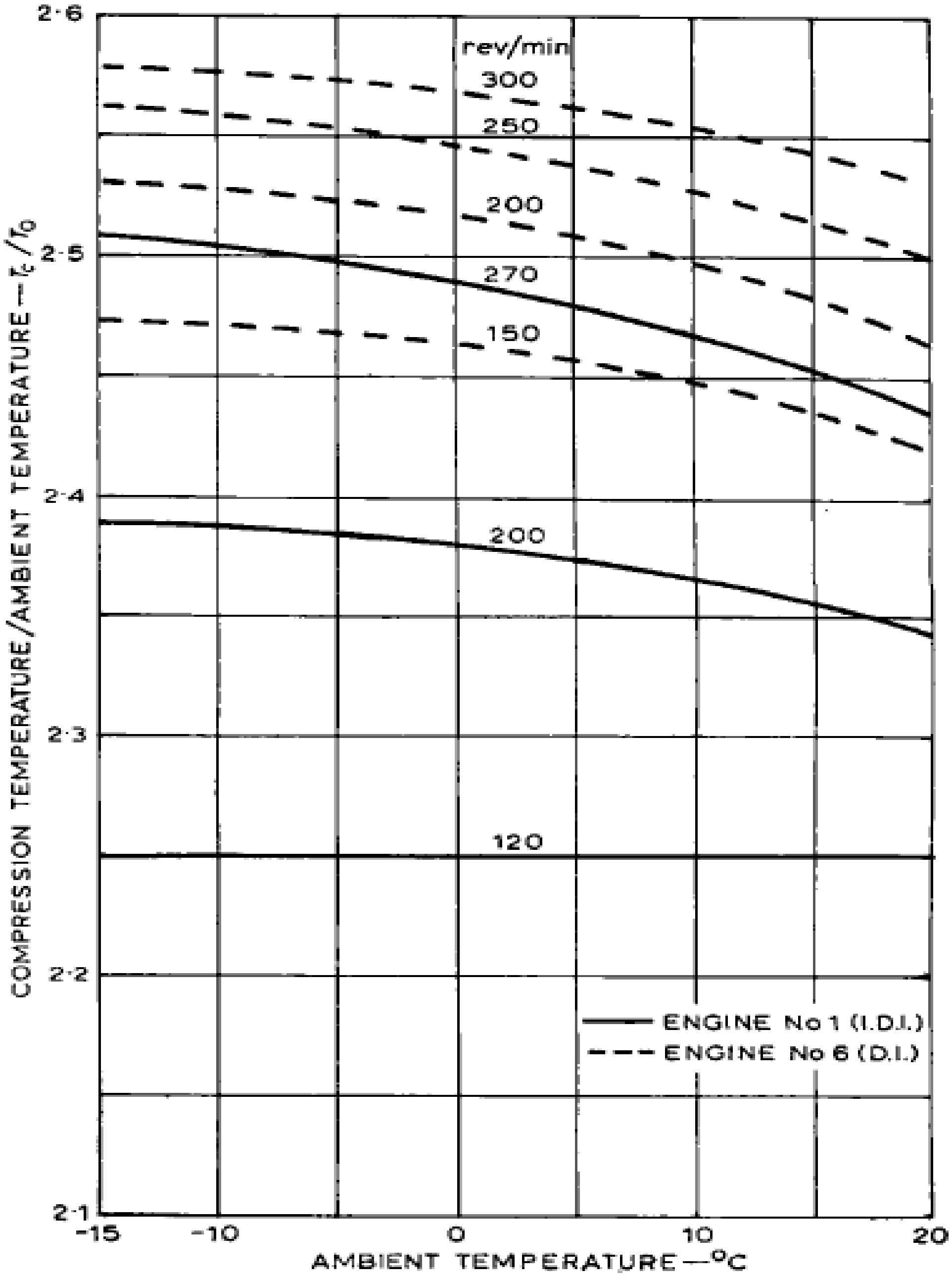

Figure 1.6 - Effect of cranking speed on compression temperature [13]

Figure 1.6 illustrates the effect of cranking speed on the ratio of compression temperature to the ambient temperature as observed during the cranking of several ambient temperatures ranging from -15 to 20^{0}C. Biddulph *et al* [13] identified that higher the cranking speeds higher will be the ratio of compression temperature to the ambient temperature, which means higher compression temperature. This effect is especially significant in raising the compression temperatures under lower ambient temperature in compared with the variation in cranking speed at higher ambient temperatures.

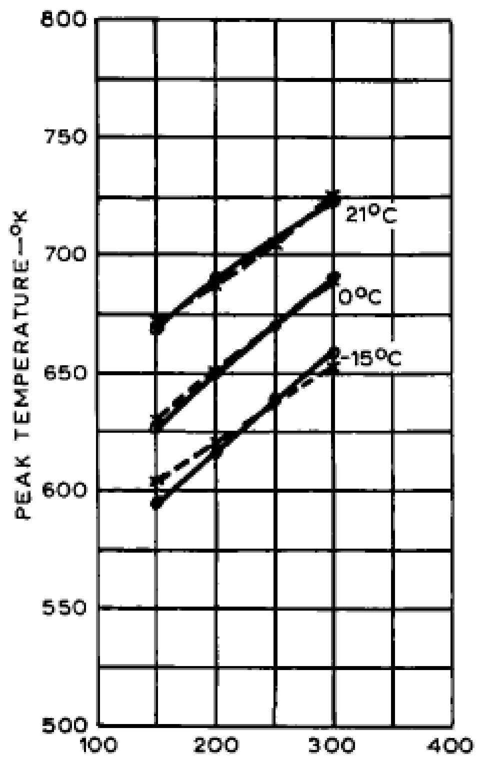

Figure 1.7 - Effect of Cranking Speeds on Peak Temperature [13]

Figure 1.7 [13] shows the correlation between the cranking speed and the peak compression temperatures for three different ambient temperatures (21 C, 0 C and -15 C) as observed in a 0.6 liter 4 cylinder diesel engine. Increase in cranking speed of 150 rpm at -15°C the peak compression temperature increases from 595k to 660k which is a significant temperature increase especially at the low ambient temperatures which will help reduce the ignition delay.

1.2.5 Accumulated Fuel

Austin *et al* [12] argued that there are some possible benefits for the excess fuel present in the cylinder during cold start. They argued that the excess accumulated fuel will increase the total quantity of air burnt because in starting not only must there be ignition, but there must also be sufficient power to increase the speed. They also discussed that too much fuelling may increase heat loss to an extent at which starting is worsened.

Since the total injection duration will be higher with excess fueling the optimum timing for cold starting will be different from the normal fuelling conditions. They mentioned that it can be expected that the actual optimum injection timing for starting will be advanced with excess fuel.

1.3 Effect of Engine Speed on Ignition Delay

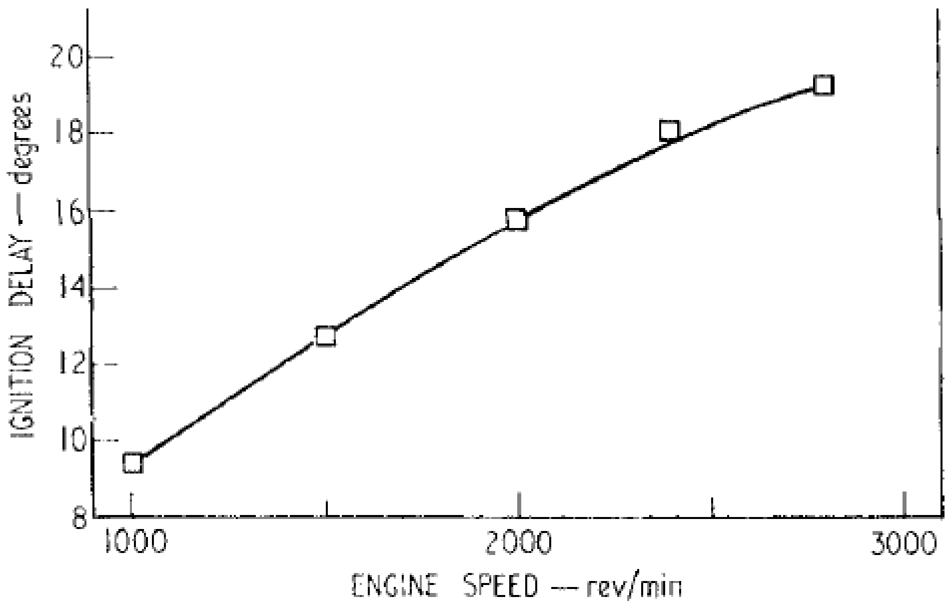

Figure 1.8 - Effect of increase in Engine Speed on Ignition Delay [30]

Bolt *et al* [30] conducted a series of tests to identify the effect of engine speed on the ignition delay. The variation in engine speed resulted in changes in other parameters that affect the combustion process, such as cylinder pressure temperature, and injection timing. The injection timing was kept constant at 21 deg BTDC at all engine speeds for this study. They observed that the ignition delay, measured in crank angle degrees, increased with increase in engine speed as shown in figure 1.8

1.4 Cold Start Misfire Identification

Han [5] described several ways in which a misfiring cycle can be identified. He explained that misfiring doesn't mean that the chemical reactions did not occur; instead the reactions may be weak enough to result in any significant combustion.

1.4.1 Dynamic Indicator

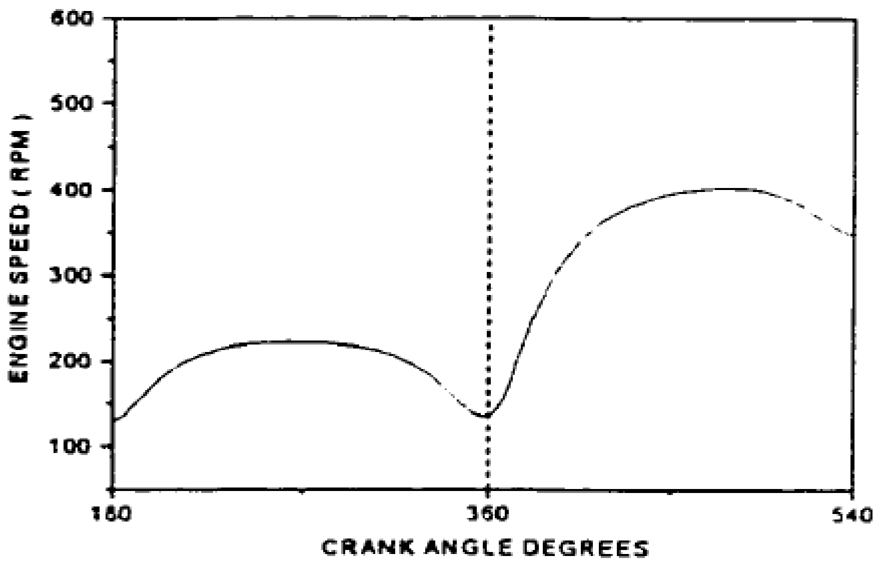

Figure 1.9 - Instantaneous speed during a fired cycle [5]

Han [5] explained that when there is a misfire the instantaneous speed drops suddenly such that the engine speeds during the expansion stroke will be lower than that of the compression stroke, because of the fact that no energy was added to the combustion chamber through combustion. During the firing cycle (Figure 1.8) this will be vice versa

1.4.2 Thermal Indicator

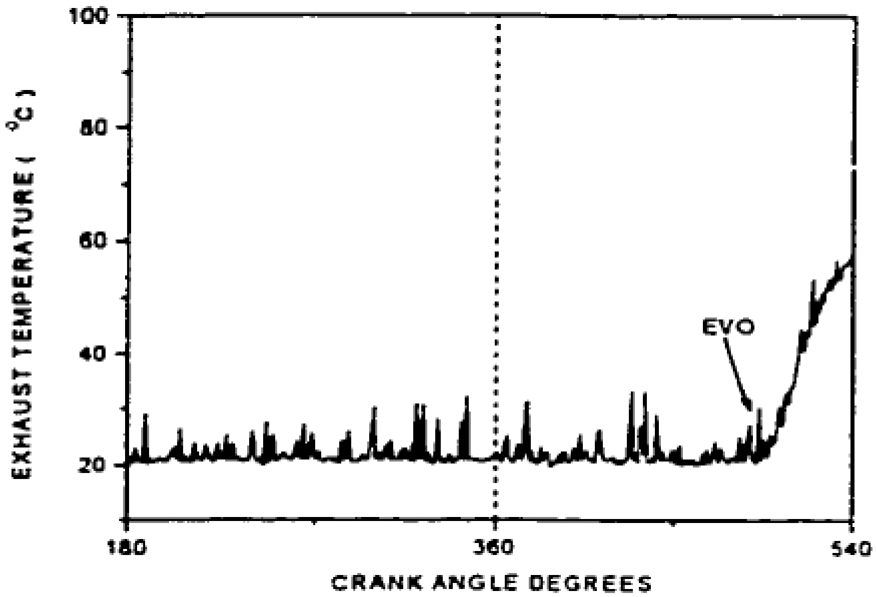

Figure 2.0 - Exhaust Temperature Trace [5]

Han [5] described that one of the ways to detect a misfire is to look at the cylinder exhaust temperature. After the successful combustion, exhaust temperature has to increase (Figure 1.9) after the exhaust valve opening (EVO), but if the exhaust temperature decreases this indicates a misfire

1.4.3 Cylinder Pressure

Han [5] described that in cylinder peak pressure usually occurs after the TDC during combustion .If there is a misfire the peak pressure occurs a few crank angle degrees after TDC .it never occurs at TDC because of the blow by losses in the cylinder. Also cylinder pressure before the EVO will be less than the intake pressure

1.4.4 Work done

Misfired cycles produce a negative IMEP as observed by Han [5], it has to be noted that there might be several cycles without any fuel injection (fuel cut off by the governor) which shouldn't be regarded as a misfired cycle.

1.5 Conclusions

- Higher the engine cranking speed higher will be the in cylinder compression temperature and pressure
- Higher the cetane number of the fuel better the startability characteristics
- The Lower the ambient temperature the higher the heat losses to the engine coolant, higher will be engine oil frictional losses as a result of increased oil viscosity
- Ignition delay is a strong function of in cylinder compression temperature and pressure
- Ignition delay increases in crank angle degrees with increase in engine speed.
- It is imperative to allow adequate timing for the fuel air mixture to auto ignite. Increase in engine speed results in shorter time period of the piston around TDC hence the injection timing must be advance in order to allow ample time for the auto ignition reactions.
- Lower the ambient temperature, higher will be the time taken for a successful cold start

CHAPTER 2

ENGINE TEST SETUP AND INSTRUMENTATION

A six cylinder 7.2 liter turbocharged Mercedes MBE 926 diesel engine is installed in the cold start diesel engine test cell of Wayne state university. All the components of the engine along with the fuel tank is kept inside the cold room to ensure uniform ambient temperature. Before starting each test, the entire cold room was soaked for minimum of 8 hours to ensure a constant engine oil temperature.

The experimental work is performed on a inline 6 cylinder 7.2 liter, single stage turbocharged, water cooled, four stroke, direct-injection, MBE 926 diesel engine which has a bore of 106mm and a stroke of 136 mm. Each cylinder has two intake valves and one exhaust valve. Each unit has a separate electronic unit pump (EUP) with a short injection line to the injection nozzle, which is located in the center of the combustion chamber. The engine is equipped with a fully electronic control system. The firing order is 1-5-3-6-2-4. Besides the engine and its related sensors, this system is composed of the Motor Control Module (MCM), and the Common Powertrain Controller (CPC). The two units are connected by a proprietary data link through which all the necessary data and information can be exchanged. Inorder to meet the on-highway EPA 2007 regulation applications, the engine uses a water cooled EGR system along with an Aftertreatment System to meet the emission standards. The EGR is fed from first three cylinders. The engine is connected to an AVL crankshaft encoder and the data was

Descriptions	6–Cylinder EGR Engine
Engine Type	Vertical, inline cylinder block with turbocharger and charge–air cooler
Engine Length	1057 mm (41.6 in.)
Engine Width	862 mm (33.9 in.)
Engine Height	1138 mm (44.8 in.)
Cooling System	Liquid Circuit
Combustion Principle	4–Stroke direct–injection diesel
Number of Cylinders	6
Bore	106 mm (4.17 in.)
Stroke	136 mm (5.35 in.)
Displacement (total)	7.2 liters (439 in^3)
Compression Ratio	18:1
Starting Speed	Approximately 100 rpm
Direction of Engine Rotation (viewed from flywheel)	Counterclockwise
Starter	Electric Motor
Coolant Capacity of Engine (Does not include capacity of cooling system.)	Max. 12.5 liters (13.2 qt.)
Lubricating Oil Fill Capacity **(In standard pan, including oil filter.)**	Max. 29.0 liters (30.6 qt.)
Cold–Start Temperature Limit (Without starting aids and with battery 75 percent charged)	Down to –15°C (+5°F)
Engine "Dry" Weight — Single -Stage Turbocharger Engine "Dry" Weight — Dual -Stage Turbocharger	613 kg (1362 lb) 648 kg (1428 lb)
Valve Lash (with engine cool)	Intake = 0.40 mm (0.016 in.)
	Exhaust = 0.60 mm (0.024 in.)
Valve Lift (at maximum valve clearance)	Intake = 9.7 mm (0.38 in.)
	Exhaust = 10.7 mm (0.42 in.)
Engine Oil Pressure	At idle rpm = 50 kPa (7 psi)
	At maximum rpm = 250 kPa (36 psi)
Fuel Injectors	Minimum opening pressure = 24,500 kPa (3553 psi)
	Maximum opening pressure = 25,700 kPa (3727 psi)
Coolant Thermostat	Opening temperature = 81° to 85°C (178° to 185°F)
	Normal operating temperature = 95°C (203°F)

Table 2.1 – Engine configuration

recorded at a resolution of every 0.5 CAD using the AVL Indicom data acquisition system. Table 2.1 represents the engine configuration.

2.1 Engine Features

Figure 2.1 indicates the standard engine setup in the cold room .Because of the absence of the dynamometer in the test cell, all the experiments conducted are at no load conditions.

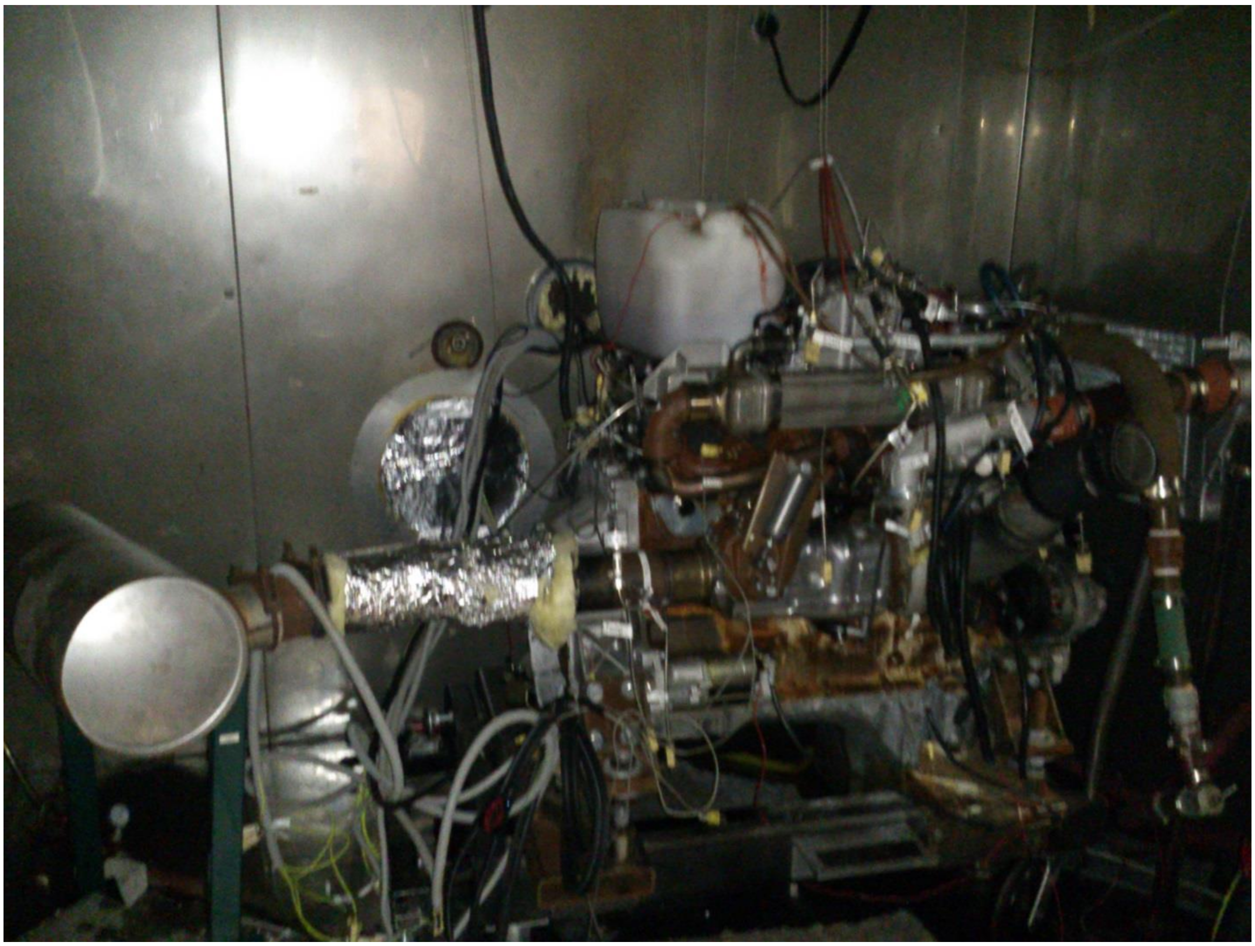

Figure 2.1 – standard engine setup inside the cold room facility

The engine was mounted on a wheel cart for easy movement within the cell. The exhaust gas pipe was connected to a muffler for noise reduction which was then connected with the suction pump to remove the exhaust gases out of the test cell.

Aluminum wraps and fiberglass were used for the heat isolation from the exhaust downpipe.

2.1.1 Fuel Injection System

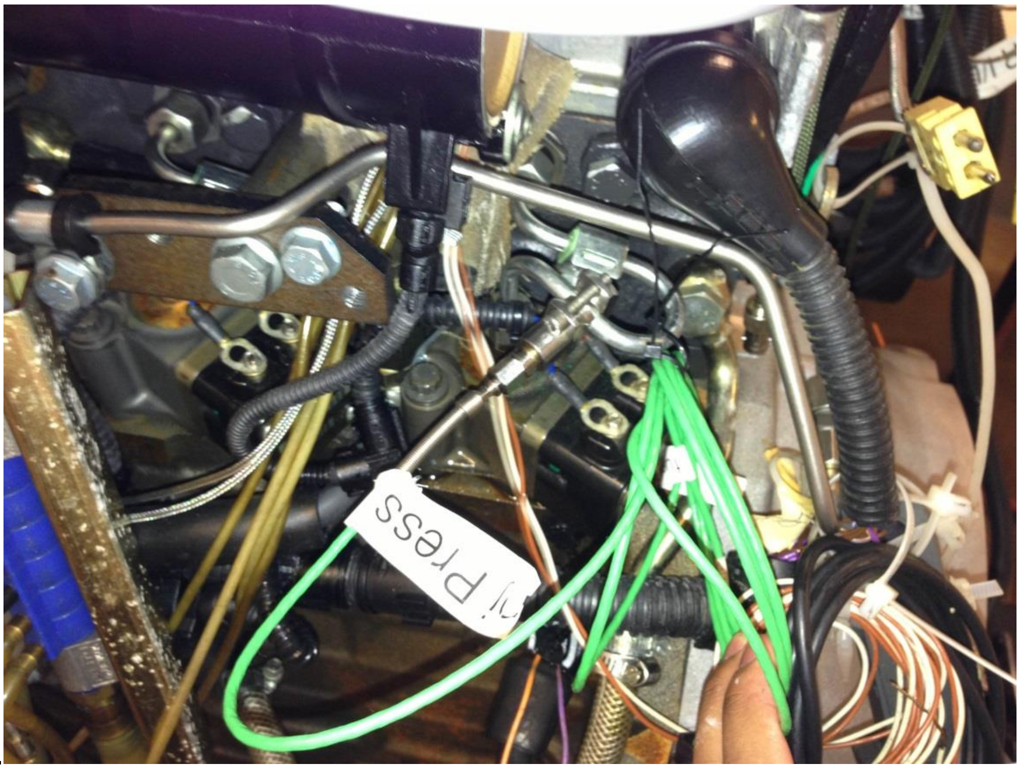

Figure 2.2 – Fuel injection pump and rail pressure sensor location

This engine has an electronically controlled unit injection system which is mechanically actuated with the aid of the camshaft and is electronically controlled. This pump can reach maximum injection pressures of up to 2200 bar. Each unit has a separate unit pump with a short injection line to the injection nozzle, which is located in the center of the combustion chamber (Figure 2.2). Operation of the injector is described in the following section.

2.1.1.1 Delphi Smart Injector

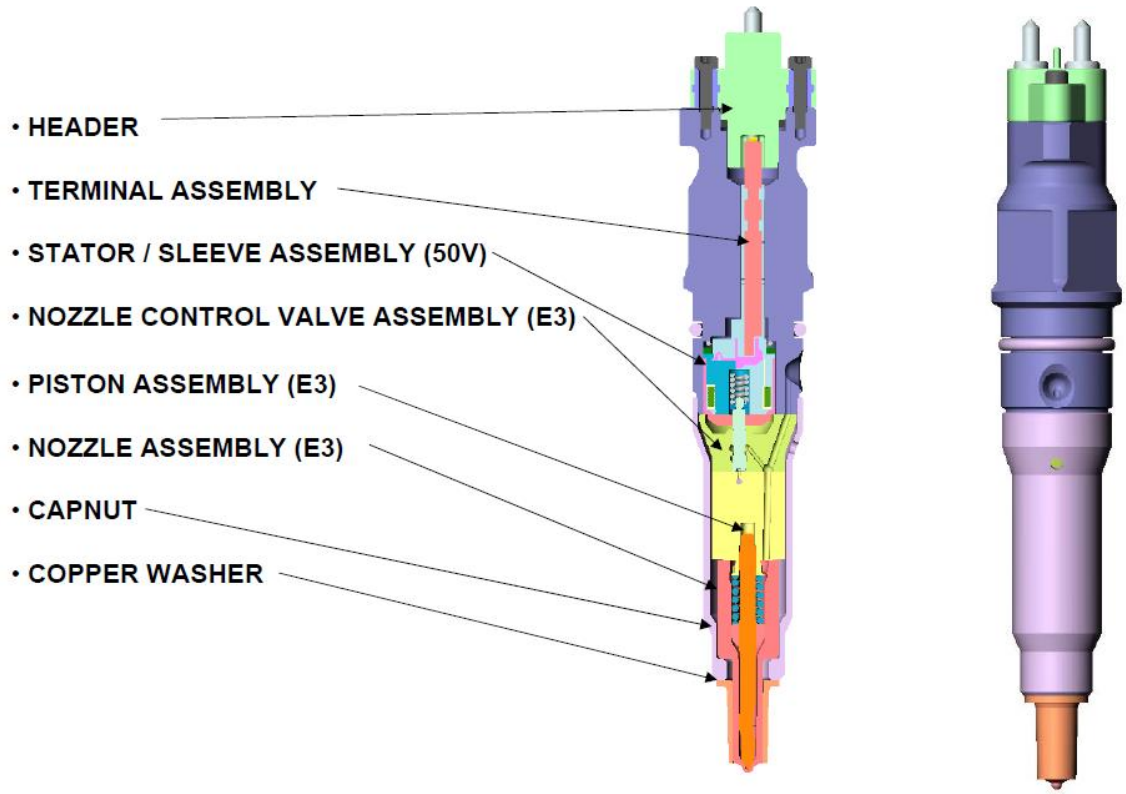

Figure 2.3 – Delphi Electronic Unit Injector

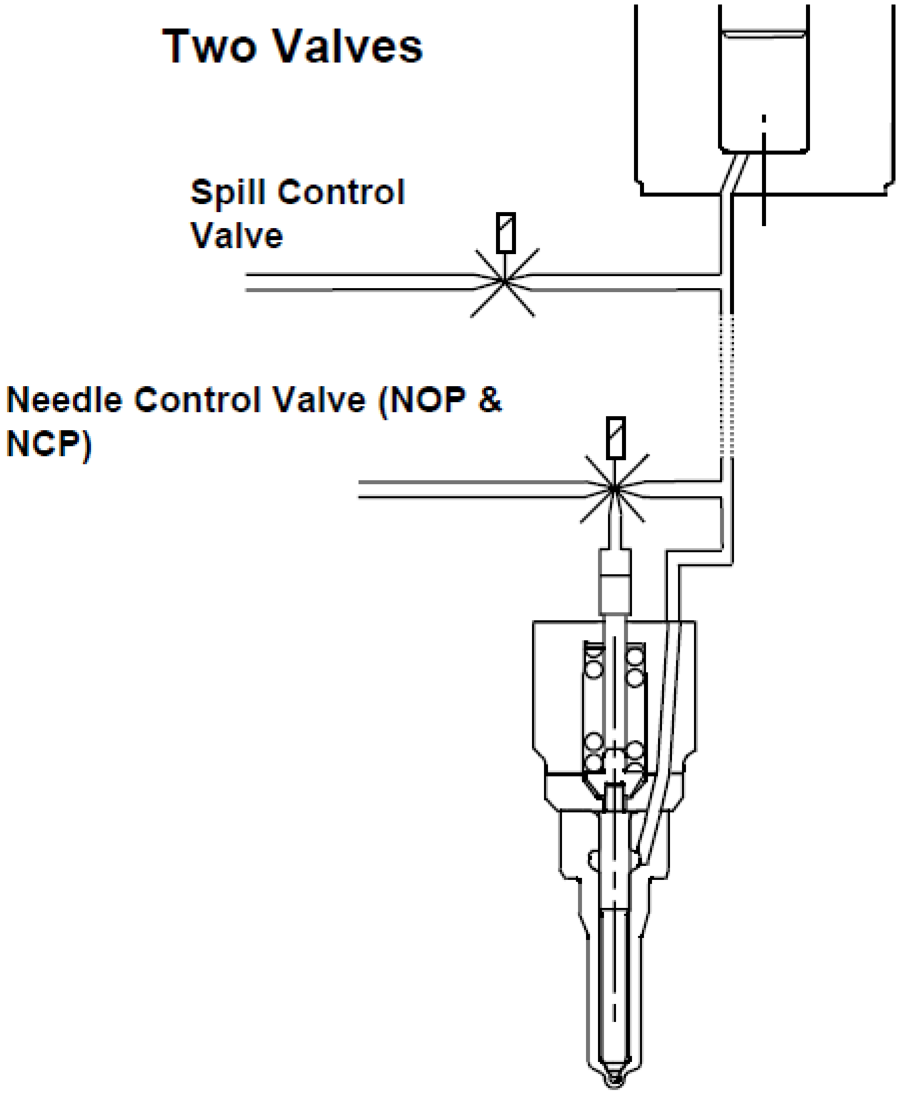

Figure 2.4 – Electronic Unit Injector Spill valve and Nozzle control valve

As illustrated in figure 2.4 the Delphi electronic unit injector consists of two valves for its operation. One is spill valve and the other the needle control valve. Spill valve is situated in between the pump and the injector and the needle control valve is situated on the injector needle. Spill valve along with the needle control valve controls the injection pressure, timing as well as the injection quantity as commanded by the ECU current signal. Figure 2.4 [14] represents the valves present in the electronic unit injector which are the spill valve and needle control valve, which are the two main valves used in the operation of the unit injector. Detailed operation of the injector can be classified as described below,

- At Rest condition
- Pressurizing event
- Injection event

2.1.1.1.a At Rest Condition

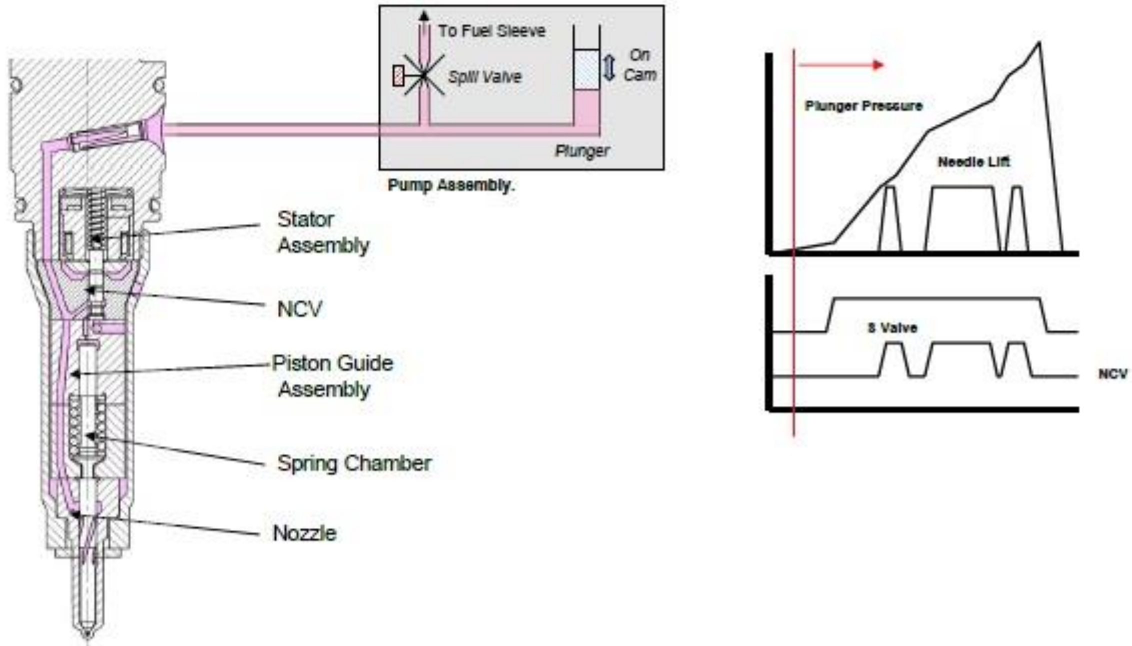

Figure 2.5 – Injector and ECU signals at rest condition

The red line in the figure 2.5 represents this condition. During the resting condition (where there is no fuel injection), the spill valve (SV) and the needle control valve are deactivated, which results in low pressure build up in the sleeve for fuel injection as a result of the pump plunger operation since the pump is connected to the camshaft of the engine. Fuel Pressure built by the pump plunger operation during the rotation of the cam will try to force fuel injection, but that event will be prevented by the preloaded injection nozzle opening pressure of 260 bar. Since there is no way for the fuel to pass through the injectors, it will be circulated in and out of the fuel sleeve around the pump assembly. Thus the fuel injection is prevented at the rest condition.

2.1.1.1.b Pressurizing Event

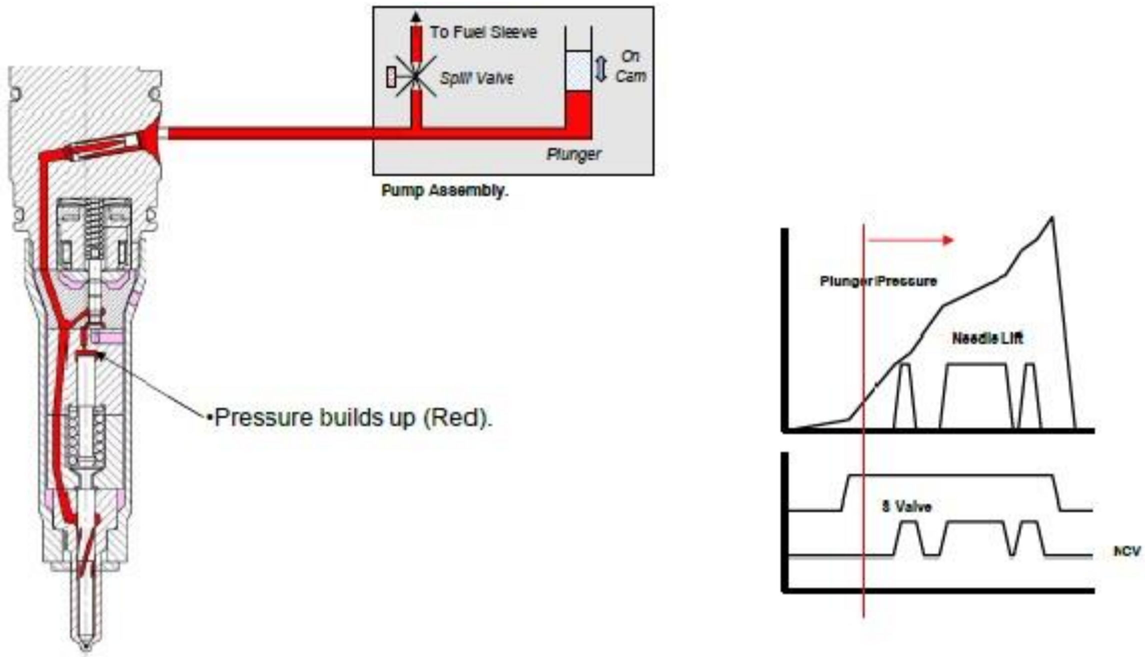

Figure 2.6 – ECU signals during pressurizing event

Figure 2.6 represents the ECU signals as well as a reference plunger pressure and needle lift signal during the pressurizing event. Initially the spill valve is activated, which prevents the fuel from escaping the fuel line, as a result the pressure builds up in the fuel line. Fuel pressure thus built will act closely on the back of the needle in the nozzle assembly. Fuel is stopped from injecting by the closed needle control valve (NCV). The pressurizing event position is indicated by the red line in figure 2.6

2.1.1.1.c Injection Event

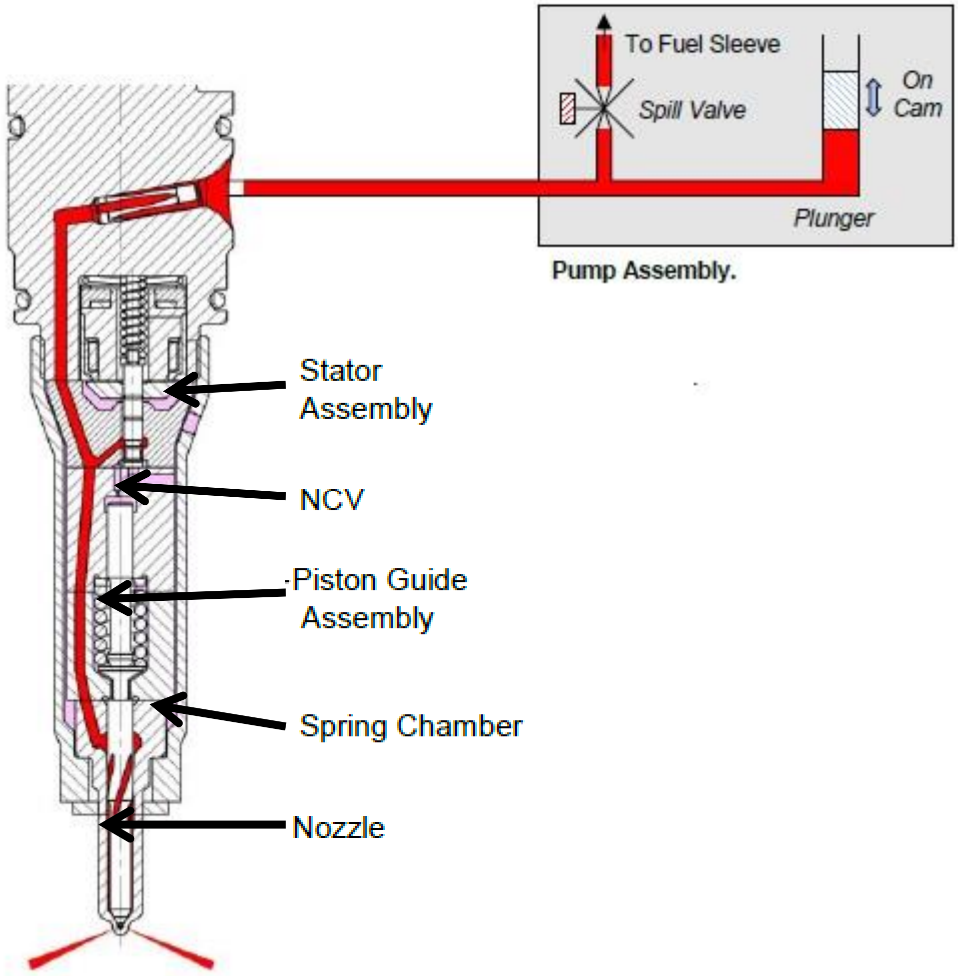

Figure 2.7 – Fuel Injector during the Injection Event

Figure 2.7 represents the fuel injector condition during the injection event. The red color indicates the pressurized fuel in the line. The Nozzle Control valve is activated at the desired ‘Nozzle Opening Pressure (NOP) and desired timing. The fuel pressure is removed from the back of the nozzle needle. The needle can now lift, so long as the fuel pressure is greater than the nozzle pre-load (260 bar, Spring Nozzle Opening Pressure, NOP). Thus the fuel is injected into the cylinder. To end injection either valves (Needle control valve and Spill valve) can be deactivated.

Nozzle Control Valve (NCV) can be utilized to allow pressure to continue building for multiple injections or both NCV as well as spill valve (SV) can be used. When the Spill Valve is de-activated the pressure in the fuel line is lost. The injection duration, pressure and number (multiple) depend on the operating region of the engine and can be controlled by the ECU current signal.

2.1.2 Crank Angle Encoder:

In order to record the data on crank angle basis, an optical shaft encoder was used. The output from various transducers is usually recorded on a crank angle basis in order to synchronize the data recorded from the transducers to the position of the piston. An AVL angle encoder (type 356CC) was used in this investigation and was installed on the free end of the crank shaft. The sensitivity of this encoder was 0.1 of a crank angle degree. The optical encoder is made up of an optical pickup with permanently connected cable and the optical transmitter. The marker disk has 720 angle marks, one of them “trigger” is longer. The marker disk is scanned with infra-red light via fiber optic cables fed through a flexible hose between the pickup and the optical transmitter. The light signal is converted to an analog voltage signal in the optical transmitter. The marker disk is scanned using the reflection method. Table 2.1 shows the technical specifications of the shaft encoder used for this investigative study.

Table 2.2 – Shaft Encoder Specifications

SPECIFICATIONS	DESCRIPTION
Model	AVL Optical Encoder 365CC
Speed range	50 rpm.........20,000 rpm
Supply voltage	5V Standard; 9V TO 36V Optional
Temperature	-40 °C – 70 °C
Moment of inertia of rotating masses	3.8×10^{-5} kgm^2

2.1.3 Data Acquisition System

Two data acquisition systems were used in the present setup. A high speed data acquisition system (Indiset Advanced plus 641) was used for crank angle based signals. It includes 2 data acquisition modules with 08 analog input channels each for high speed data acquisition as typically required in engine indicating. The AVL Indiset Advanced plus 641 is a multi- channel indicating system for combustion engines. Its main application area is the recording of measurement data, such as cylinder pressure, fuel rail pressure in relation to the crank angle.

Parameterization, measurement control, data display and data evaluation are performed using the AVL Indicom software. It has 16 channels with a resolution of 12 bit each, and the output voltage range is from -10V to +10 V. Data is recorded at an overall throughput rate of up to 800 kHz/channel.

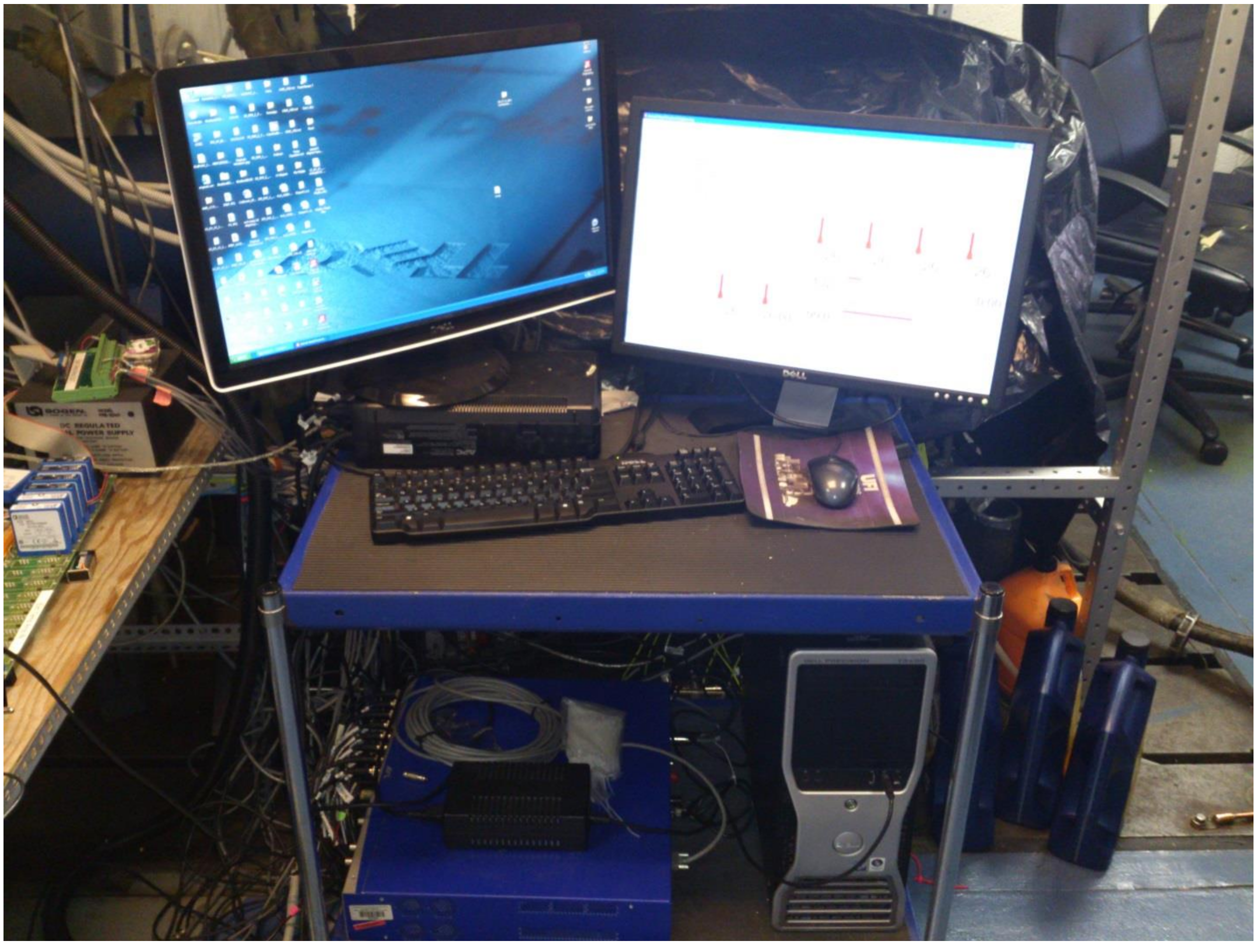

Figure 2.8 – PC along with the Indicom Data Acquisition System

The following channels were recorded by the Indicom during this study,

- In-cylinder Pressure#1
- In-cylinder Pressure#2
- In-cylinder Pressure#3
- In-cylinder Pressure#4
- In-cylinder Pressure#5
- In-cylinder Pressure#6
- Fuel Rail Pressure
- Current Probe Signal
- Air inlet manifold pressure.
- Total exhaust manifold pressure (after the turbocharger)
- Exhaust manifold pressure (for cylinders 1,2,3 before t/c)
- Exhaust manifold pressure (for cylinders 4,5,6 before t/c)
- EGR cooler inlet pressure
- EGR cooler outlet pressure
- Exhaust temperature Cylinder #5
- Exhaust temperature at the intersection of cylinders 4, 5 and 6

2.1.4 Electronic Control Unit

The engine is equipped with a stock Electronic Control Unit (ECU) which is a fully electronic control system. This system is composed of a Motor Control Module (MCM), and the Common Powertrain Controller (CPC). The two units are connected by a proprietary data link through which all the necessary data and information is shared. The MCM monitors both the engine and the data link. When a malfunction or other problem is detected, the system selects an appropriate response.

2.1.4.a Motor Control Module

The engine mounted MCM includes control logic to provide overall engine management. The MCM processes the data received from the CPC, for example the position of the accelerator pedal. This data is evaluated together with the data from the sensors on the engine, such as, charge and oil pressure and coolant and fuel temperature. The data is then compared to the characteristic maps stored in the MCM. From this data, quantity and timing of injection are calculated and the electronic unit pumps are actuated accordingly through the solenoid valves. Figure 2.9 shows the arrangement of motor control module

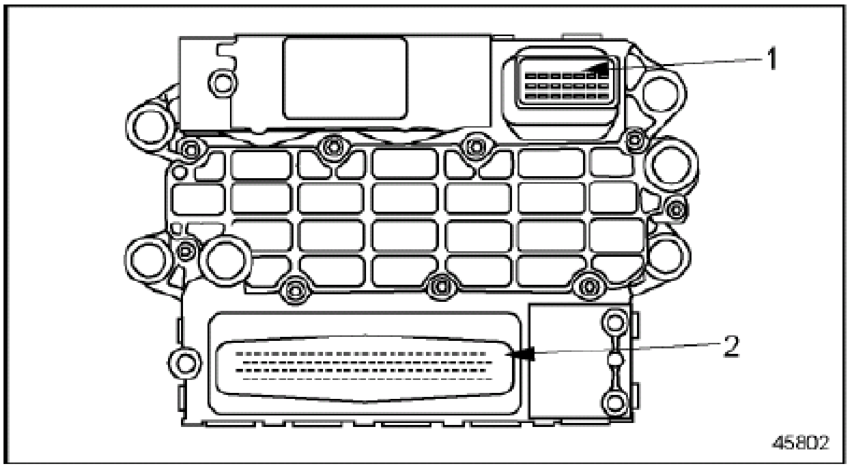

Figure 2.9 - Motor Control Module

2.1.4.b Common Powertrain Controller

The CPC has three 18-pin connectors and one 21-pin connector. The CPC is the interface between the MCM and the vehicle/equipment for engine control. The CPC receives data from the operator (accelerator pedal position, switches, and various sensors). Figure 2.10 shows the arrangement of common powertrain controller.

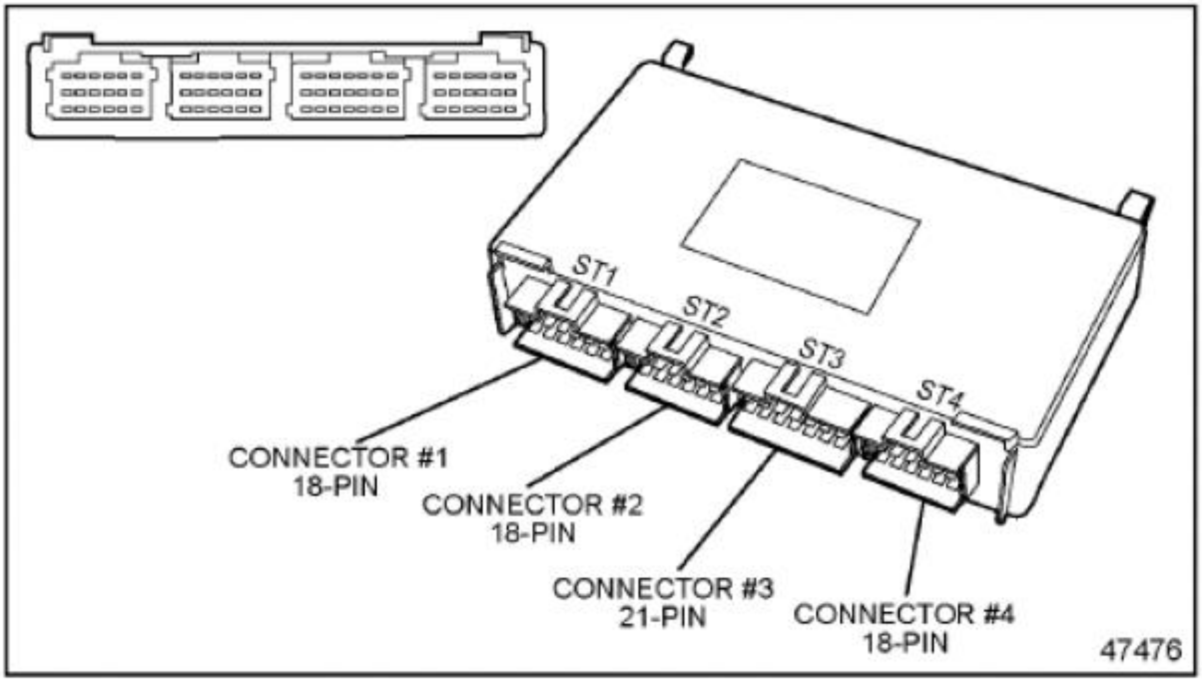

Figure 2.10 - common powertrain controller

From the data received by the CPC, instructions are computed for controlling the engine and transmitted to the MCM via the proprietary data link. Within the CPC, sets of data for specific applications are stored. These include idle speed, maximizing running speed, and the speed limitation.

2.2 Engine Instrumentation

The engine is heavily instrumented to measure cylinder pressure on each cylinder, intake manifold pressure, exhaust manifold pressure, EGR cooler inlet and outlet gas pressures, exhaust gas pressure before and after the turbocharger, and various thermocouples installed on the engine to measure temperature at different locations. Fuel rail pressure sensor is installed on the fuel high pressure line (after the electronic unit injection pump) on cylinder # 6 due to the ease of mounting. The engine has a stock ECU. The needle lift sensor could not be incorporated in the injector due to cost and the space constraints.

2.2.1 Pressure transducers

The cylinder head of the engine was replaced with a customized cylinder head. The sleeves for installing the in-cylinder pressure transducers could be mounted in the customized cylinder head. Six Kistler (Type 7061B) pressure transducers were used in this investigation. The signal from these in-cylinder transducers was amplified by six Kistler (5010) amplifiers respectively. Figure 2.9 shows the Kistler (Type 7061 B) pressure transducer and table 2.3 illustrate the technical specifications of the in-cylinder pressure transducer.

Table 2.3 – Specifications of the In-Cylinder Pressure Transducer

SPECIFICATIONS	DESCRIPTION
Measuring range	0 to 250 bar
Overload	300 bar
Sensitivity	5.52 pC/psi
Natural frequency	45 khz
Operating temperature range	-58 to 662 °F

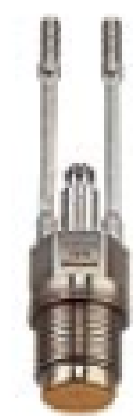

Figure 2.11 – Kistler In-Cylinder Pressure Transducer

These transducers were water cooled. The technical specifications of the Kistler (5010) amplifier used by these transducers are illustrated in table 2.4.

There were seven additional pressure transducers which were installed on the engine. The transducers were installed for the measurement of intake manifold pressure, EGR cooler inlet pressure, EGR cooler outlet gas pressure, gas pressure in the exhaust manifold for units # 1,2,3, gas pressure in the exhaust manifold for units # 4,5,6, fuel rail pressure (installed on unit #6), exhaust gas pressure after the turbocharger.

Table 2.4 – Specifications of the Pressure Transducer amplifier

SPECIFICATIONS	DESCRIPTION
Measurement range	+10,-10 to 999000 pC
No. of channels	1
Frequency range	0 to 180 khz
Supply voltage	115 V(AC)
Operating temperature range	32 to 122

2.2.2 Thermocouples:

Omega k type thermocouples were used for this investigation. The diameter of the wire was 1875 inches and the junction was grounded. The temperature range for measurement was from -200°C to 1250°C and the standard limit of error was 2.2°C or 0.75% (whichever was greater). Figure 2.12 shows an omega K type thermocouple.

Figure 2.12 - Omega Thermocouple

2.2.3 Current Probe

Due to space limitation considerations, the needle lift sensors for the fuel injectors could not be installed on this engine. Instead of that a current probe (fluke 80i-110s) is used for this investigation. This probe is jaw shaped and it is clamped around all the six conductors through which the electrical signal goes to the respective fuel injectors .The signal from this current probe can be used to detect if there is a fuel injection or not . This device is used to measure current through any conductor. The magnetic flux strength around the conductor is measured, from which the current is calculated.

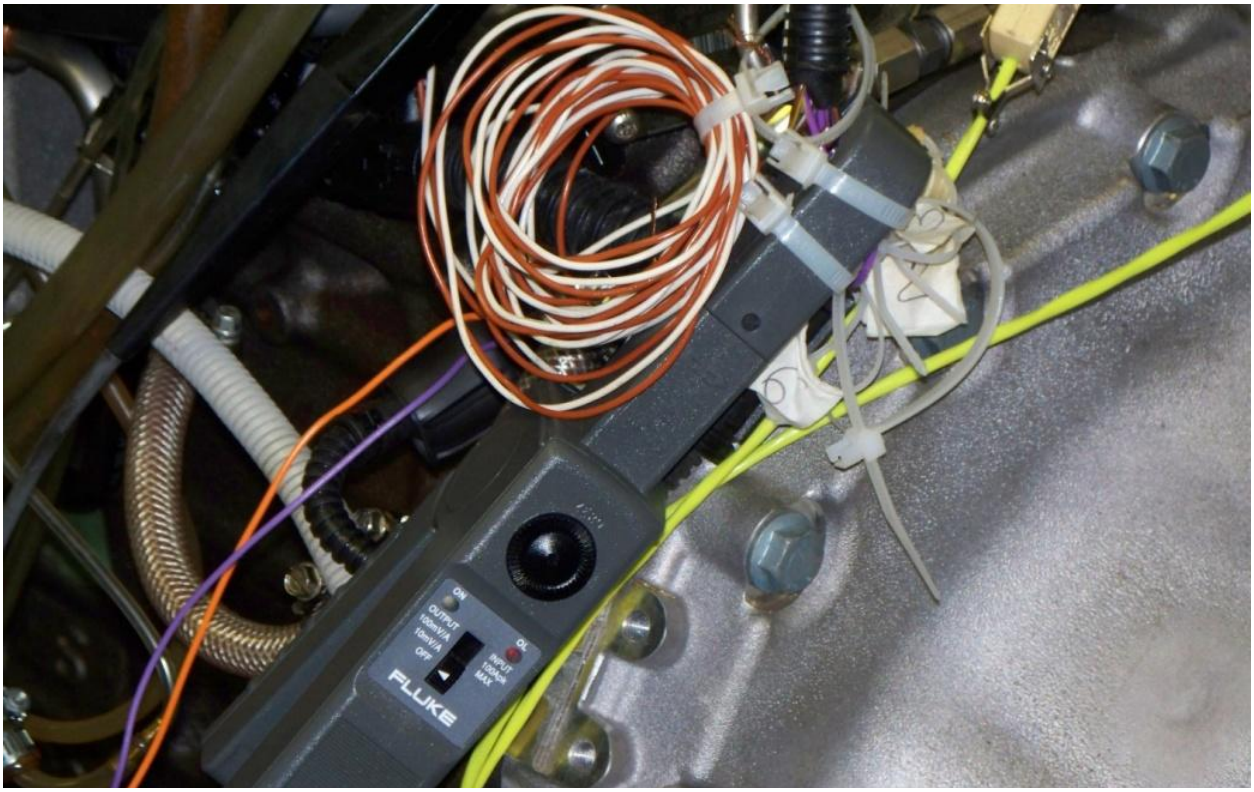

Figure 2.13 - Current Probe Installation

Table 2.5 - Current probe specifications

SPECIFICATIONS	DESCRIPTION
Dimensions	67 x 231 x 36 mm
Weight	330 gm (battery included.)
Max conductor size	11.8 mm
Max jaw opening	12.5 mm
Operating temperature	-30 to 70°C

2.3 Cold Room Description

The Wayne State cold room is capable of maintaining the ambient temperatures as low as -50 C which utilizes the Watlow control systems. Figure 2.14 illustrates the fans situated inside the cold room.

Figure 2.14 – Giant fans installed inside the Cold room cooler

Figure 2.15 – Watlow control panel used by the Cold Room Controller

Figure 2.16 – Timer Switch for Cold Room Cooler

Figure 2.17 – Temperature Setpoint control for the Cold Room Cooler

Figures 2.14 and 2.15 illustrate the fans installed in the cold room facility as well as the controller used for the temperature control of the cold rom cooler. Figure 2.16 illustrates the timer switch used to set the cold room cooler to operate at a specific temperature for a predetermined time as set in the timer. Figure 2.17 illustrates the switch used to control the ambient temperature Setpoint inside the cold room. The controller as shown in figure 2.15 is operated automatically by the temperature setpoint control switch (Figure 2.17) and the timer switch (Figure 2.16).

2.4 Instrumentation Challenges

1. Start of Injection cannot be exactly determined in the engine because of the absence of needle lift sensor. ECU Injector current signal might be used for an approximate start of injection prediction. In this experimental study in order to calculate the approximate SOI , the timing at which the ECU injection signal reached its peak value was assumed to be the SOI timing as illustrated by the red vertical line in the figure 2.18

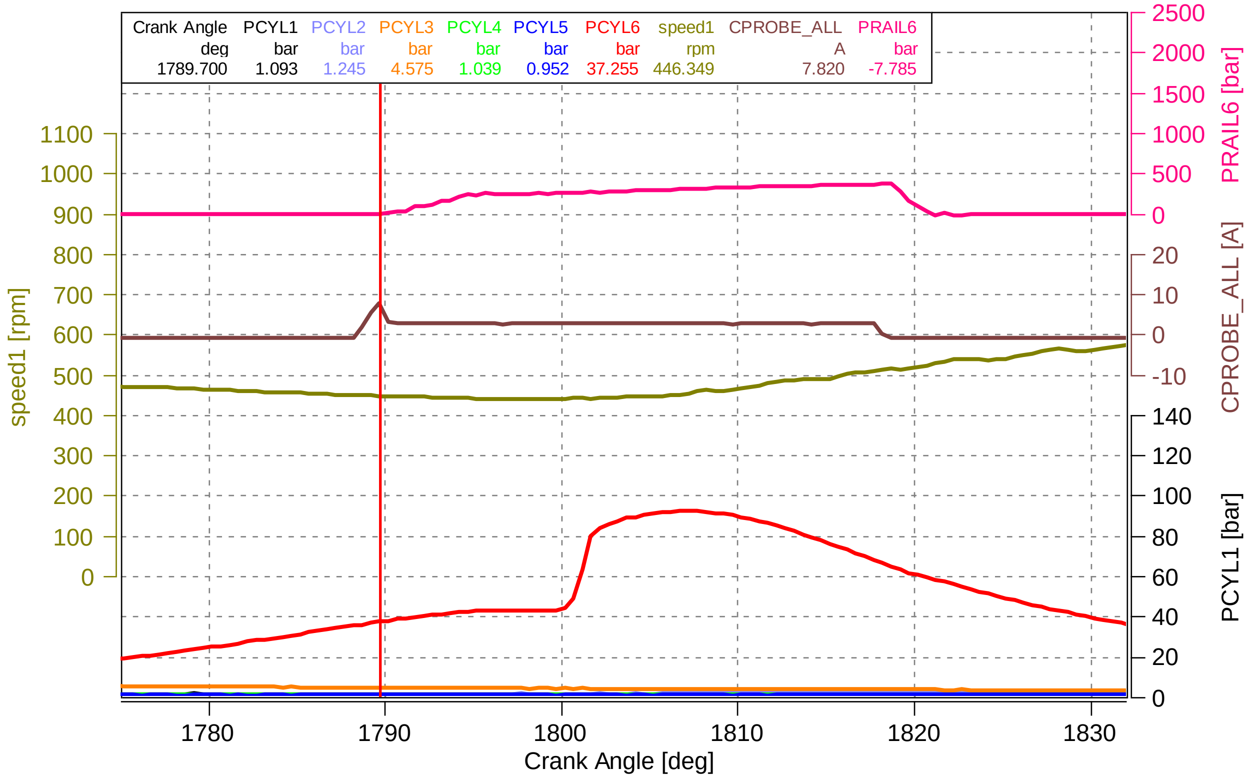

Figure 2.18 – Start of Injection determination from the ECU Injection Signal

2. Injection timing cannot be accurately calculated from the injection current signal from the ECU. There will always be a small timing delay between when the ECU sends the signal to open the NCV valve and when the actual mechanical fuel injection happens
3. Injection pressure cannot be accurately measured from the pressure trace in the fuel line, since it is a function of the time at which the mechanical injection happens in the injector which cannot be accurately measured without a needle lift sensor
4. The fuel injection can be controlled by two valves (Needle Control Valve and Spill Valve) as discussed earlier. In our engine we only measure the current flow through the NCV and not the spill valve. Under certain circumstances engine might appear to misfire by analyzing the NCV position and the pressure in the fuel rail, but the spill valve might be open, thus releasing the pressure required for adequate fuel injection. The only way to prevent this from happening is to install a current probe to monitor the current flow in the spill valve, which was not a viable option at the time of the cold room setup
5. Engine ECU used is a closed ECU and the calibration setup (injection timing, injection pressure, injection quantity as a function of temperature) cannot be identified which further complicates the data analysis process

CHAPTER 3

TEST MATRIX AND TEST CONDITIONS

3.1 Test Matrix:

All the cold start tests were conducted on the cold room test cell of Wayne state university. The engine fuel storage tank, the batteries and the engine itself are all placed inside the cold room to make sure not just the engine, but also the fuel is at the desired ambient temperature before conducting the experiment.

Cold start characterization of Mercedes Benz MBE 926 engine was done with two fuels, Ultra low sulfur diesel (ULSD) and JP8.

Test procedure involves soaking the cold room at the desired ambient temperature for at least 8 hours and then using the ECU oil temperature sensor, engine oil temperature was verified to be the desired temperature. Subsequently followed cranking and data recording using AVL Indicom data acquisition system. The engine was not connected to a dynamometer; hence all the testes were performed at no load condition. The table 3.1 illustrates the test matrix.

Table 3.1 - Test Matrix

Fuels Used	Ambient Temperature (^{o} F)						
JP8(HCN)	77	35	25	16	10	5	0
ULSD	77	40	35	25	20	10	

3.2 Fuel Properties

Fuel properties such as density, viscosity and cetane number play a very important role in the cold starting. For example fuels with higher cetane numbers tend to have less ignition delay period during the cold start and hence exhibit better cold starting characteristics. Table 3.2 illustrates the fuel properties of Jp8 and ULSD used in this study.

Table 3.2 - Fuel Properties

Fuel	ASTM	ULSD	JP-8 (HCN)
Cetane Number	D613	42.3	49
Derived Cetane Number	D6890	42.1	50.1
Flash point (°C) min	D93	69	49.5
Density (@15°C) kg/m^3	ASTM 85H	842	798
Viscosity (cSt, 40°C)	D445	2.438	1.367
Heating Value (MJ/kg)		41.2	43.2
Aromatic content (%Mass)	D2425	27.8	16.3

3.3 Detailed Steps to Run the Engine for a Single Test:

1. Program the cold room air cooler:

Prior to each run, the engine is required to be soaked for at least 8 hours at the desired ambient temperature. The Cold Room air conditioner can be programmed to run for desired number of hours at a desired temperature. In order to soak the engine at the desired temperature, adjust the thermostat knob to read that value. The microprocessor controlled cooler maintains the temperature as defined in the thermostat using a timer switch. This switch is used to turn on and turn off the cold room air cooler. The timer switch and the thermostat are shown below.

Figure 3.1 – Timer Switch for Cold Room Cooler

Figure 3.2 – Temperature Setpoint control for the Cold Room Cooler

The procedure to program this switch is as follows.

❖ To turn the cooler ON:

- Press “Mode” button until it shows the “SCH” sign below the time in the display
- Next press “hour / min” button to set the required time and then press the “Event” button to turn it on.
- Next select the “Day” button to choose the required day on which the cold room refrigerator has to be turned on.
- After everything is set, press the “Enter” button to save the entered configuration.

❖ To turn the cooler OFF:

- Press “Mode” button till it shows the “SCH” sign below the time in the display.
- Next press the “hour / min” button to set the required time and then press the “Event” button to turn it off.
- Next select the “Day” button to choose the required day on which the cold room refrigerator has to be turned off.
- After everything is set, press the “Enter” button to save the entered configuration.

2. Turn the main power switch ON and start charging the batteries so that a sufficient power is supplied to the starter motor to crank the engine

3. Start the in-cylinder pressure sensor cooling system and check the coolant flow to each of the pressure sensors. This ensures that the pressure transducers are not overheated and increases the life of the sensor.

4. Switch the ECU ignition ON

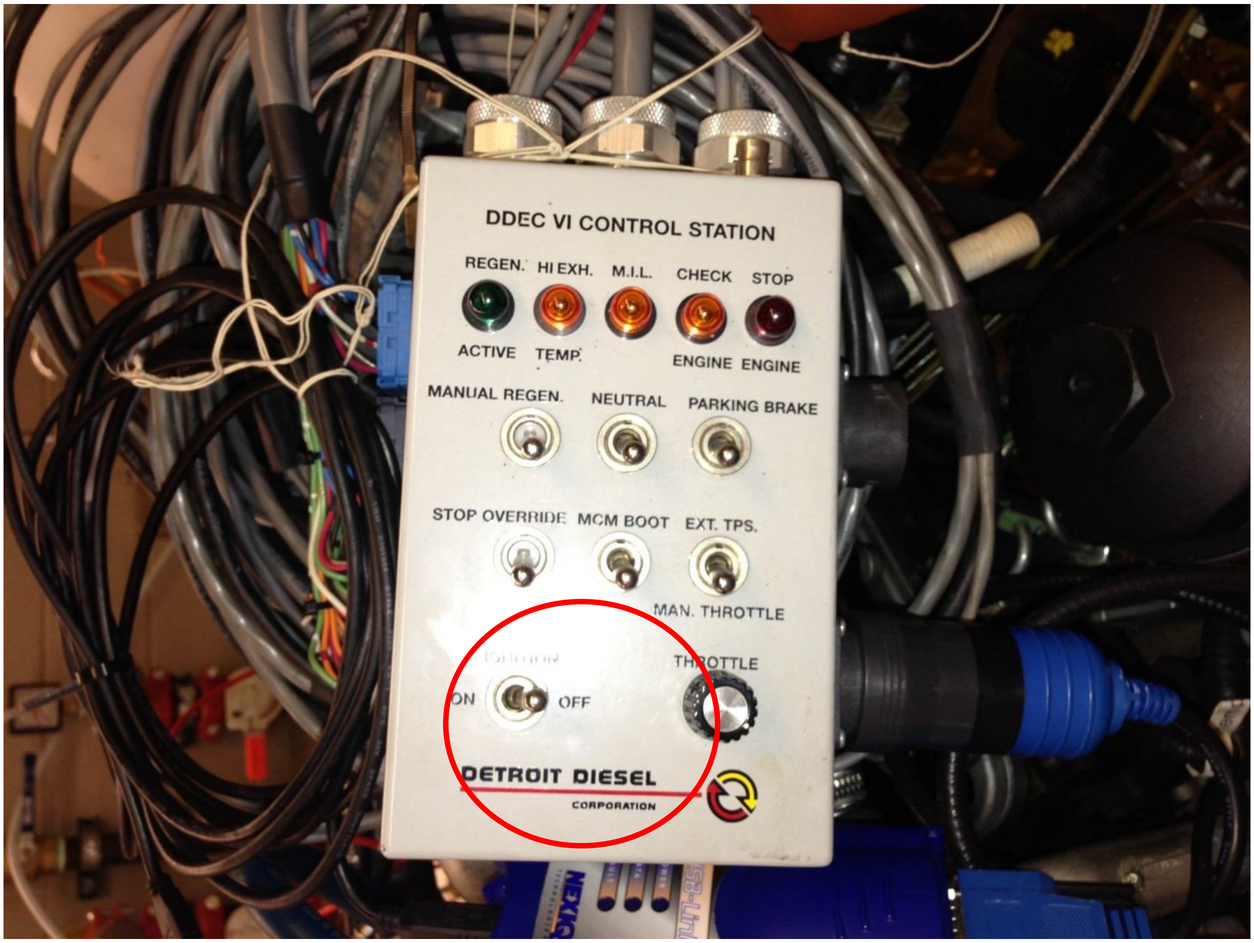

Figure 3.3 - ECU Ignition Switch

5. Turn on the data acquisition computer (INDICOM) and the engine ECU computer.

Figure 3.4 - Indicom and ECU PCs

6. Verify that the ECU computer reads the engine oil temperature and related data

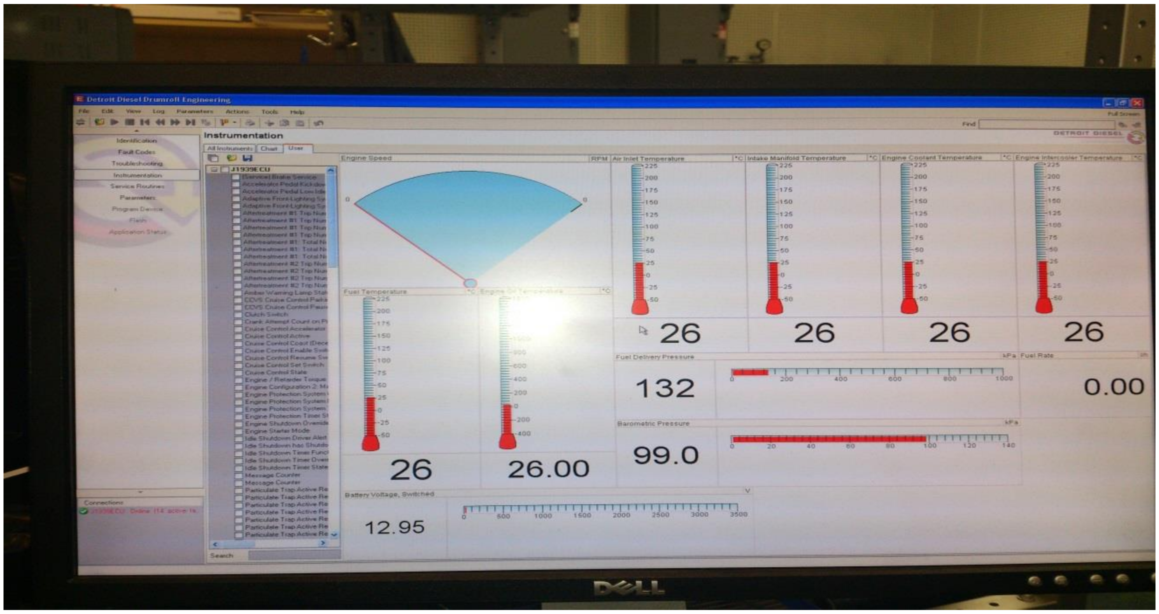

Figure 3.5 - ECU Temperature Display

7. Turn the pressure transducer amplifiers to the “Operate” mode.

Figure 3.6 - Pressure Transducer Amplifier

8. Start the engine exhaust fan.

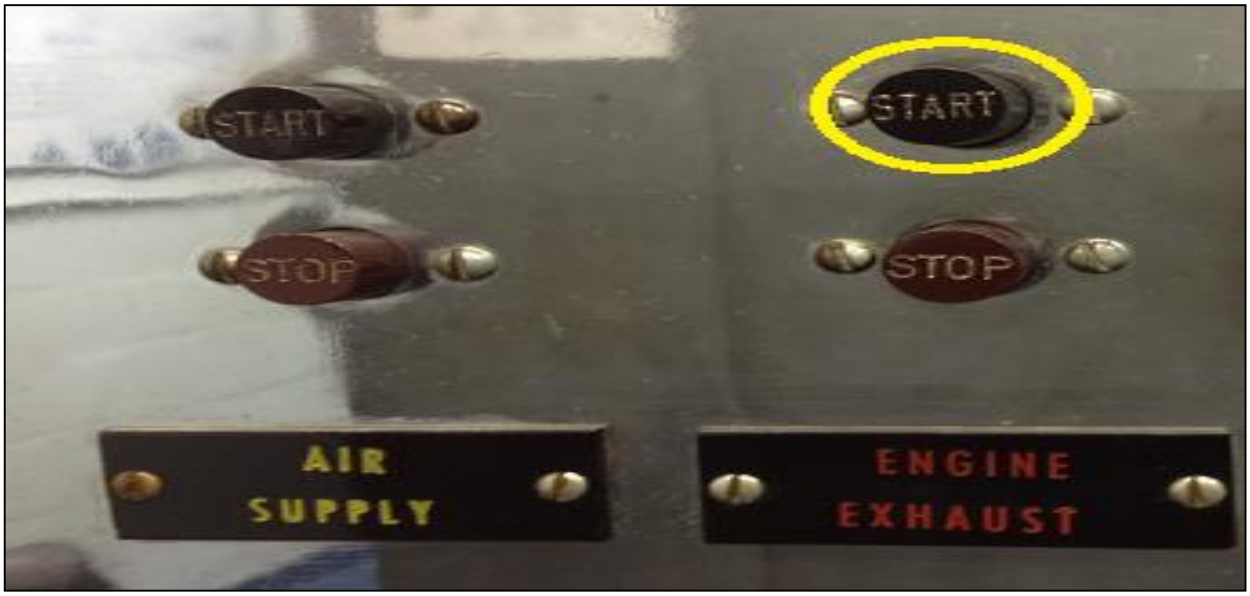

Figure 3.7 - exhaust fan switch

9. Run the ECU software in the INDICOM PC
10. Run the data acquisition software INDICOM and make sure the transient measurement option is checked.
11. Start cranking the engine through the starter motor till the engine runs.
12. Keep the engine running until it is warmed up so that the engine oil temperature reaches 80 C. After the warm up turn off the ECU.

CHAPTER 4

COLD START EXPERIMENTAL RESULTS

First set of engine tests were conducted using the ULSD fuel in the MBE926 engine in order to have a base data for the comparison purposes, since the initial engine calibration was done in ULSD by the engine manufacturer. A detailed analysis of the engine cold start transient data is done in the following sections for both the ULSD and JP8 fuels. In the following section ULSD and JP8 experimental data will be presented.

4.1 Cold Start – ULSD 77 F

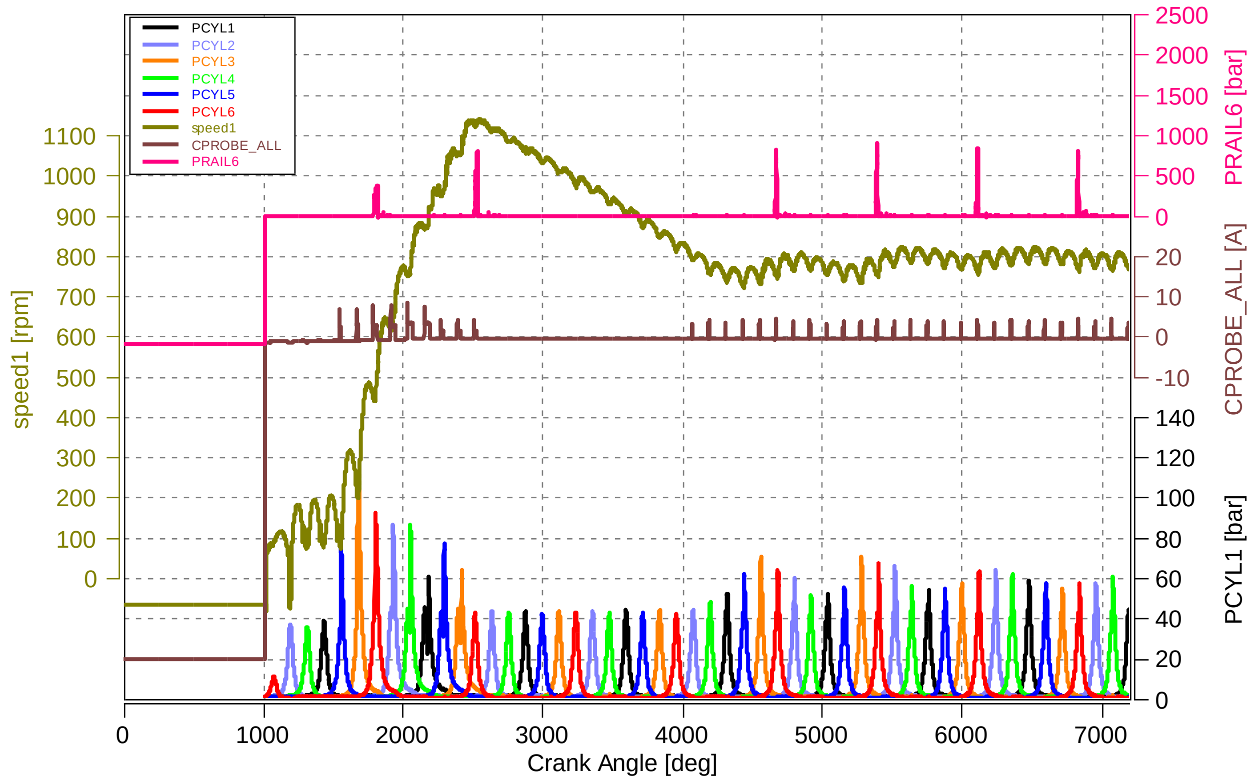

Figure 4.1 – Cold starting of ULSD at 77F

Figure 4.1 represents the transient engine speed trace recorded during the first twelve cycles at the room temperature of 77F. The engine resulted in successful start at 77F. First fuel injection started after three cycles, which was followed by a continuous increase in the fueling which resulted in a prompt engine start which led to the engine speed overshoot of more than 800 rpm and close to 1150 rpm. In general, when the engine speed increases, the injection pulse width increases in crank angle degrees. As soon as the engine speed was over 800rpm the fuel control governor kicked in and reduced the fueling inorder to maintain the engine speed close to idle. Fueling cutoff lasted for a period of two engine cycles as a result of speed overshoot, which was followed by the regular fueling strategy of a main and a pilot injection. As a result the engine speed finally stabilized at the idling speed of 800 rpm.

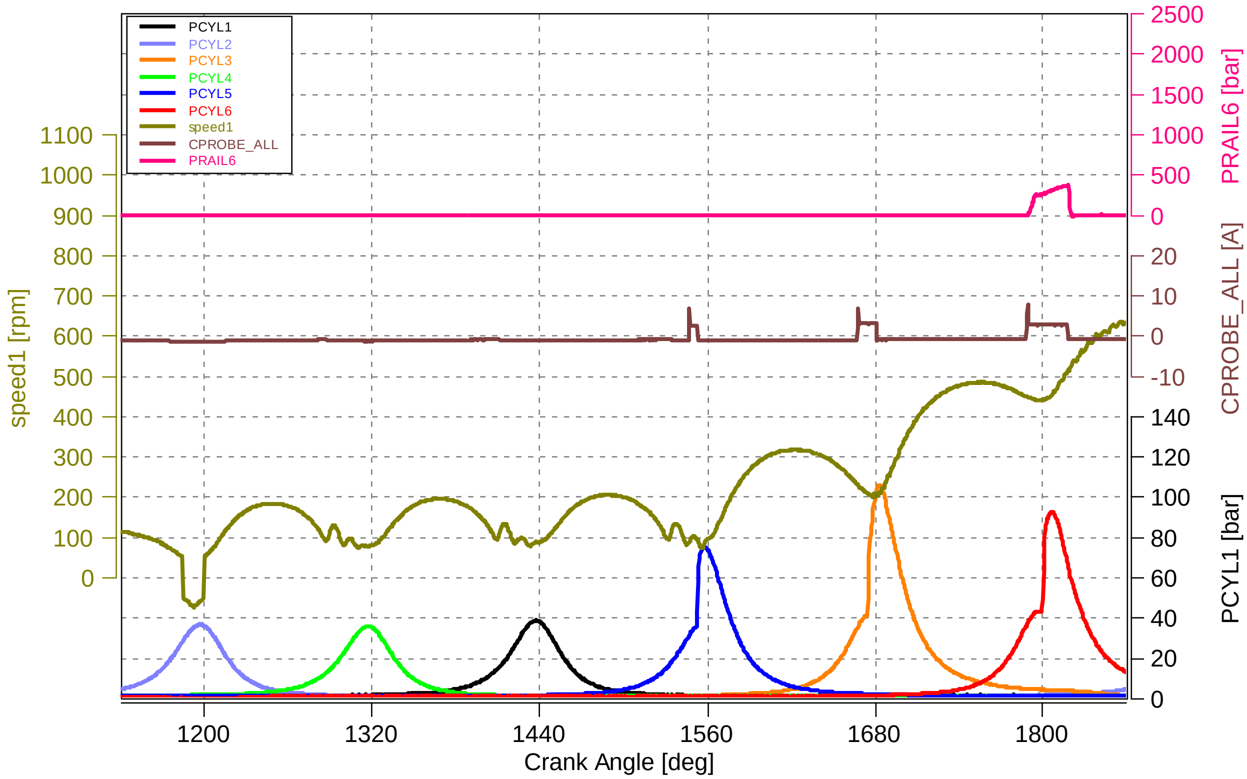

Figure 4.2 – Cold starting of ULSD at 77F-1st cycle

Figure 4.2 represents the zoomed in version of the figure 4.4 with only showing the first cycle of the six cylinders. The average cranking speed is 142rpm. The very first injection in cylinder 5 resulted in successful firing followed by cylinders 3 and 6 and the speed accelerated towards idling speed. As observed in figure 4.2 the pulse width was gradually increased as a part of the ECU calibration strategy by the manufacturer in order to allow more fueling to accelerate the engine up to the idling speed. It is recommended to advance the injection timing with increase in engine speed. It has to be noted that the engine speed did not reach the idling speed in the first cycle.

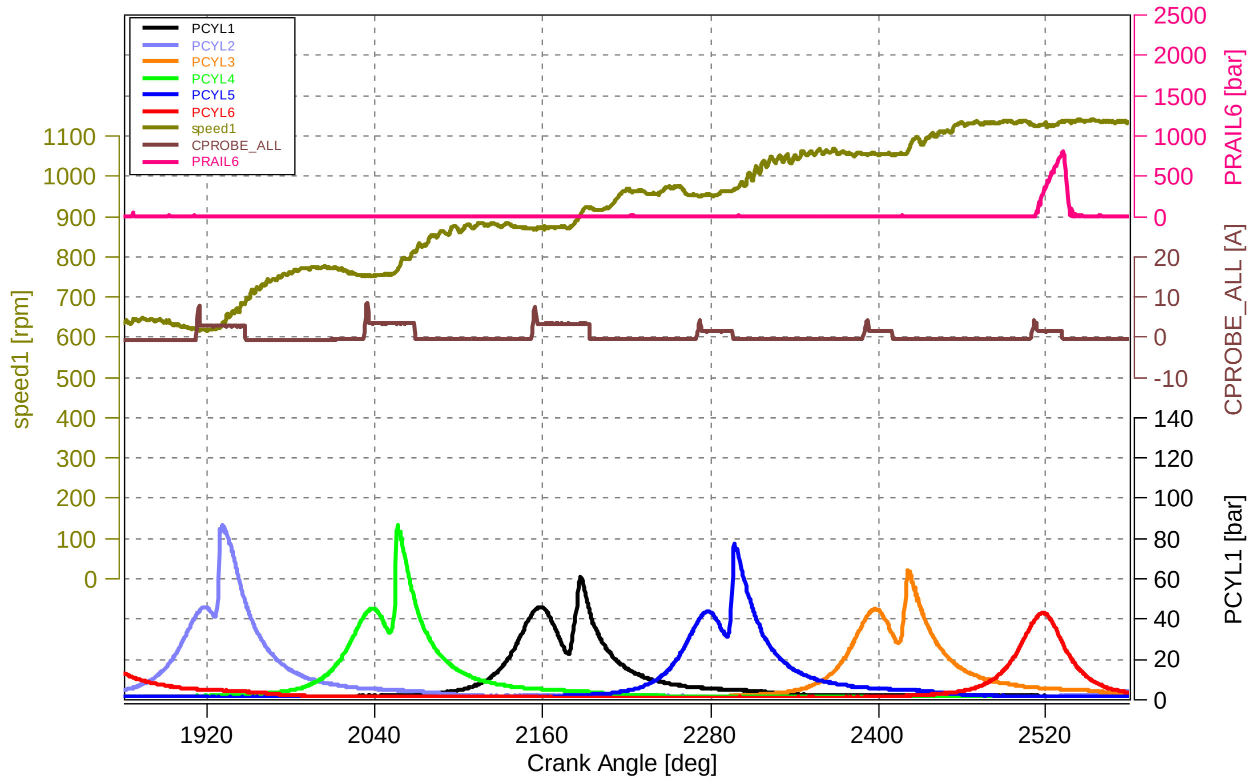

Figure 4.3 – Cold starting of ULSD at 77F-2nd cycle

It is interesting to note that from the pressure traces in 2nd cycle the first three cylinders has a same injection timing (6 deg BTDC) but resulted in increased ignition delays respectively which is attributed to the fact that the instantaneous engine speed is constantly accelerating which results in less time spent by the piston around TDC to allow sufficient time for the diesel fuel to mix with air and autoignite.

Similar phenomena can be observed in cylinders 5, 3 and 6, but in this case cylinder 6 misfired, which is indicated by the occurrence of peak cylinder pressure before TDC. The exact reason could not be concluded from the available instrumentation.

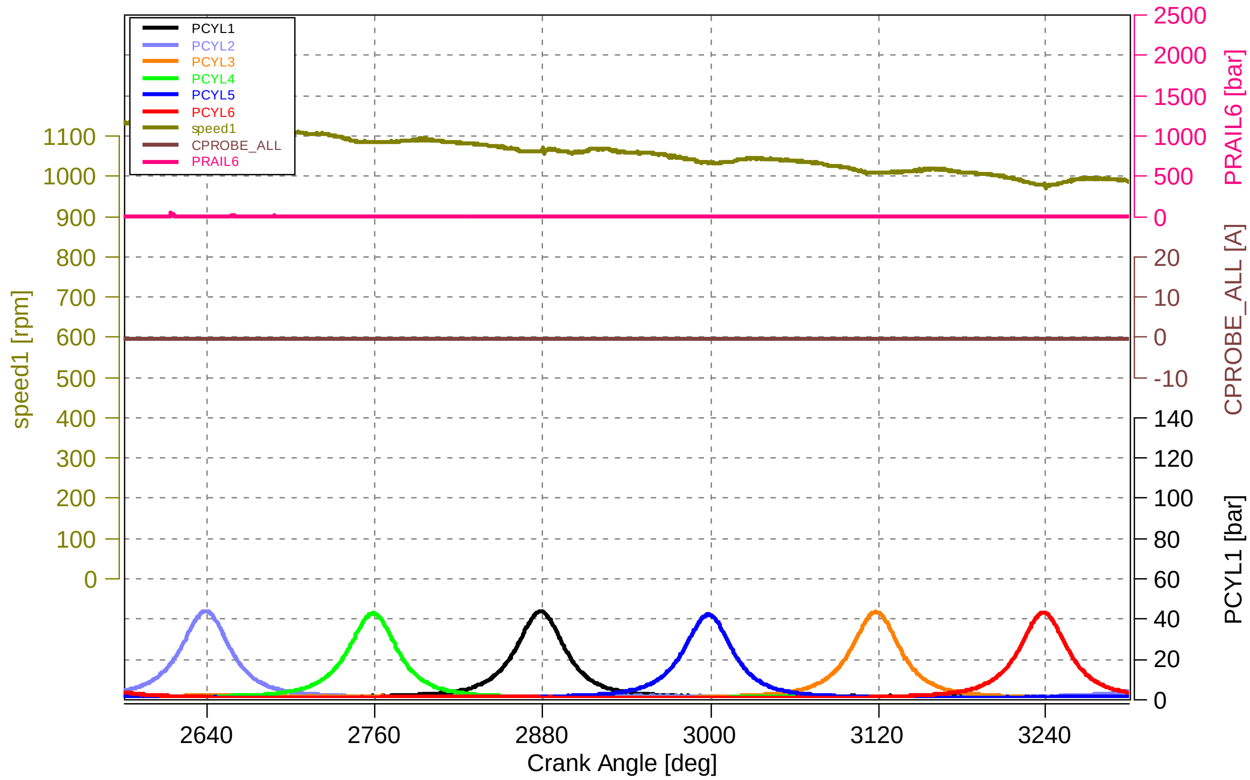

Figure 4.4 – Cold starting of ULSD at 77F-3rd cycle

Figure 4.4 represents the engine speed trace during the third cycle where there was fuel injection cutoff by the ECU because of the engine speed higher than the idling speed of 800 rpm which resulted in reduced engine speed from 1130 rpm to 1000 rpm by the end of the cycle. The fuel injection cut off continued throughout the 4th cycle as well.

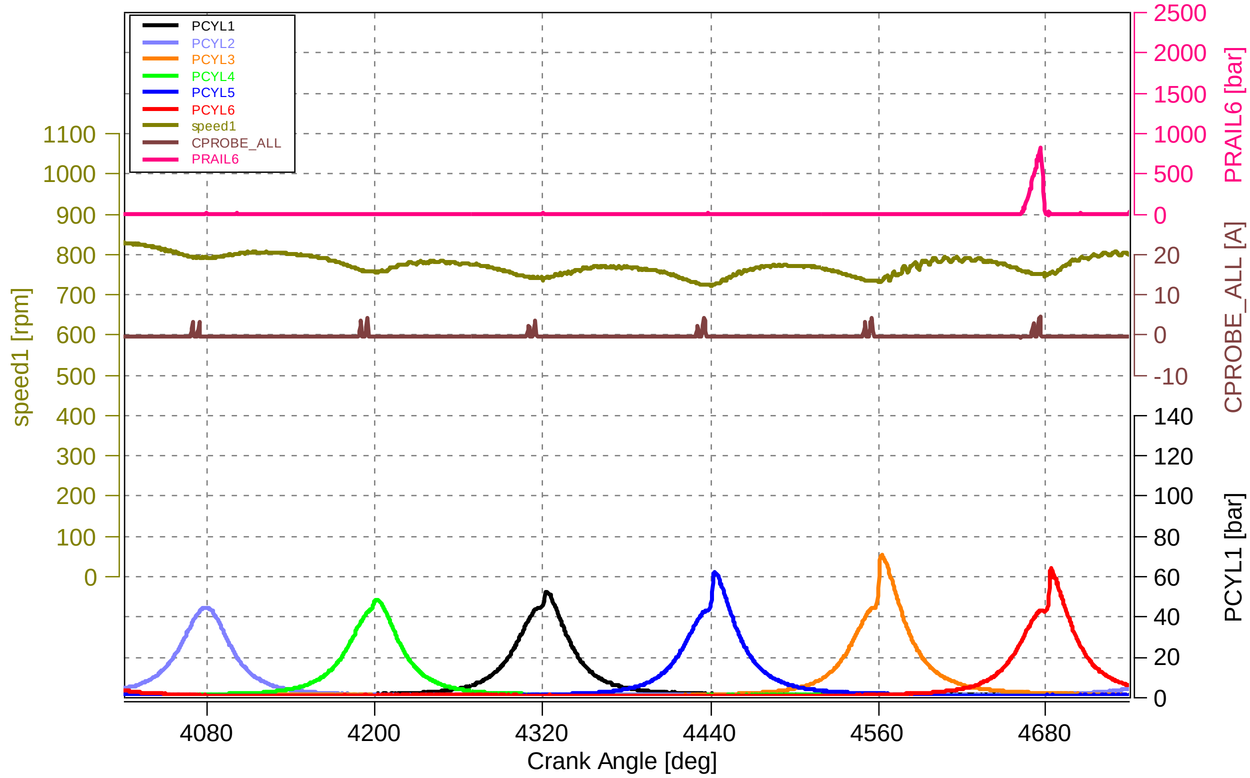

Figure 4.5 – Cold starting of ULSD at 77F-5th cycle

Figure 4.5 represents the speed and pressure traces of the 5th cycle. As soon as the engine speed reduced below 800 rpm, fuel injection started in the following cylinder. It is also interesting to note that the fueling strategy shifted from single injection to pilot + main injection as calibrated by the manufacturer. Since the engine speed was maintained at idle without any oscillation after the first pilot + main injection, the same injection pattern continued for the following cycles.

4.1.1 Conclusions – ULSD 77F

- Engine attained a stable start at room temperature without any hesitation in engine speed
- Injection timing was kept constant with increase in engine speed for a few cycles, which was not desirable from the cold start perspective and had to be advanced
- First fuel injection started after three TDCs
- One misfire occurred during 2^{nd} cycle in cylinder 6.
- Engine reached the idling speed in its 2^{nd} cycle
- Engine speed fully stabilized to the idling speed without any speed oscillation after 5 cycles
- For two cycles fuel injection was totally cut off to maintain the idling speed by the idle governor

4.2 Cold Start – ULSD 40 F

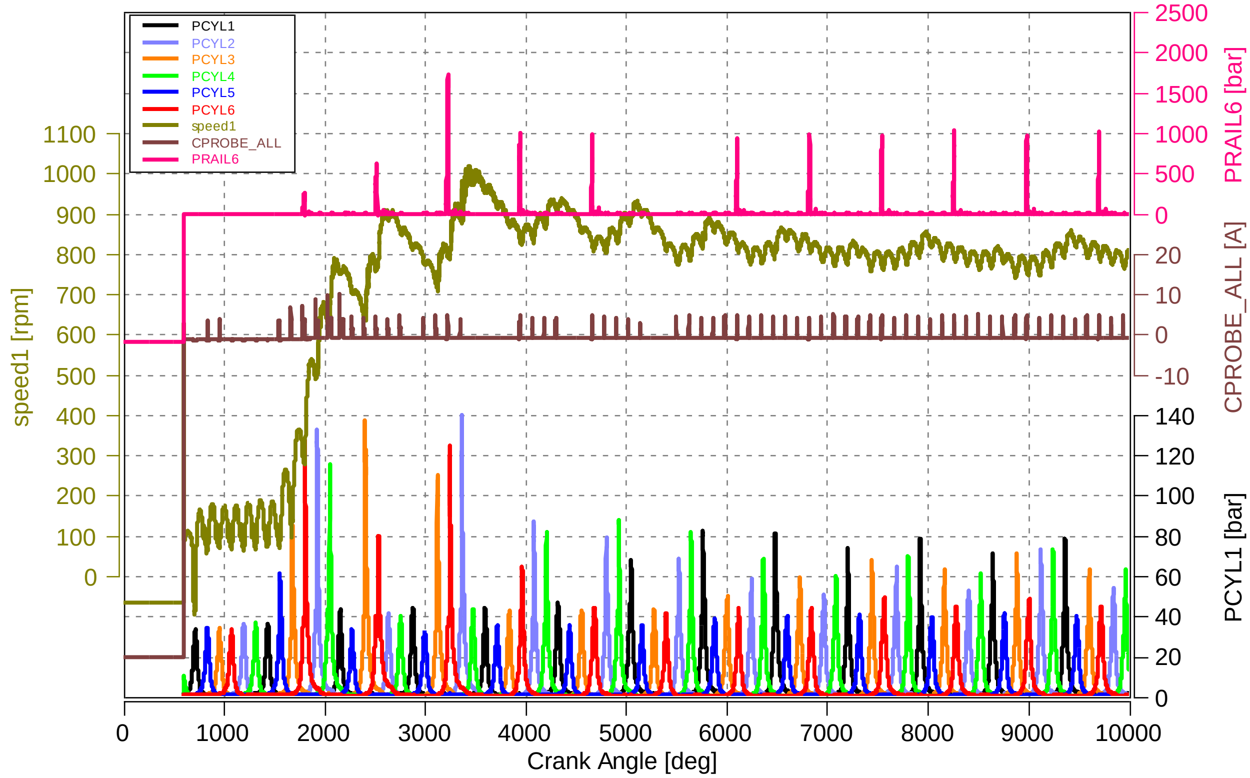

Figure 4.6 – Cold starting of ULSD at 40F

Figure 4.6 represents the engine speed as well as pressure traces for the first 13 cycles of ULSD at 40F. Initially two fuel injection events happened followed by no injection for a few cylinders, which was then followed by continuously increasing fueling for a few cycles for the prompt engine acceleration up to the idling speed. Lower ambient temperature resulted in increased heat and blowby losses which resulted in longer ignition delays and partial combustion. Engine speed oscillated around the idling speed, as a result fueling continued intermittently for a few cycles in order to maintain the idling speed. The engine speed took longer time to stabilize in the idling speed in comparison with the ULSD 77F experiment.

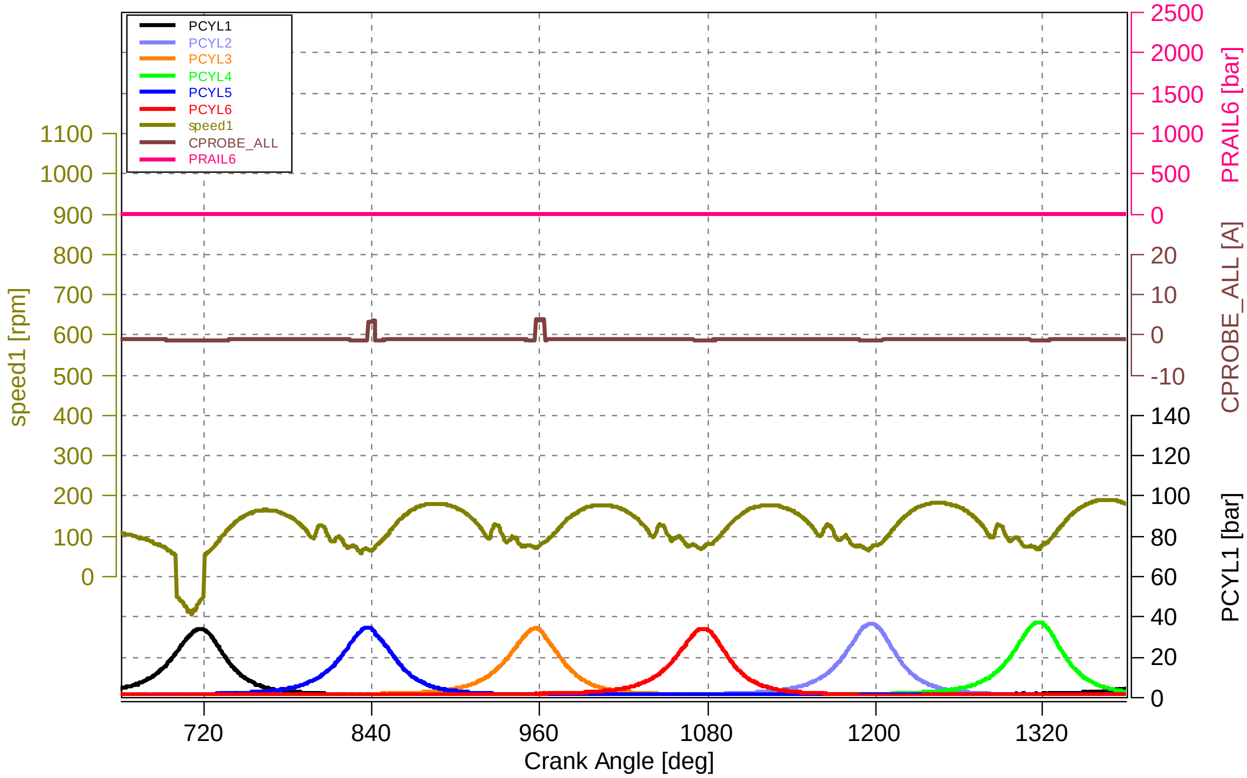

Figure 4.7 - Cold starting of ULSD at 40F-1st cycle

Figure 4.7 represents the engine speed as well as pressure traces for the first cycle of ULSD at 40F. Average cranking speed was reduced to 129 rpm. Initially two fuel injection signals were sent by the ECU which resulted in no pressure rise. It cannot be concluded whether there was a proper fuel injection or not because of the lack of instrumentation as discussed in chapter 3. There was no signal sent from the ECU for the following cylinders in the first cycle and cranking speed is lesser than the cranking speed at ULSD 77F because of the reduced charge discharge capacity and increased frictional losses as well as blow by losses at lower ambient temperatures.

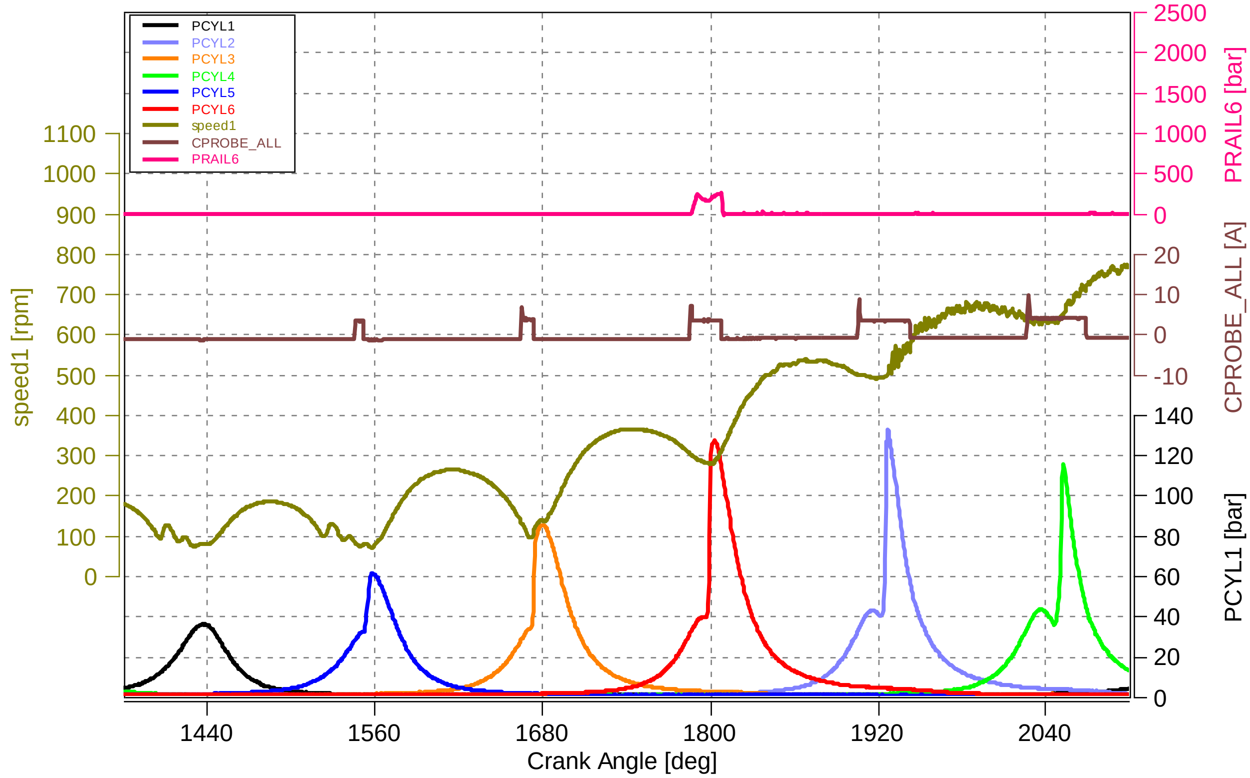

Figure 4.8 - Cold starting of ULSD at 40F-2nd cycle

Figure 4.8 represents the engine speed as well as pressure traces for the second cycle of ULSD at 40F. Injection starts in cylinder 5 and gradually the fuel injection pulse width was increased for the following three cycles and held constant. Injection duration was increased continuously for all the cycles from the start inorder to accelerate the engine to the idling speed. Constant injection timing resulted in increased ignition delays with increase in engine speed for the last three cylinders. Engine speed accelerated form cranking speed of 130 rpm to close to 800 rpm by the end of the 2nd cycle.

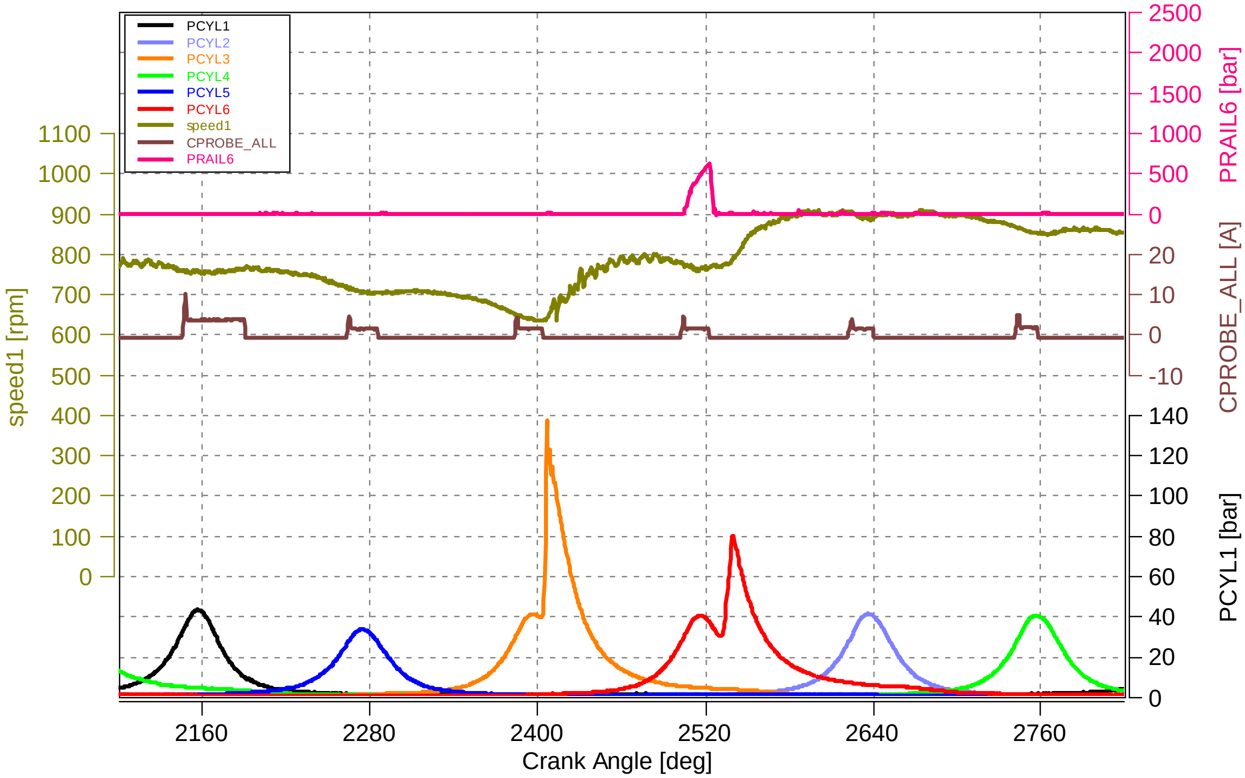

Figure 4.9 - Cold starting of ULSD at 40F-3rd cycle

Figure 4.9 represents the engine speed as well as pressure traces for the third cycle of ULSD at 40F. The engine speed was close to idling speed of 800 rpm in the first cylinder, which resulted in the reduced amplitude of the ECU current signal from the following cylinder (cylinder 5). The engine speed oscillates between 600 and 900 rpm throughout the cycle. It is interesting to note that injections in the cylinders 1, 5, 2, and 4 resulted in misfire. The reason for misfires in cylinders 1, 5, 2 and 4 couldn't be properly identified because of the lack of instrumentation. In order to maintain the idling speed rapid fuel injection in cylinder 3 resulted in pressure increase up to 130bar which is a high value at below idling speed

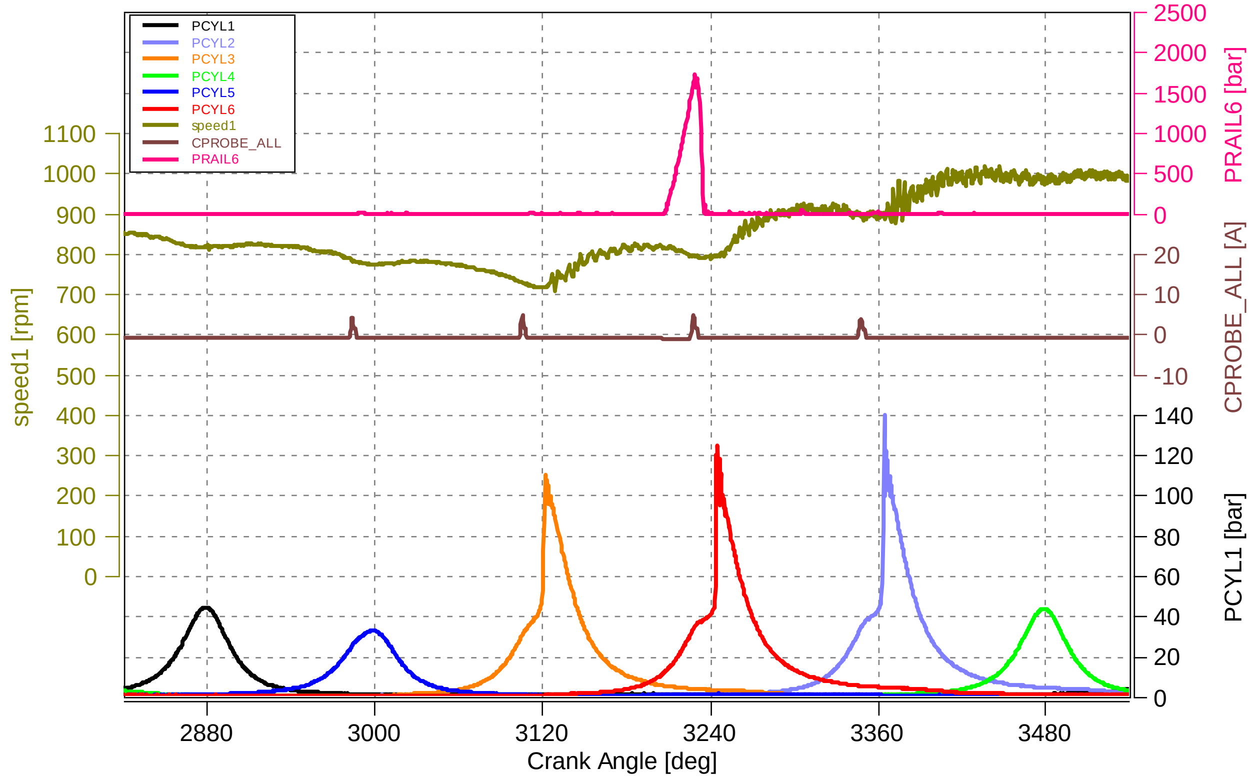

Figure 4.10 - Cold starting of ULSD at 40F-4th cycle

Figure 4.10 represents the engine speed as well as pressure traces for the fourth cycle of ULSD at 40F. Since the engine speed was higher than the idling speed of 800 rpm fuel injection was cutoff in cylinder 1 at the start of the cycle. Cylinder 5 misfired which might be because of the low compression pressure in the cylinder. Cylinder 4 has no fuel injection since the engine speed was higher than the idling speed. The cylinders 3, 6 and 2 resulted in very high peak pressures ranging from 110 bar to 140 bar because of the increased injection pressures as discussed in the following section.

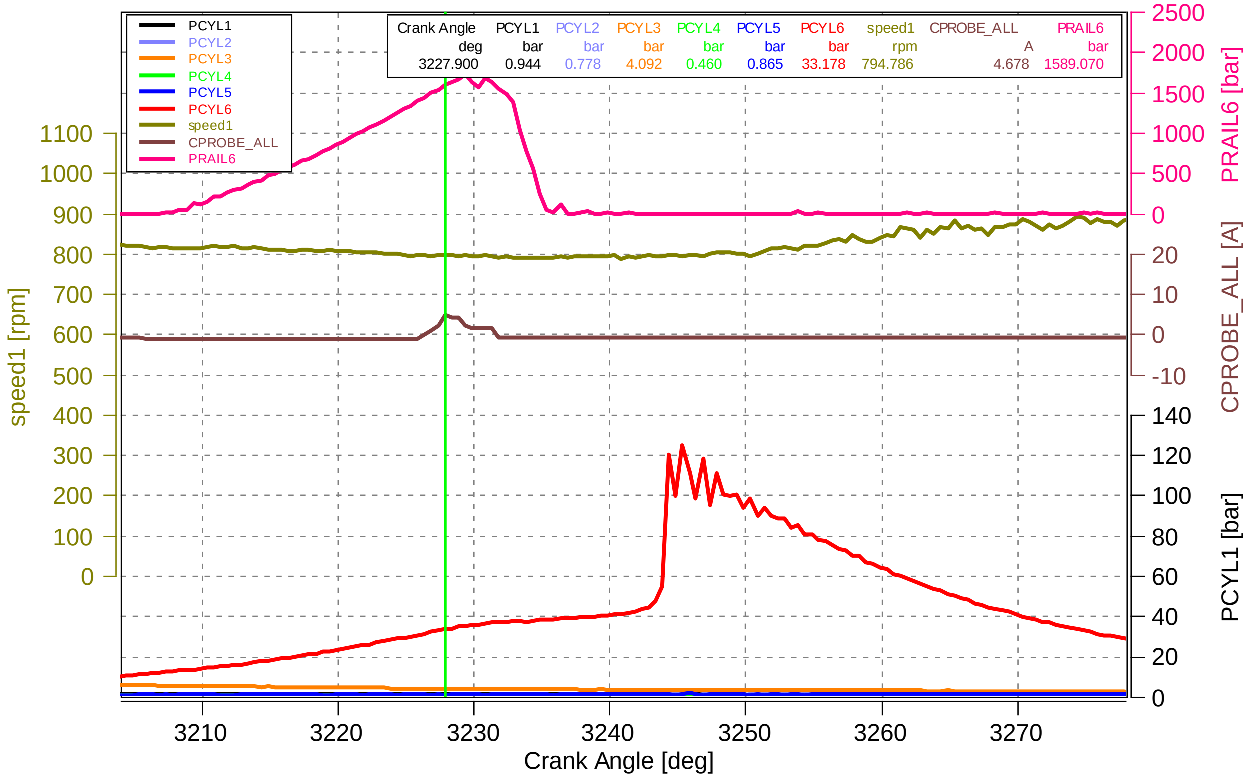

Figure 4.11 – Injection Pressure of Cylinder 6 – 4th Cycle ULSD 40F

Higher peak pressure despite shorter injection duration of 4.5 crank angle degrees occurred as a result of increased injection pressures of over 1560 bar as shown in green line of figure 4.11, which is a very high injection pressure especially when considering the fact that the engine was running at idle conditions without any load.

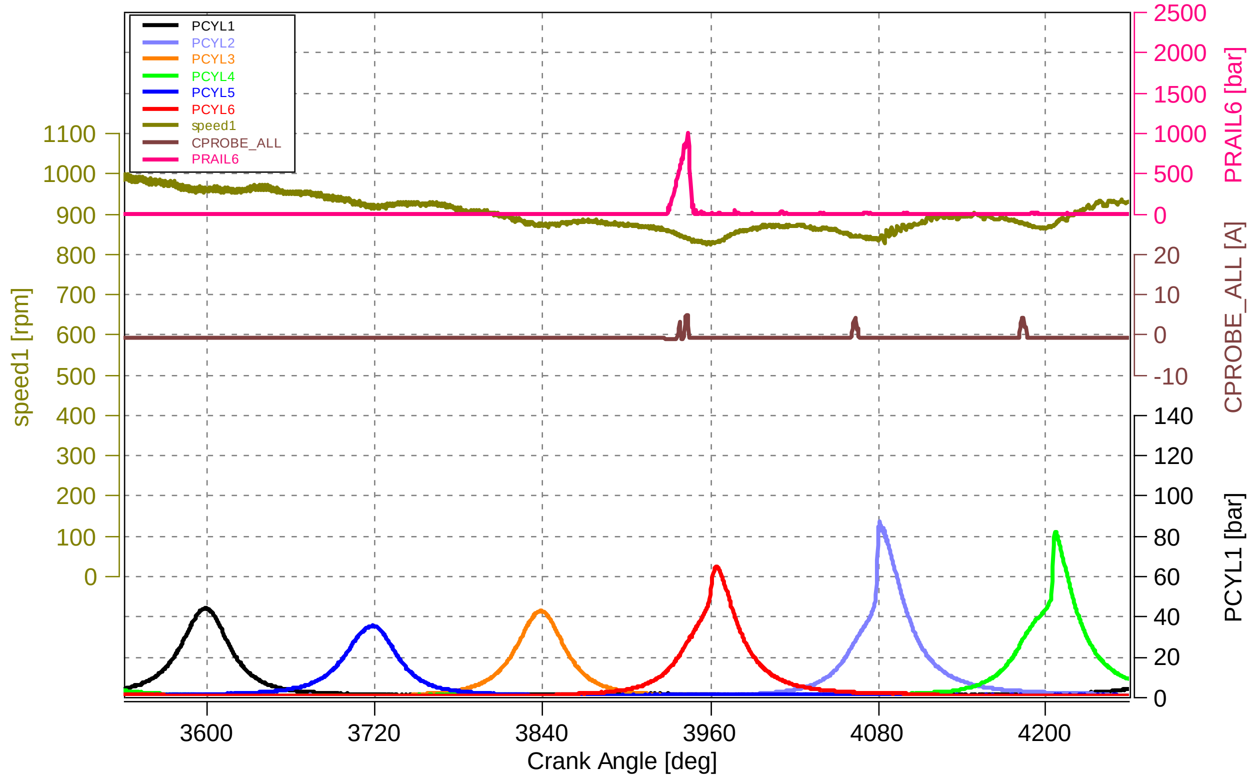

Figure 4.12 - Cold starting of ULSD at 40F-5th cycle

Figure 4.12 represents the engine speed as well as pressure traces for the fifth cycle of ULSD at 40F. Engine speed partially stabilized to the idling speed in cycle 5. ECU tried to switch the injection pattern from single injection to dual injection in cylinder 6, but after the dual injection the speed was still above 800 rpm which resulted in switching the calibration strategy from dual injection to single injection. Engine speed oscillation continued for the following cycles until the 56th cycle.

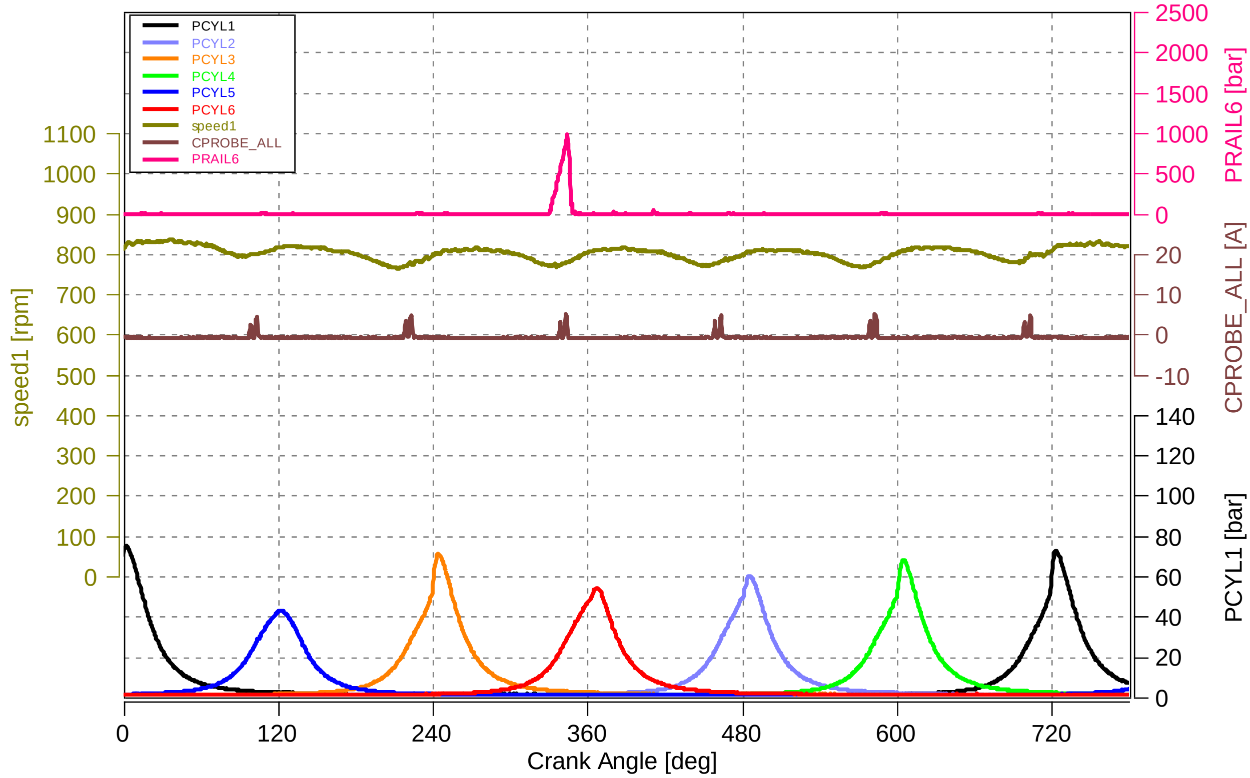

Figure 4.13 - Cold starting of ULSD at 40F-56th Cycle

Figure 4.13 represents the engine speed as well as pressure traces for the 56th cycle of ULSD at 40F. Engine speed stabilized in its idling speed at the end of 55th cycle without further more oscillations around the idling speed and the engine ECU switched to dual fuel injection strategy since the engine speed was stable around the idling speed of 800 rpm

4.2.1 Conclusions – ULSD 40F

- Engine successfully started at 40F using the ULSD fuel
- Engine speed took longer time to stabilize at the idling speed in comparison with ULSD 77F experiment as a result of the low ambient temperature which resulted in increased blowby and heat losses.
- Engine cranking speed was reduced to 130 rpm as a result of lower battery discharge capacity and increased frictional losses
- As observed in ULSD 77F, injection timing was kept constant which resulted in increased ignition delays in a few cycles (3^{rd} cycle). It is recommended to advance the injection timing with increase in engine speed.
- The engine speed oscillations took 55 cycles to stabilize at the idling speed
- Partial combustion was observed in a few cycles which resulted in a minor heat release and thus the pressure rise was much lower than other complete combustion cycles.

4.3 Cold Start – ULSD 35 F

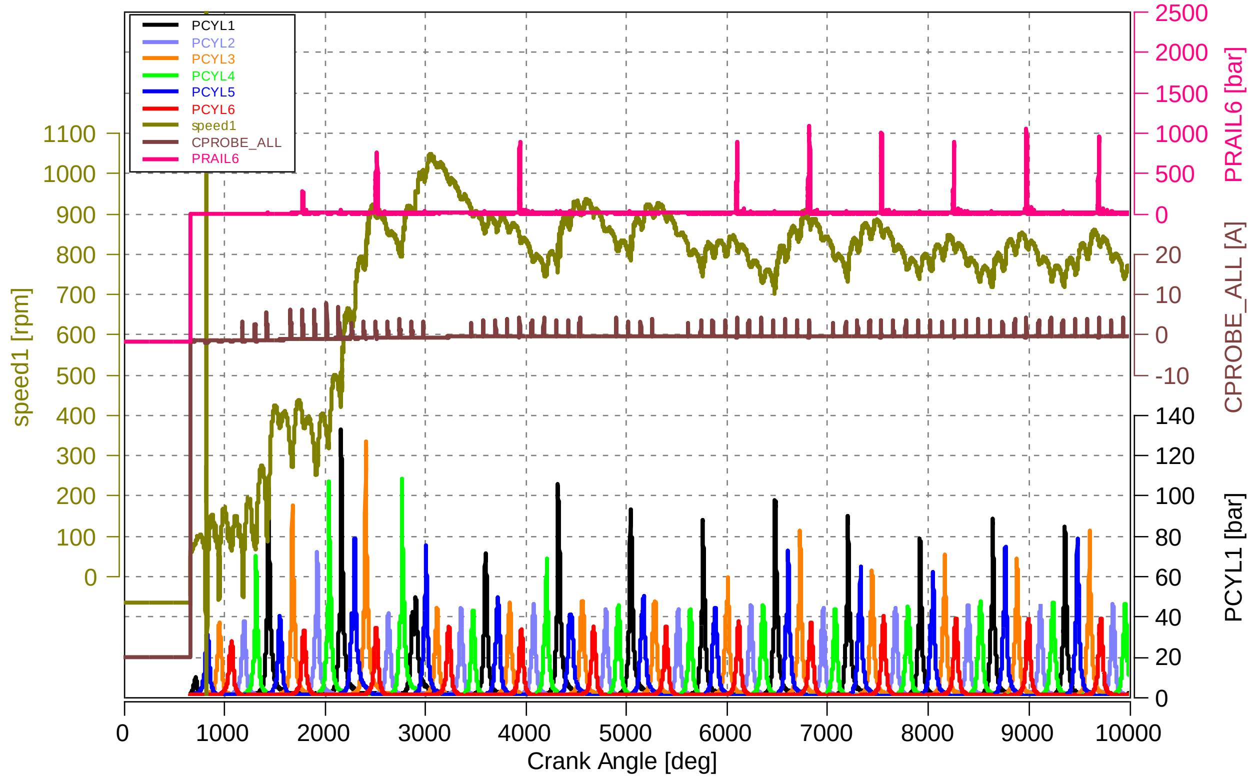

Figure 4.14 – Cold starting of ULSD at 35F

Figure 4.14 represents the engine speed trace along with the cylinder pressure recorded at an ambient temperature of 35F. First injection started after three TDCs which was then followed by increased fuel injection quantities which accelerated the engine to the idling speed. After reaching the idling speed engine speed did not fully stabilize as in ULSD 77F experiment. This fuel injection and cylinder pressure oscillation continued for longer number of cycles until the engine was completely stabilized.

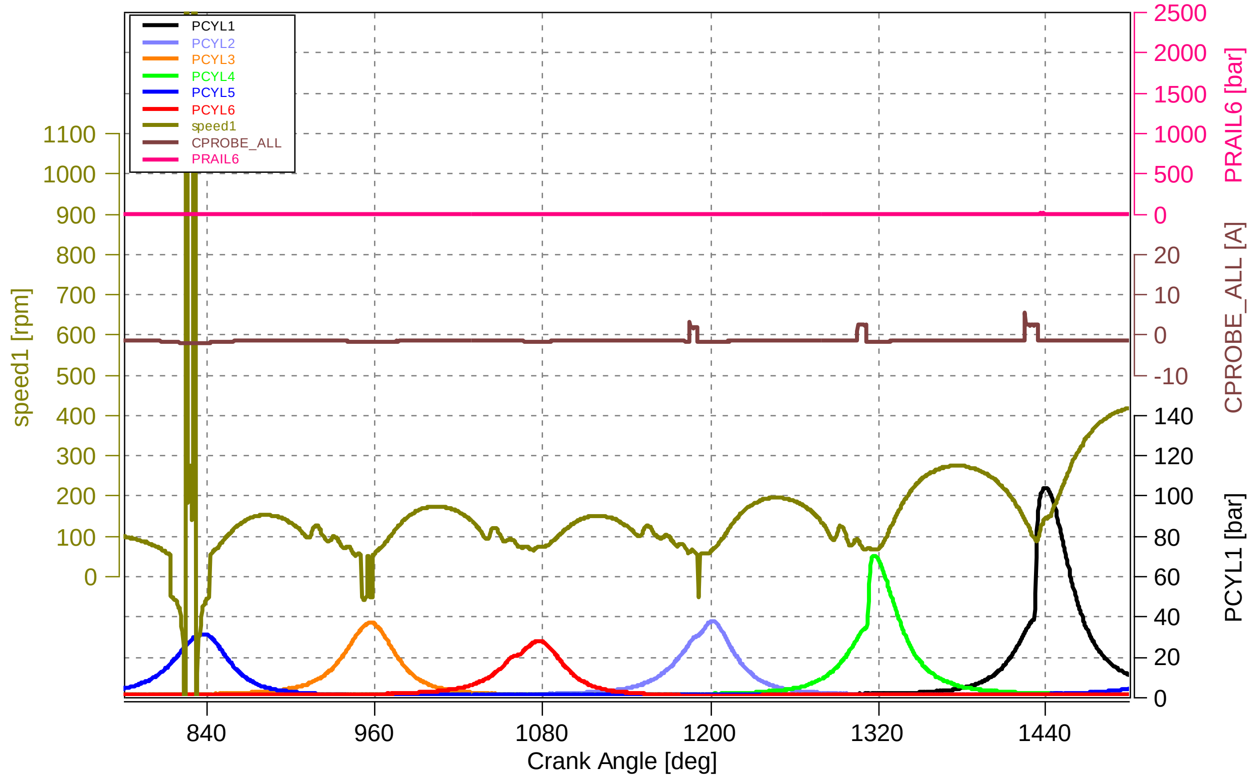

Figure 4.15 - Cold starting of ULSD at 35F-1st cycle

As the temperature was further lowered than 40F, the average engine cranking speed was reduced to 123 rpm as a result of the increased frictional as well as reduced battery discharge capacity which resulted in less compression pressures. First injection started in cylinder 2 after three TDCs in the first cycle. The injection timing was kept constant and the injection duration was increased gradually as a part of standard ECU injection strategy inorder to allow more fueling to accelerate the engine upto the idling speed which resulted in gradually increasing peak cylinder pressures for the last three cylinders. Engine speed increased from cranking speed of 123 rpm to 410 rpm at the end of the first cycle.

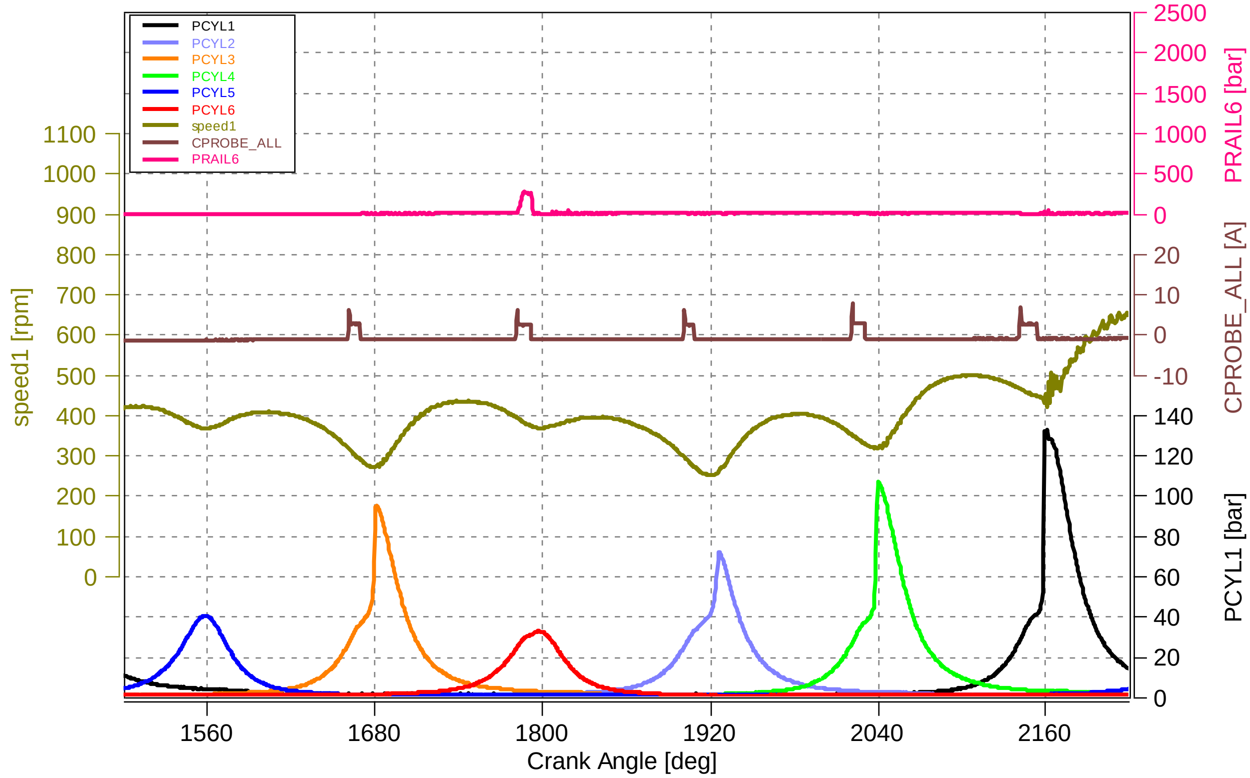

Figure 4.16 - Cold starting of ULSD at 35F-2nd cycle

Figure 4.16 represents the engine speed as well as pressure traces for the second cycle of ULSD at 35F. As observed in the figure 4.16 the first injection was cutoff even before reaching the idling speed in this experiment which was not desirable in the cold start perspective since we need as continuous fueling is needed to accelerate the engine to the idling speed. It was unclear as of this moment whether it was because of the ECU calibration error or because of the inadequate instrumentation. Pressure in the rail barely crossed the pressure of 260 bar for cylinder 6, which was the nozzle opening pressure of the injector, hence a very low amount of fuel might be injected in this cycle, which explains the slight increase in pressure of cylinder 6. Engine speed in this cycle started at 410 rpm and ended at 650 rpm.

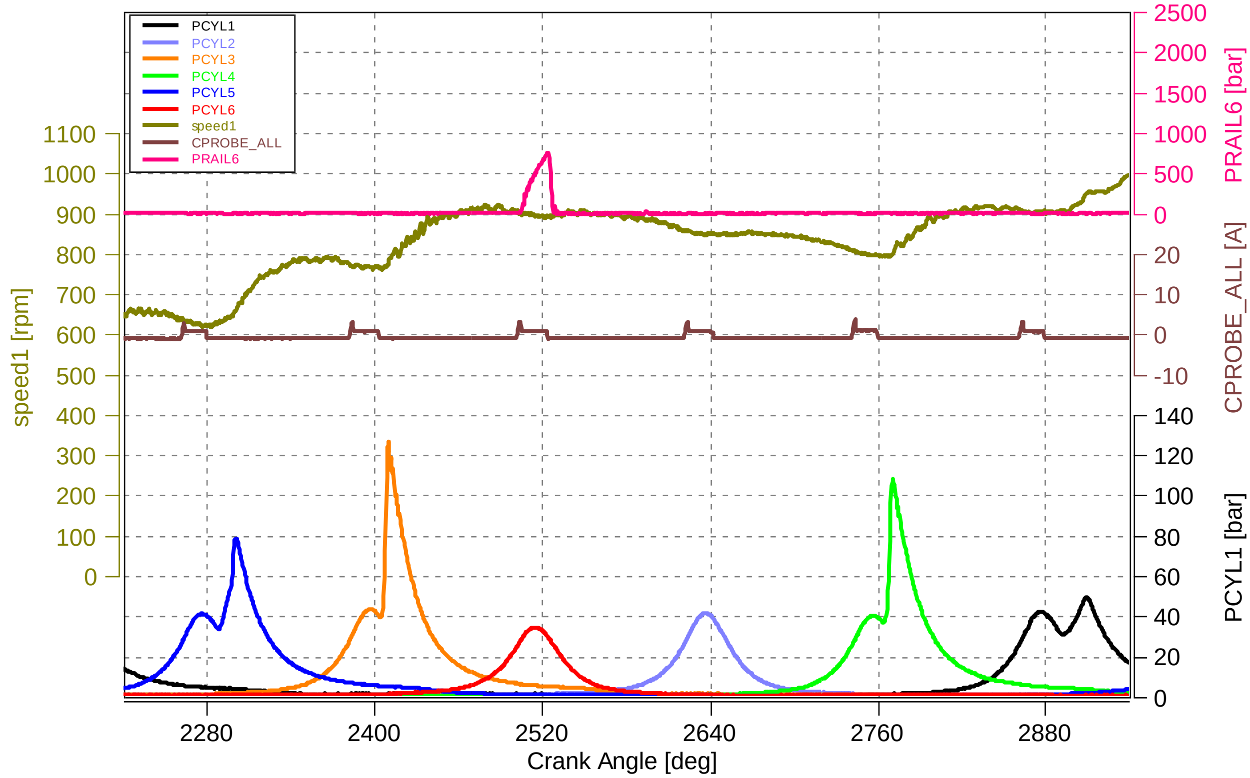

Figure 4.17 - Cold starting of ULSD at 35F-3rd cycle

Figure 4.17 represents the engine speed as well as pressure traces for the third cycle of ULSD at 35F. Engine reached the idling speed in this cycle. Instantaneous engine speed started at 650 rpm and ended up overshooting to 1000 rpm at the end of the cycle. The rapid rise in cylinder pressure from cylinder 5 to cylinder 3 resulted in engine speed increase over the idling speed. The reason for misfire of cylinders 6 and 3 resulted could be because of the constant injection timings without advancing the timing with increase in engine speed.

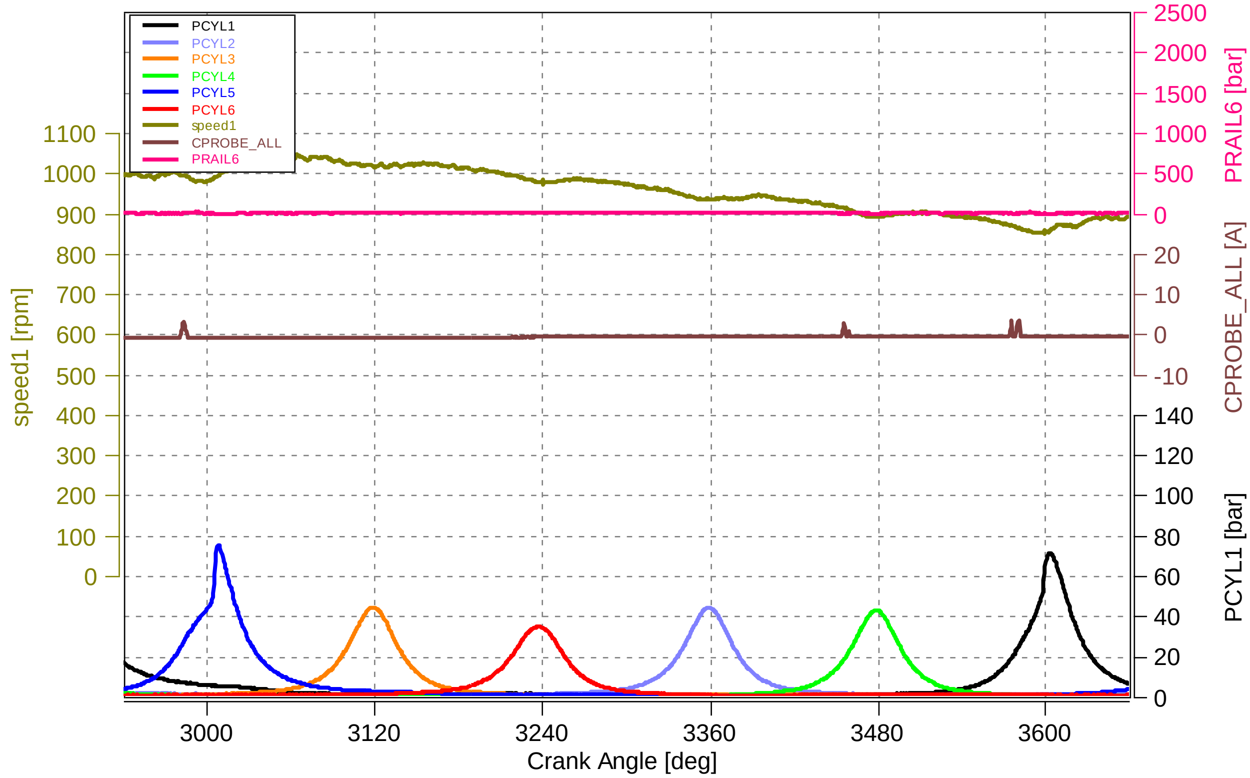

Figure 4.18 - Cold starting of ULSD at 35F-4th cycle

Figure 4.18 represents the engine speed as well as pressure traces for the fourth cycle of ULSD at 35F. As observed in the figure, fuel injection was cut off completely for three cylinders after the cylinder 5 since the engine speed was above the idling speed and to control the engine at constant idling speed. ECU tried to shift the injection strategy from single to double injection (main + pilot), but the engine speed couldn't be maintained at the constant idling speed after the double injection hence the ECU switched back to the single injection strategy in the following cycles. The speed oscillation and the fuel injection switch between single and dual injection continued for 83 cycles.

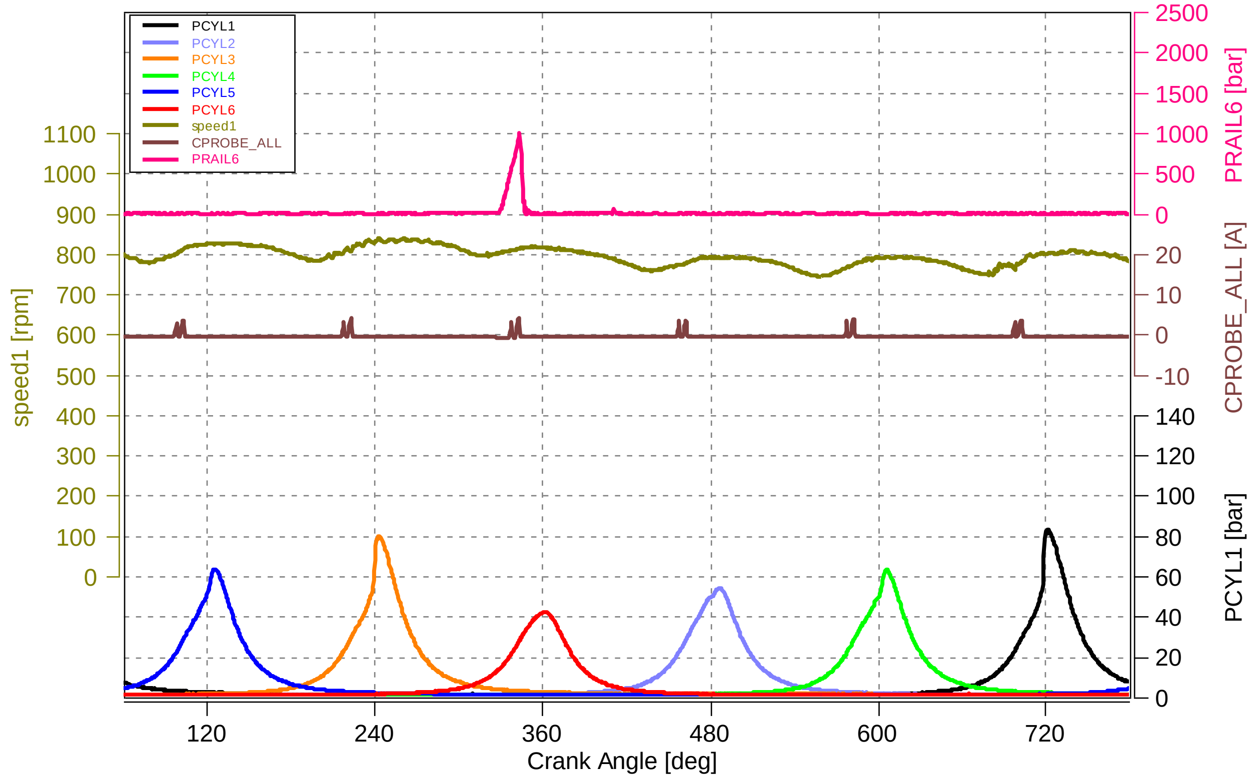

Figure 4.19 - Effect of Ambient Temperature on Cylinder Pressure-84th Cycle ULSD 35F

At 84th cycle the engine speed fully stabilized at idle ECU fully switched to dual (pilot + main) injection strategy in order to main the idling speed. Engine ECU switched to dual fuel injection (main + pilot) strategy since the engine speed was stable around the idling speed of 800 rpm.

4.3.1 Conclusions – ULSD 35F

- Engine successfully started at the ambient temperature of 35F.
- Average engine cranking speed was reduced to 123 rpm because of the decreased current flow from the battery as well as because of the increased blowby and heat losses along with increased frictional losses.
- Fuel injection was cutoff for the fourth injection following the first three fuel injections. The exact reason couldn't be identified.
- Engine speed oscillated for 83 cycles before stabilizing to the constant idling speed (800 rpm) and at 84^{th} cycle switched form single injection to pilot + main injection.

4.4 Cold Start – ULSD 25 F

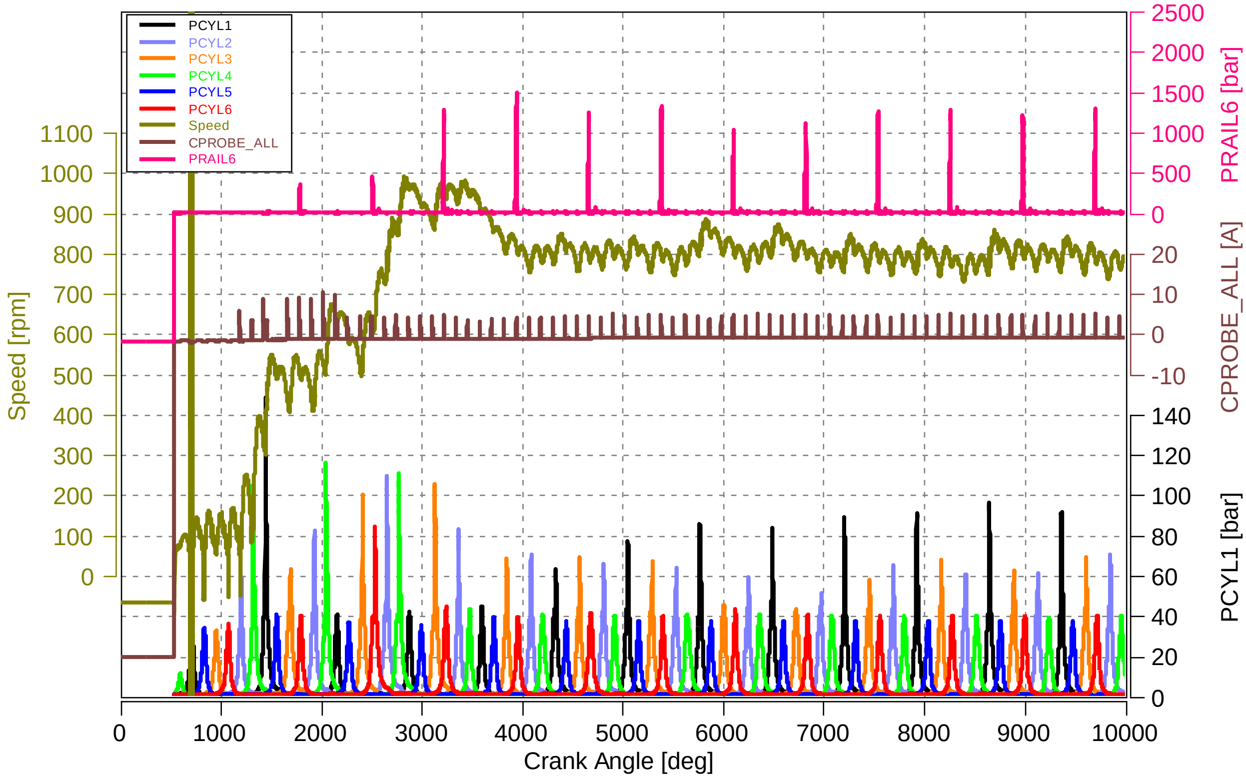

Figure 4.20 – Cold starting of ULSD at 25F- ULSD 25F

As expected the engine took longer time to reach the idling speed when compared with the previous cases. Initial fuel injection started after 4 TDCs which was followed by rapid increase in fuel injection pulse with which resulted in increased fuel injection quantities hence higher peak cylinder pressures which accelerated the engine speed upto 500 rpm. The engine speed was held at an average of 500 rpm for a cycle which was then followed by rapid fuel injection increase which resulted in crossing the idling speed. Unlike previous cases fuel injection cutoff inorder to maintain idling speed occurred only for a few cycles, Fuel injection signal was sent by the ECU for the majority of cycles. One important observation is increased fuel rail pressures as high as

1200 bar or more was observed during this experiment, which is higher than the earlier cases using the ULSD fuel. Engine speed oscillations were little less when compared with the ULSD 35F case. One reason could be because of the increased injection pressures, which resulted in improved atomization of the fuel which resulted in better mixing of air and fuel, thus a much stable combustion.

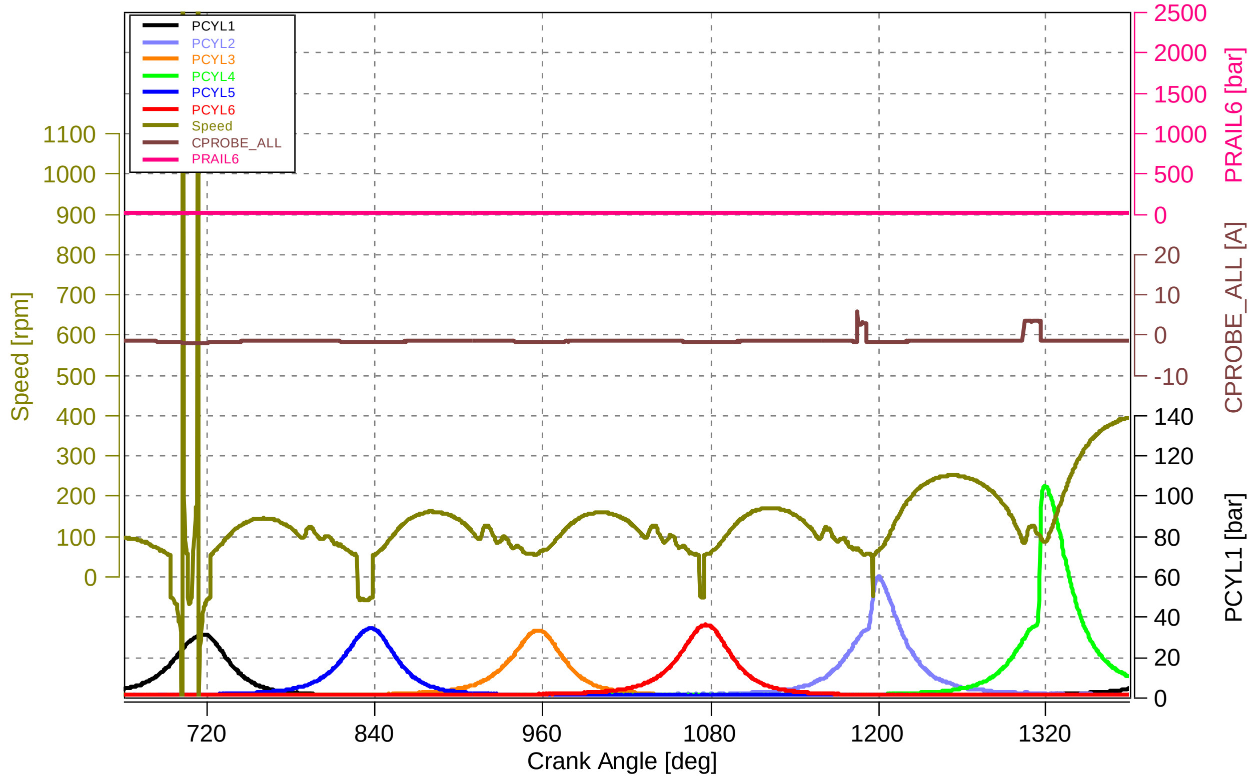

Figure 4.21 - Cold starting of ULSD at 25F-1st cycle

Figure 4.21 represents the engine speed as well as pressure traces for the first cycle of ULSD at 25F. Initially the engine was cranked at an average cranking speed of 112 rpm which was followed by the first fuel injection in cylinder 5. The first and second injections in cylinders 2 and 4 resulted in rapid pressure rise which resulted in increasing the engine speed from the cranking speed to 400 rpm at the end of the cycle. The peak cylinder pressures were 60 bar and 104 bar for the cylinders 2 and 4 respectively.

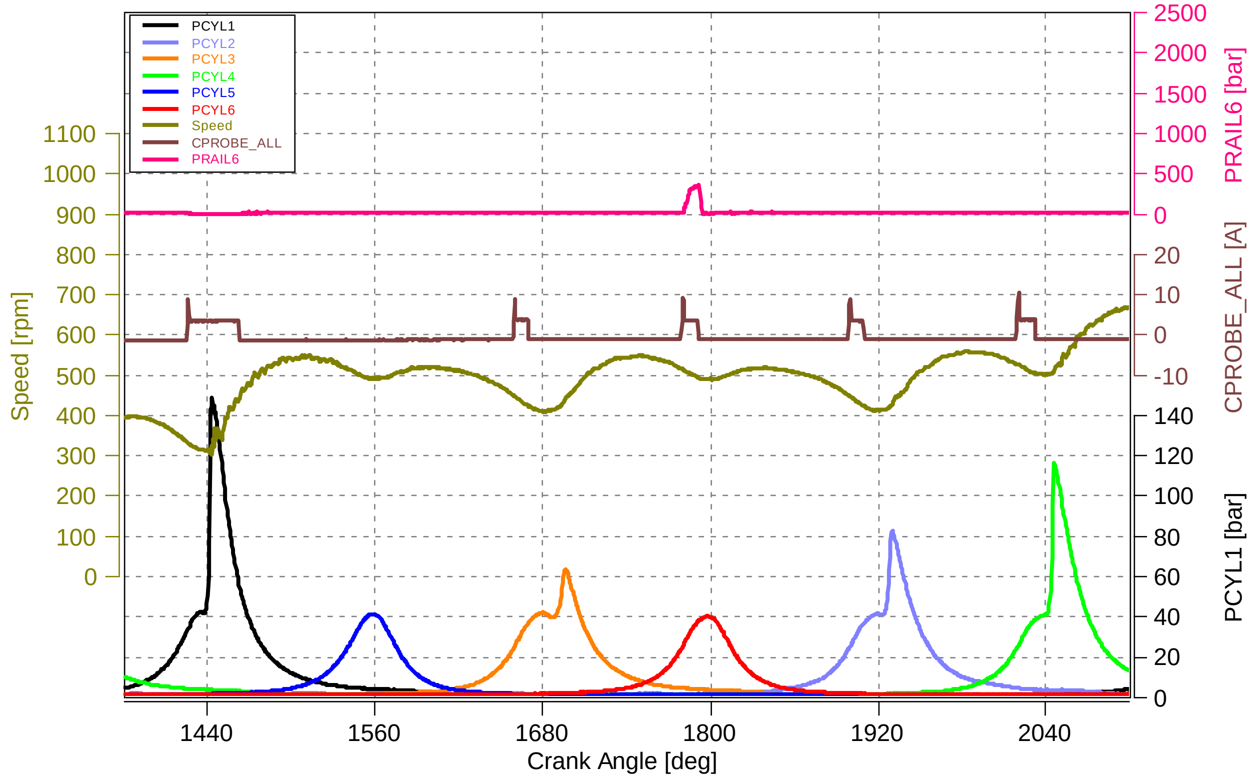

Figure 4.22 - Cold starting of ULSD at 25F-2nd cycle

Figure 4.22 represents the engine speed as well as pressure traces for the second cycle of ULSD at 25F. First injection resulted in increased amount of fueling which resulted in a steep pressure rise of more than 140 bar (cylinder1). The following injection (fourth injection) was cut off by the ECU as observed in ULSD 35F experiment for which the reason couldn't be identified without sufficient instrumentation. Even though there was injection signal from the ECU and the pressure in the rail was more than the nozzle opening pressure of 260 bar, Cylinder 6 misfired. The engine speed at the start of the cycle was 400 rpm and at the end of the 2nd cycle it was 680 rpm.

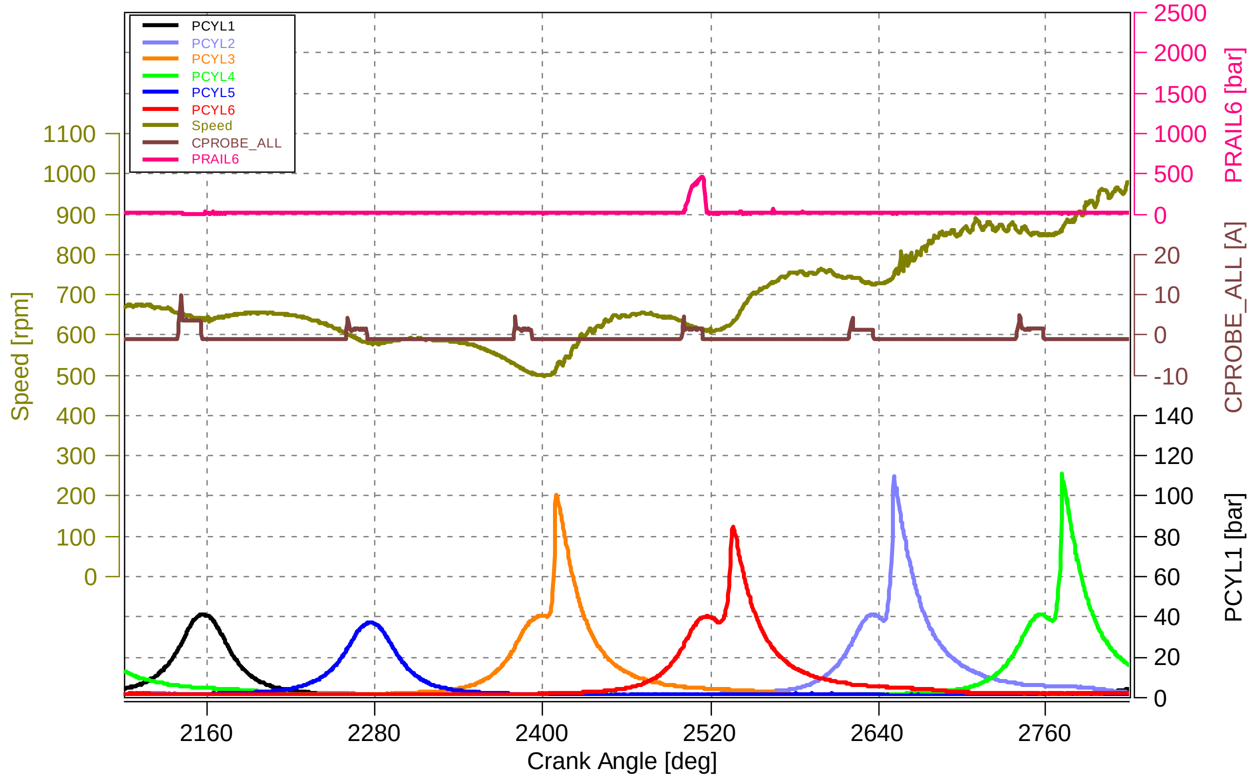

Figure 4.23 - Cold starting of ULSD at 25F-3rd cycle

Figure 4.23 represents the engine speed as well as pressure traces for the third cycle of ULSD at 25F. Even though the cylinders 1 and 5 misfired the engine crossed the idling speed in the third cycle. Successful firings from the cylinders 3, 6, 2 and 4 resulted in increase in engine speed from 660 rpm from the start of the cycle to 990 rpm at the end of the cycle.

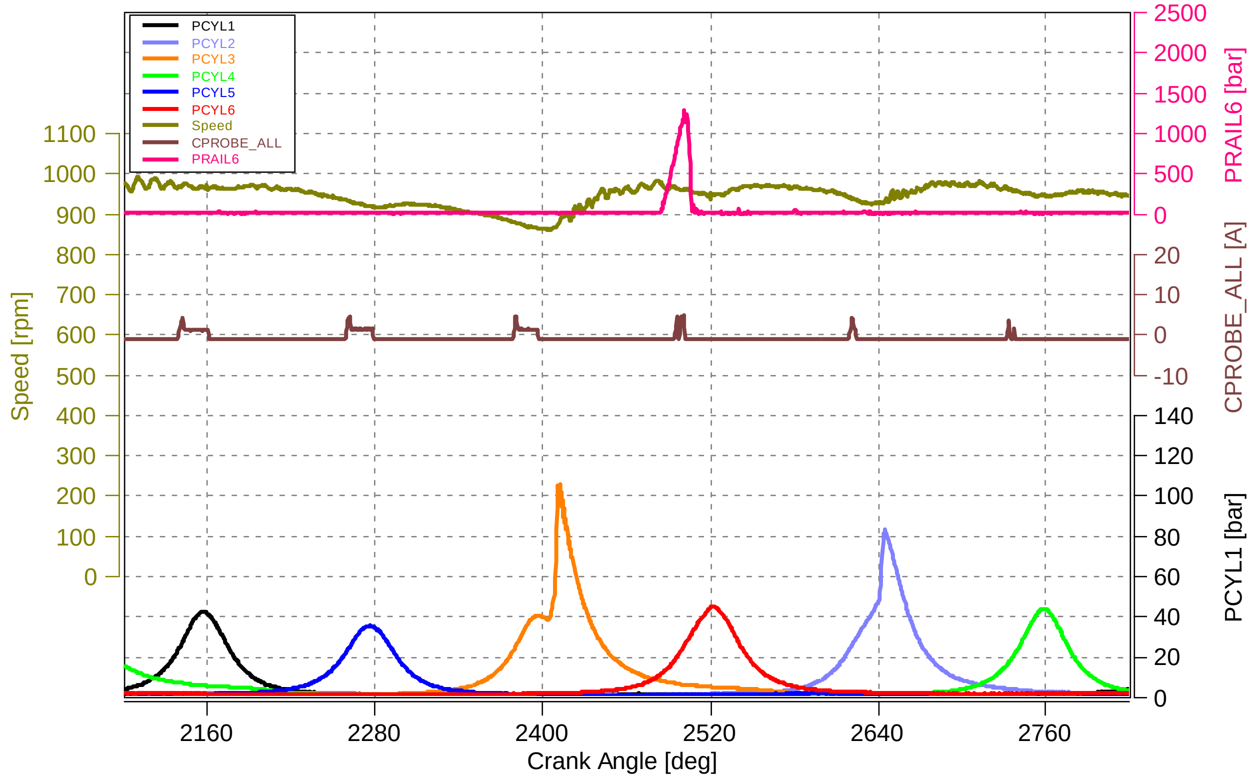

Figure 4.24 - Cold starting of ULSD at 25F-4th cycle

Figure 4.24 represents the engine speed as well as pressure traces for the fourth cycle of ULSD at 25F. It is interesting to note that the cylinders 1 and 5 misfired. In general the injection timing needs to be advanced with increase in engine speed to produce a proper combustion. The engine tried to switch the injection strategy to dual injection, but the engine speed was still over 800 rpm after the combustion of cylinder 3, hence the injection strategy was again switched to single injection for cylinder 2. The pilot + main injection in cylinder 4 at the end resulted in a misfire which was indicated by the occurrence of peak cylinder pressure before the TDC. The engine speed was varied from 965 rpm from the start of the cycle to 945 rpm at the end of the 4th cycle.

Number of misfires after reaching the idling speed was considerably higher in this case which is because of the energy released by the combustion in a lot of cycles was not high enough to overcome the frictional and blowby losses at very low ambient temperatures.

This trend of misfires, combined single and double injection, sudden increase in peak pressures and the speed instability continued until the 175th cycle in the ULSD 25F experiment. At the 175th cycle the injection switched from single main injection to pilot + main injection and the engine speed stabilized at 800 rpm (idle speed).

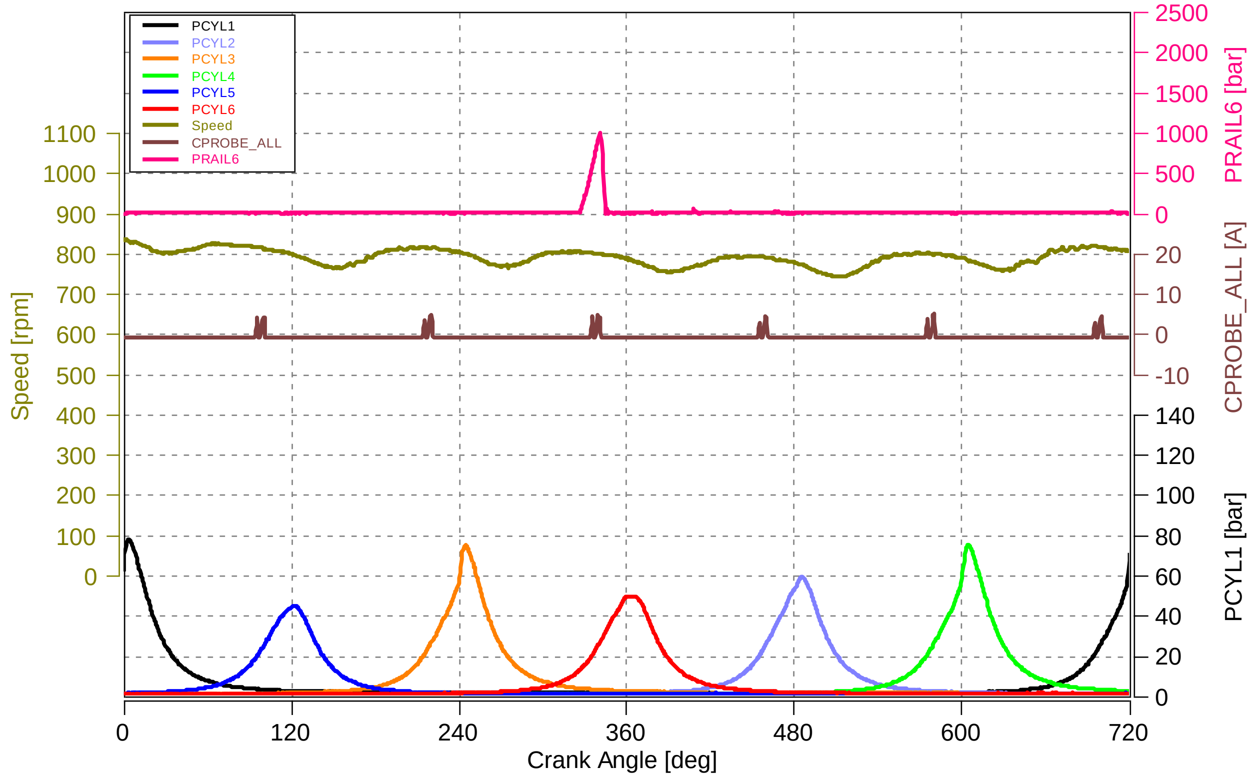

Figure 4.25 - cold starting of ULSD 25F-175th Cycle

Figure 4.25 represents the engine speed as well as pressure traces for the 175th cycle of ULSD at 25F. As illustrated in the figure even though the pressure traces were not the same, the engine speed was much stable around the idling speed of 800 rpm. The injection strategy switched from single main injection to pilot + main injection.

4.4.1 Conclusions – ULSD 25F

- Engine successfully started at the ambient temperature of 25F
- Average engine cranking speed was reduced to 112 rpm because of the decreased battery discharge capacity at very low ambient temperature
- The fuel injection was cut off for only one cylinder during the 2^{nd} cycle in the entire experiment
- Engine reached the idling speed in the third cycle
- Engine took a total of 175 cycles to fully stabilize and switch to multiple injection strategy

4.5 Cold Start – ULSD 20F

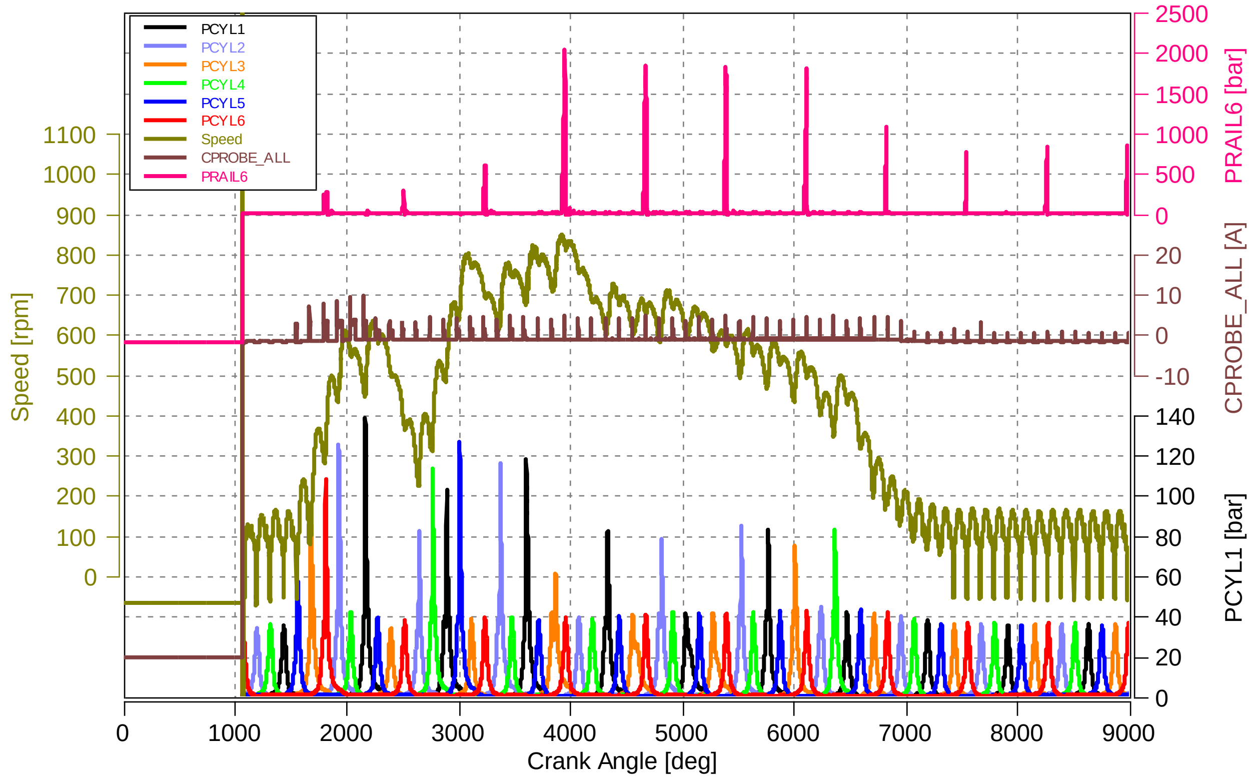

Figure 4.26– Cold starting of ULSD at 20F

Figure 4.26 represents the engine speed trace recorded at 20F using ULSD fuel. As illustrated in the picture initially the engine accelerated upto a speed of 610 rpm which was followed by reduced fueling which reduced the engine speed as low as 200 rpm which was then followed by the engine acceleration upto the idling speed. As evident in the figure, engine misfired a few cycles before as well as after reaching the idling speed. Lower ambient temperature of 20^{o} C resulted in poor oxidation reactions which partially explain the misfires observed in the experiment. In the 10th cycle the engine speed was reduced to cranking speed because of the reduced injection pulse width as a result of inadequate ECU fueling strategy. Higher fuel pressures (close to 2000 bar) were observed in the fuel rail in comparison with the earlier experiments (1000 bar – ULSD 77F)

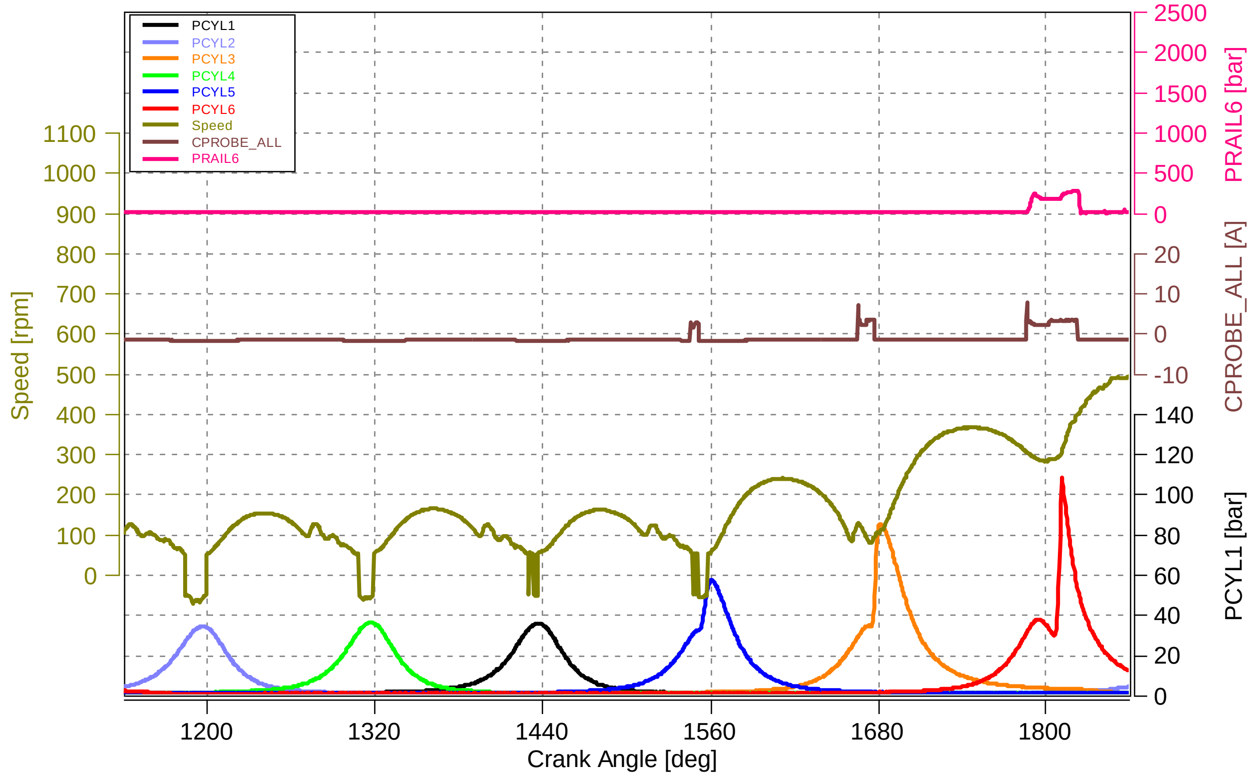

Figure 4.27 - Cold starting of ULSD at 20F-1st cycle

Figure 4.27 illustrates the engine speed trace for the first cycle of ULSD at 20F. First fuel injection started after three TDCs with an average cranking speed of 108 rpm in cylinder 5. Continuous fuel injections in the following cylinders 3 and 6 resulted in engine speed acceleration from the idling speed at the start of the cycle to 500 rpm at the end of the first cycle.

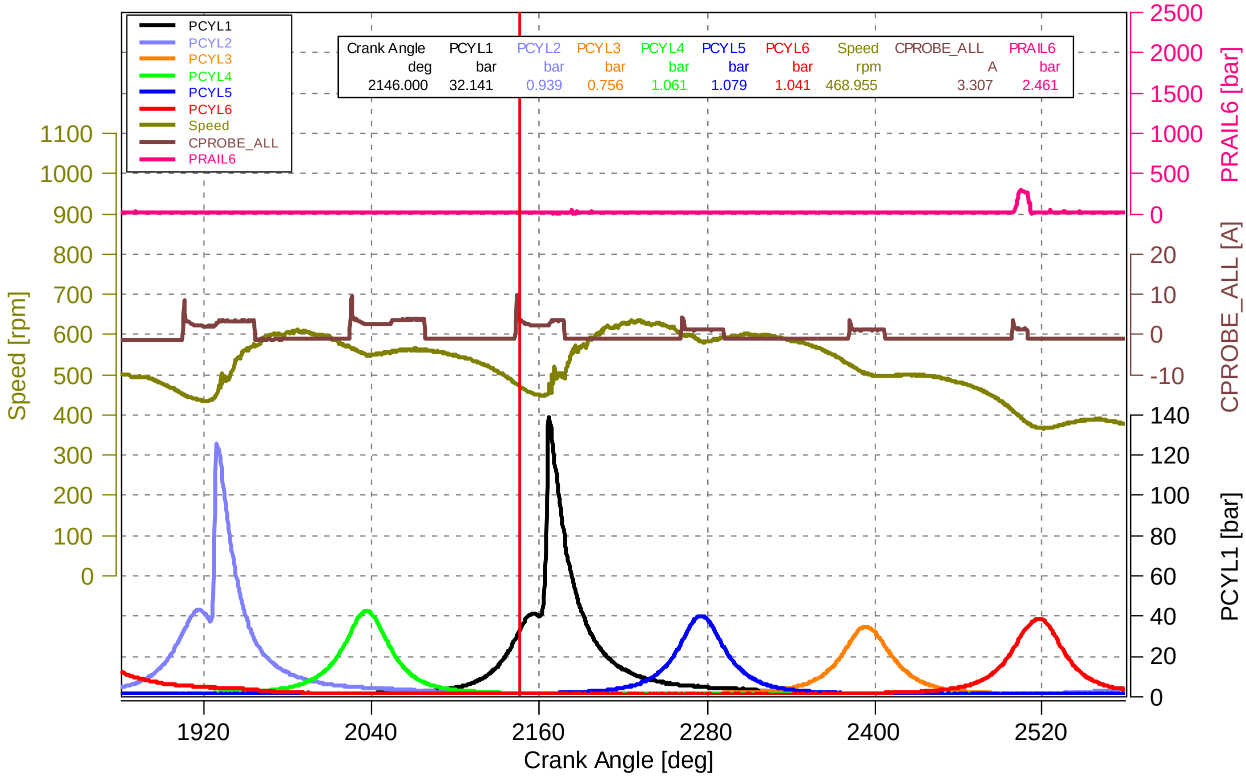

Figure 4.28 - Cold starting of ULSD at 20F-2nd cycle

Figure 4.28 illustrates the engine speed trace for the second cycle of ULSD at 20F. The misfire of cylinders 3, 5 and 6 could be because of the inadequate fuel injection strategy at low temperatures. The engine speed started at 500 rpm at the beginning of the cycle and ended at less than 400 rpm.

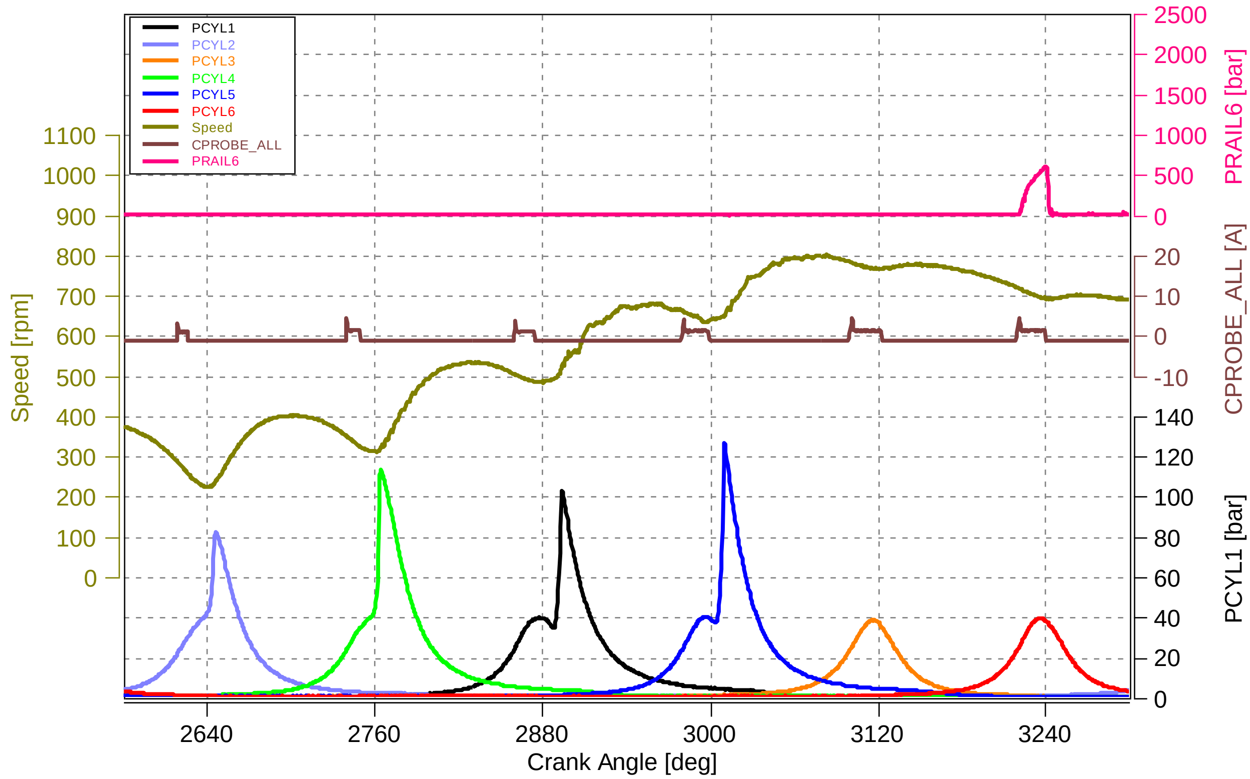

Figure 4.29 - Cold starting of ULSD at 20F-3rd cycle

Figure 4.29 illustrates the engine speed trace for the third cycle of ULSD at 20F. Engine speed at the start of the cycle was less than 400 rpm and at the end of the cycle it was 700 rpm as a result of the four continuous firing cycles. The injection timings of cylinders 1 and 5 are 19 degBTDC, but resulted in different ignition delays. The instantaneous engine speed during the cylinder 5 was higher than the cylinder 1. Constant injection timing with increase in engine speed should result in increased ignition delay, but in this case it appears opposite. Further investigation is required to identify the root cause. This trend of misfiring after firing continued until the 8th cycle at which the fuel injection pulse width was so low which resulted in no combustion as explained in the following section.

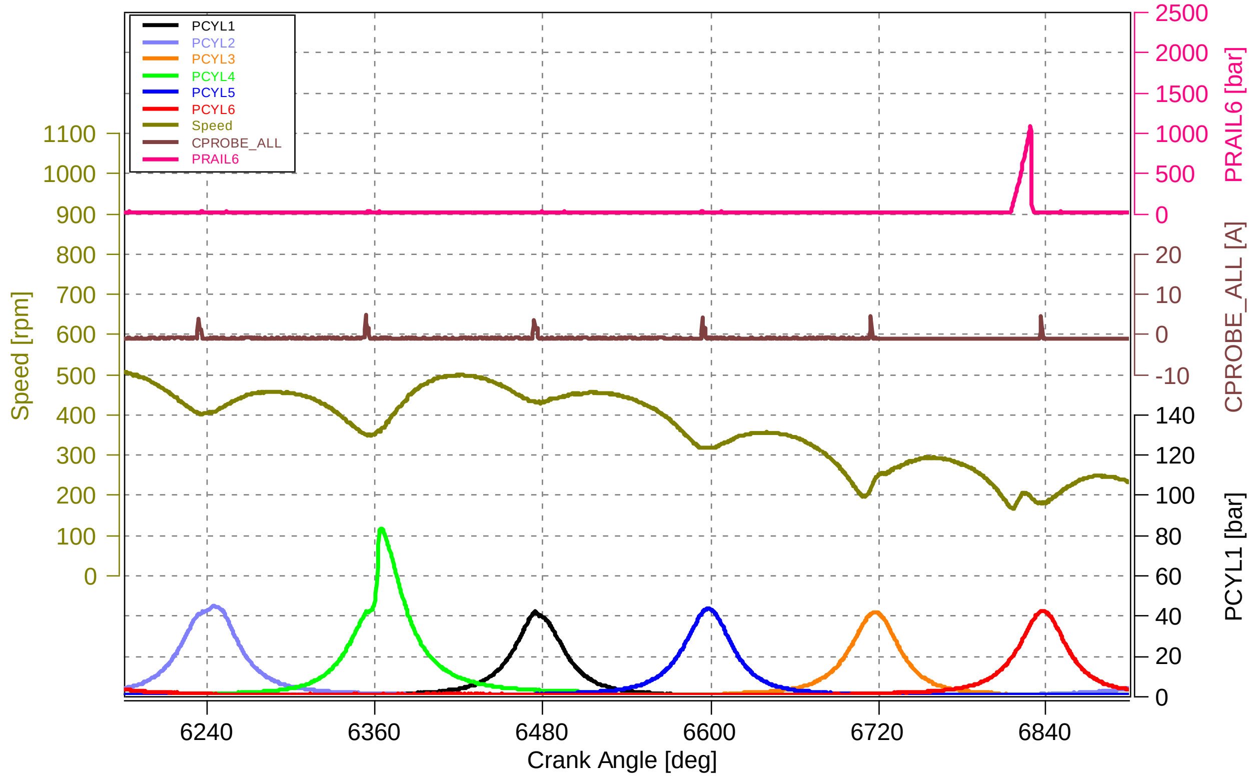

Figure 4.30 - Cold starting of ULSD at 20F-8th cycle

Figure 4.30 illustrates the engine speed trace for the eighth cycle of ULSD at 20F. As illustrated, the engine speed at the start of the cycle was 500 rpm which was then reduced to 200 rpm as a result of the inadequate fuel injection strategy. The negligible fueling pulse width resulted in no fuel being injected into the cylinder which resulted in no combustion. Zoomed in version of the 6th cylinder during the eighth cycle is shown below.

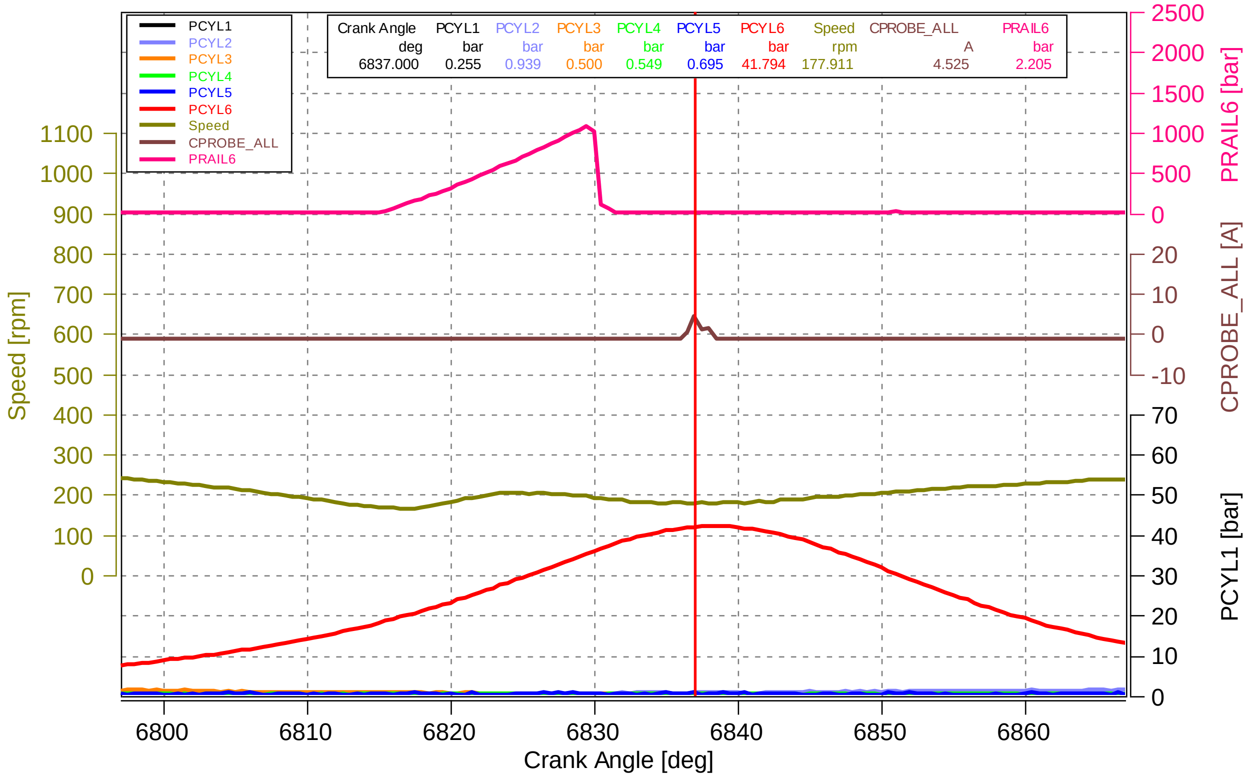

Figure 4.31 - Delayed fuel injection in 6th cylinder - 8th Cycle ULSD 20F

As illustrated in the figure the start of fuel injection signal was sent by the ECU after the pressure in the fuel line was dropped by the spill valve into the fuel return line. This results in no fuel being injected as a result of the absence in fuel pressure in the fuel line. This is determined to be the result of inadequate fueling strategy.

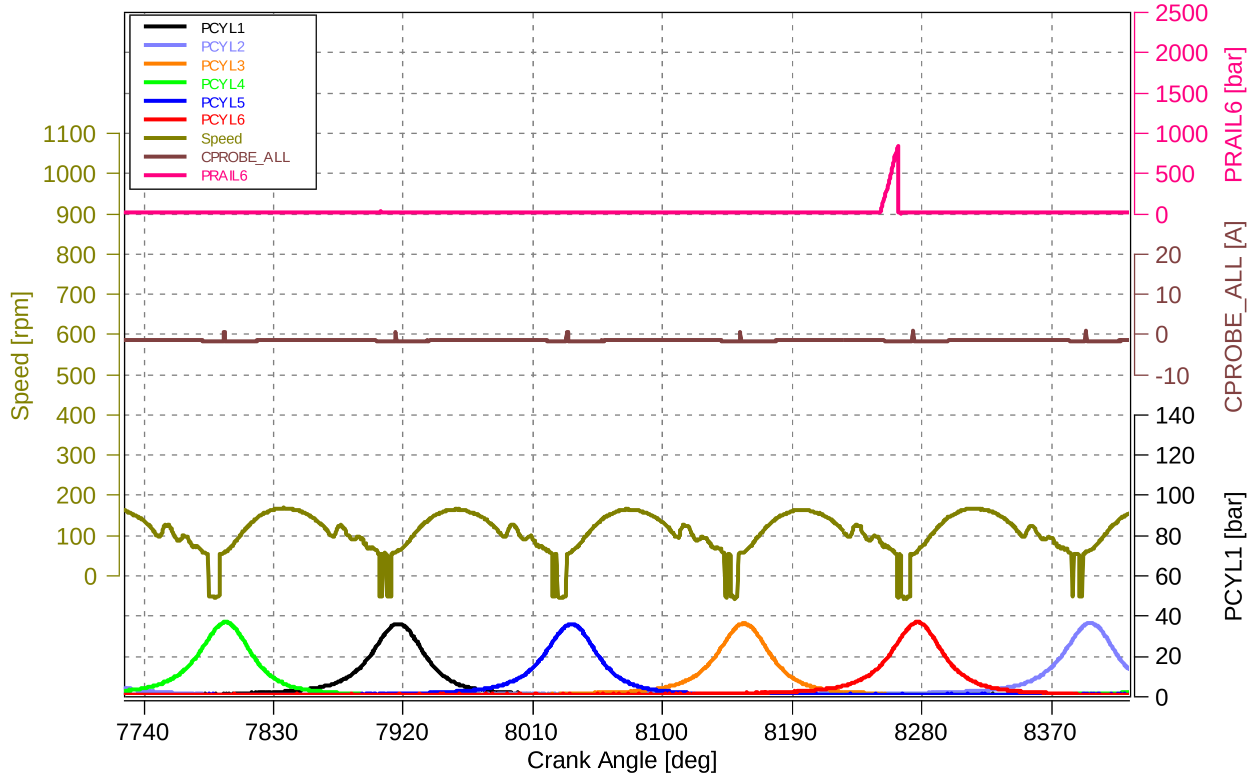

Figure 4.32 - Inadequate Fueling Strategy – ULSD 20F

Following the 8th cycle for the rest of the cycles the same strategy with very minimal fuel injection signal lead to the engine cranking without any combustion as illustrated in the figure 4.32. Since no combustion occurred the engine was stopped after a few cycles.

4.5.1 Conclusions – ULSD 20F

- Engine successfully started at first and failed to maintain the idling speed as a result of the inadequate fueling strategy by the engine ECU at the 20 degrees ambient temperature using ULSD fuel.
- Cranking speed observed was 108 rpm which was lower than the higher ambient temperature experiments as discussed earlier sections
- Starting from the 8th cycle, ECU fuel injection pulses were so low which resulted in the very low/ no fuel being injected into the combustion chamber, which reduced the engine speed to the cranking speed..
- At ambient temperature of 20F the engine reached idling speed, but didn't start due to premature fuel injection cut-off.
- When fuel injection was stopped, the peak compression pressure in the cylinders reached about 42 bar, the same value at which engine started under room temperature. Engine start could occur if enough fuel would have been injected

4.6 Cold Start – ULSD 10F

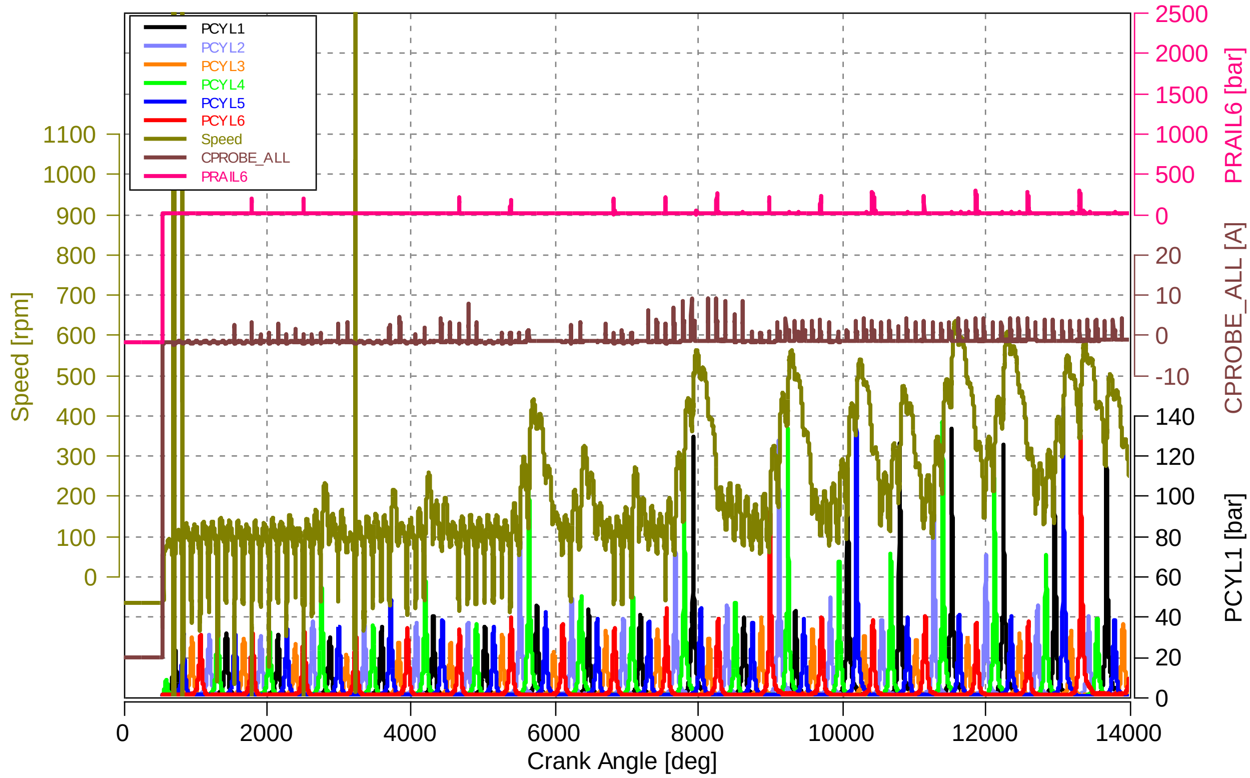

Figure 4.33 – Cold starting of ULSD at 10F

Figure 4.33 represents the engine speed trace recorded at 10F using ULSD fuel. During the engine cranking as illustrated in the figure, engine failed to go through a steady acceleration and instead it followed a misfiring followed by a firing pattern. Even though the engine crossed 19 cycles it failed to reach the idling speed of 800 rpm.

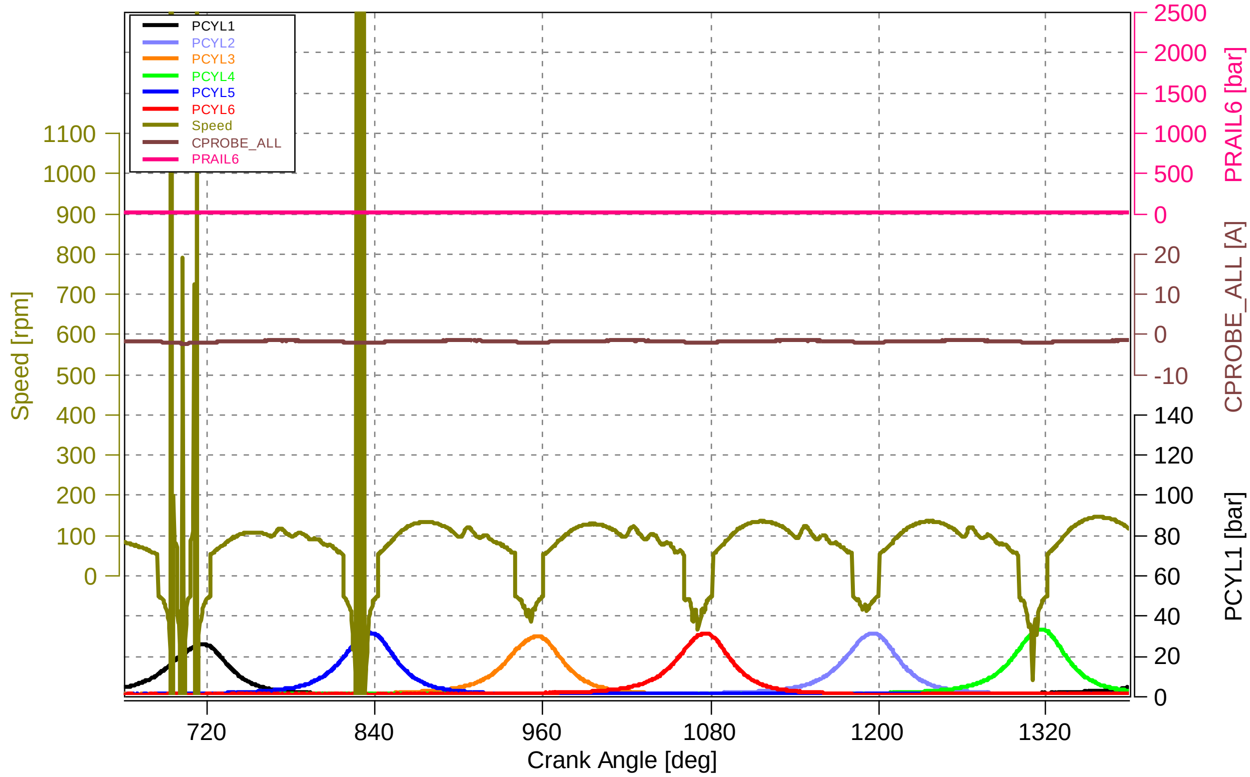

Figure 4.34 - Cold starting of ULSD at 10F-1st cycle

Unlike the previous experiments in which the fuel injections started at the first cycle, the first cycle in ULSD 10F experiment contained no combustion as a result of the absence of the fuel injection which resulted in the engine just motoring at 95 rpm for the first cycle without any increase in engine speed. It is unclear as of this moment whether this is because of the calibration or because of the issues in fueling system. Further investigation into the engine calibration is required to identify the root cause.

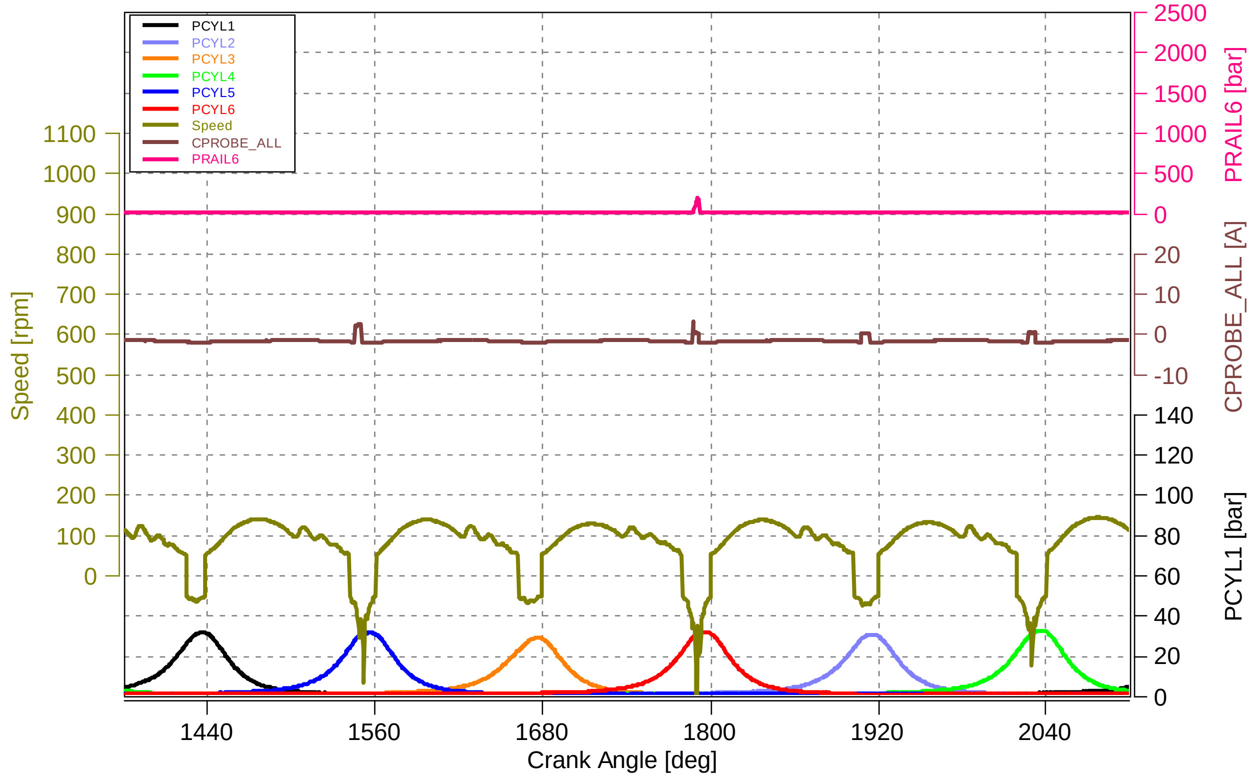

Figure 4.35 - Cold starting of ULSD at 10F-2nd cycle

Figure 4.35 illustrates the engine speed trace for the second cycle of ULSD at 10F. One of the reasons could be the very low pressure in the fuel rail might not be sufficient enough to overcome the spring loaded pressure of 260 bar in the fuel injector and successfully inject fuel for combustion, which might have resulted in no fuel injection. This similar trend in fuel injection continued for six cycles.

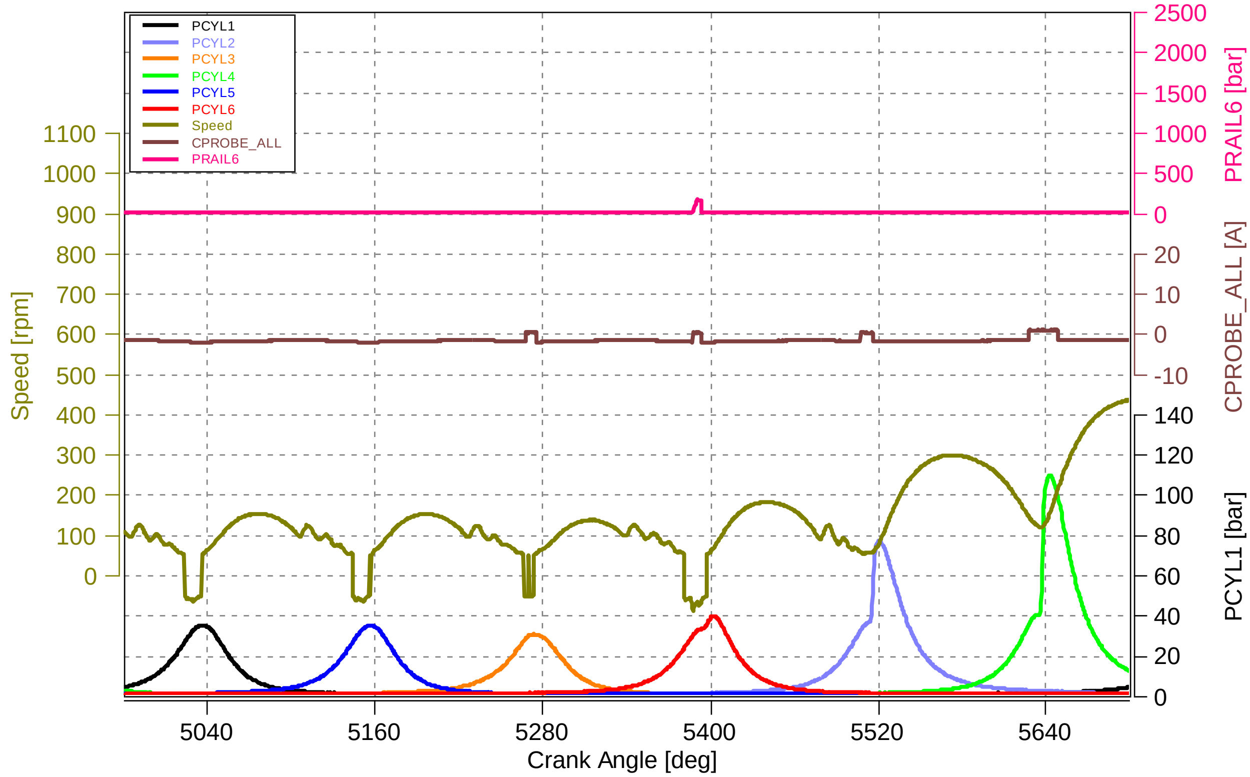

Figure 4.36 - Cold starting of ULSD at 10F-7th cycle

Figure 4.36 illustrates the engine speed trace for the seventh cycle of ULSD at 10F. The engine speed accelerated from the cranking speed at the start of the cycle to more than 400 rpm at the end of the cycle as a result of the continuous combustion in three cylinders 6, 2 and 1. The injection pulse width increases with increase in engine speed starting from the cylinder 6 in order to allow more time for the fuel oxidation reactions. The trend of firing following misfire was continued for fourteen cycles.

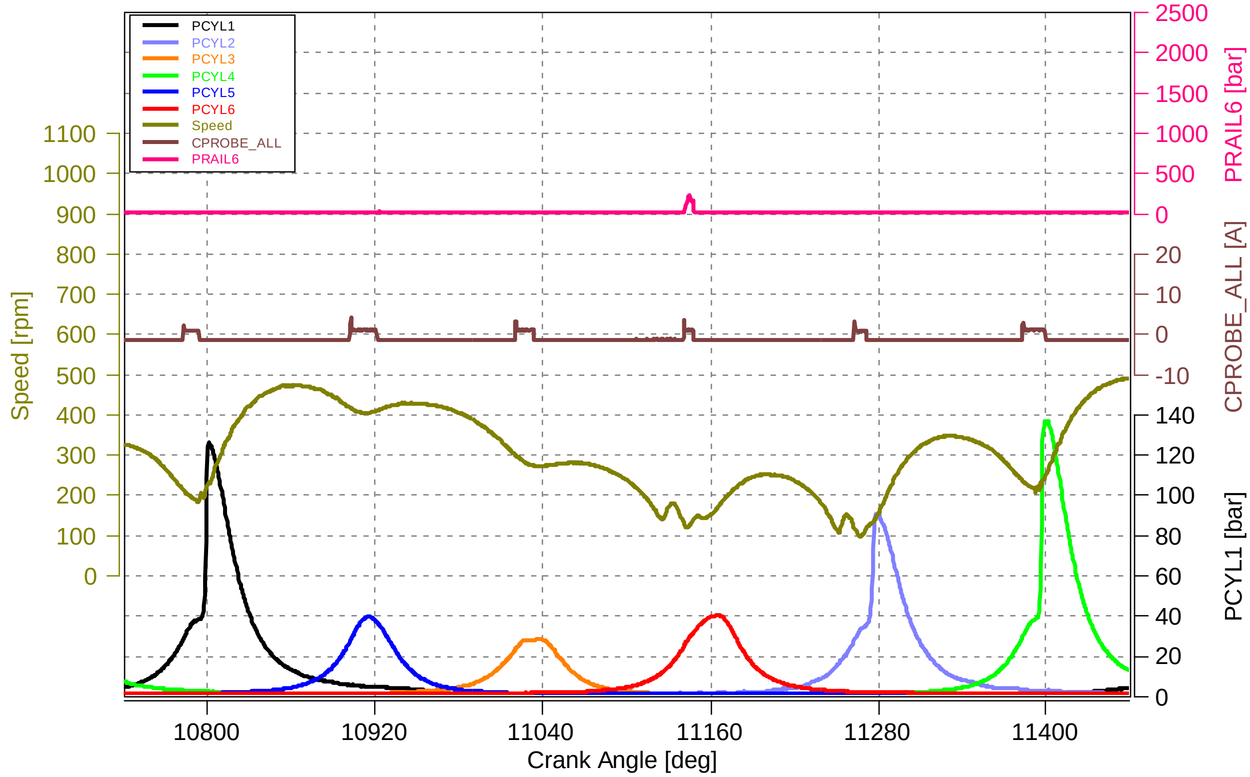

Figure 4.37 - Cold starting of ULSD at 10F-14th cycle

Figure 4.37 illustrates the engine speed trace for the fourteenth cycle of ULSD at 10F. Even after 13 cycles the engine was still following a pattern of firing after misfiring and didn't reach the idling speed. The pressures in the fuel line was still under 400 bar which was a low value and might not be enough to initiate a proper combustion at this low ambient temperature. It was decided to stop the experiment at this stage because of the continuous charge drain from the battery to the starter motor. It was concluded that the engine was not capable of operating below 10^{o}F without any starting aid.

4.6.1 Conclusions – ULSD 10F

- Engine failed to achieve a prompt start and reach the idling speed even after 14 cycles in ULSD 10F experiment

- Average cranking speed of the engine was 95 rpm at 10^{o}F ULSD experiment
- Pressures in the fuel line were observed to be below 400 rpm throughout the experiment which might not be a perfect choice for cold starting at very low ambient temperatures and should be increased
- ECU fueling strategy for the cold start is inadequate under very low ambient temperatures.
- Cold Start failed at 10^{o}F using ULSD fuel in MBE 926 engine

4.7 Cold Start – JP8 77 F

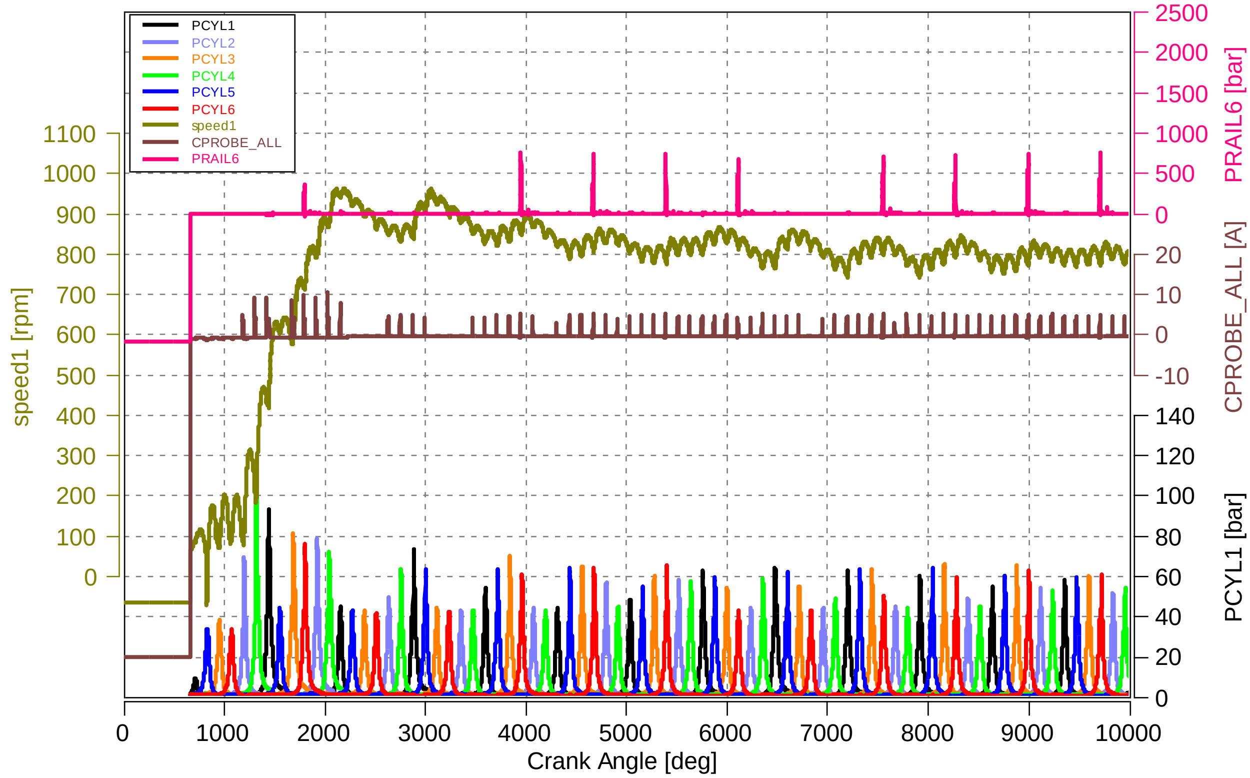

Figure 4.38 – Cold starting of JP8 at 77F

Figure 4.38 represent the first 13 cycles of cold start using the JP8 fuel. Majority of the cycles using JP8 are closely comparable with the ULSD 77F data. Starting form the first fuel injection the fueling was gradually increased by the ECU in order to increase the engine speed from the cranking speed to the idling speed. Continuous fueling resulted in engine speed overshoot till 960 rpm, which less than the 1100 rpm overshoot as is observed in the ULSD fuel. It is interesting to note that after speed overshoot in the ULSD fuel at 77F fueling was totally cutoff, as soon as the fueling resumed, the engine speed was stabilized. But in the JP8 case the engine oscillates around the idling speed. A partial reason for this phenomenon might be the difference in the fuel physical properties as well as the energy density. JP8 fuel has a less energy density on a volumetric basis. The fueling after reaching the idling speed might not be sufficient enough to maintain the engine speed; hence the engine oscillates around the idling speed and maintains the idling speed after 5 cycles. These phenomena could be explained by the engine calibration, since no calibration changes were made to the JP8 fuel run to adjust the combustion characteristic differences between JP8 and ULSD fuels.

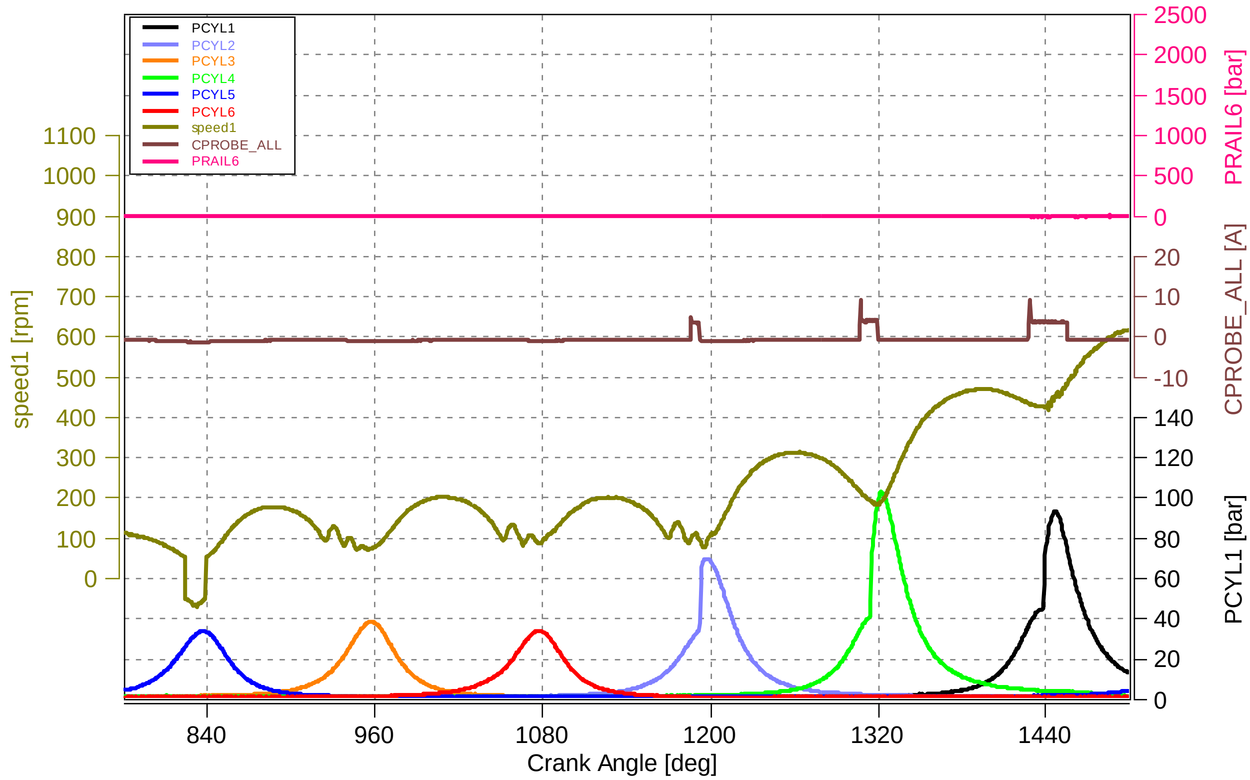

Figure 4.39– Cold starting of JP8 at 77F-1st cycle

The first fuel injection started after 3 cycles as observed with the ULSD fuel at 77F. JP8 fuel tends to develop low injection pressure as a result of low bulk modulus values as compared with ULSD fuel in the first injection. The average cranking speed is 142rpm as observed in the picture which was the same as ULSD 77F experiment. The very first injection in cylinder 2 resulted in successful firing followed by cylinders 4 and 1 and the speed accelerated towards idling speed. The pulse width was doubled as of first injection during the second injection (cylinder 3) and pulse width for the third injection (cylinder 6) is doubled as that of the second injection which is the same as that of the ULSD 77F experiment. ECU calibration was developed by the manufacturer in this way in order to allow more fueling to accelerate the engine up to the idling speed.

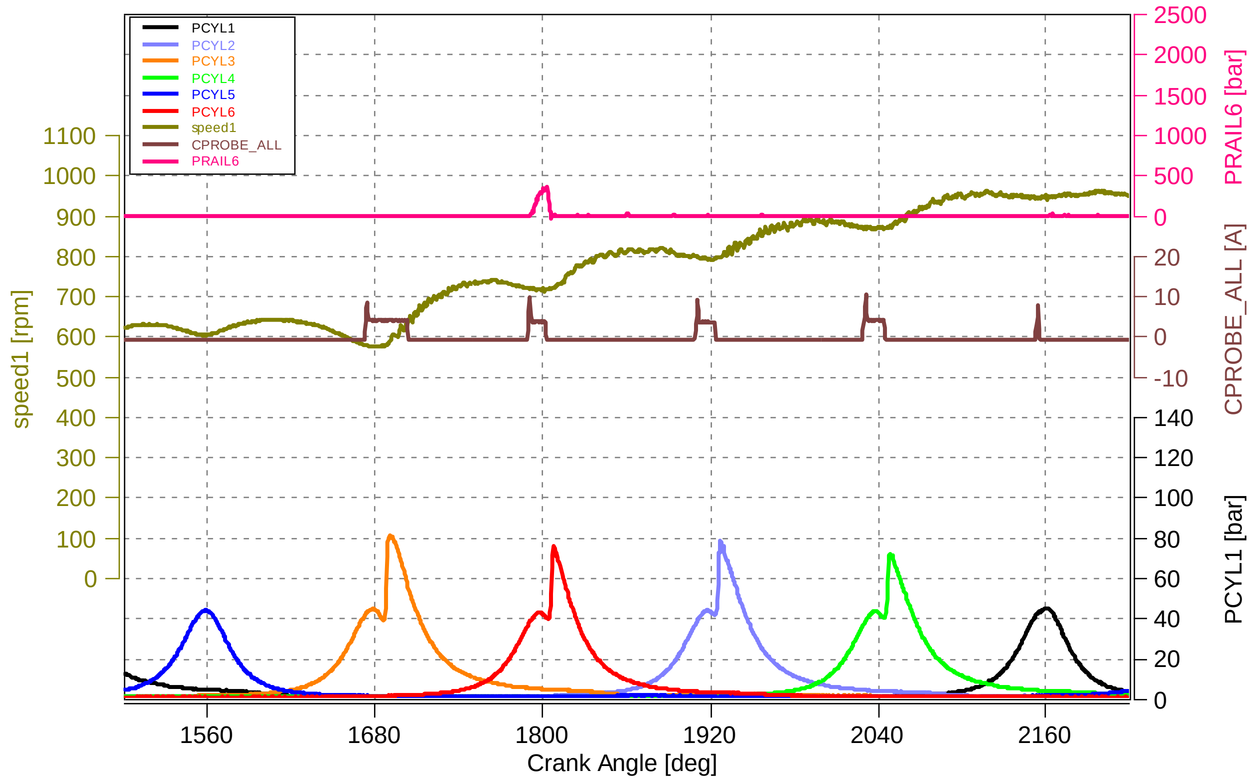

Figure 4.40 – Cold starting of JP8 at 77F-2nd cycle

Figure 4.40 represents the engine speed as well as pressure traces for the second cycle of JP8 at 77F. The third injection was cut off in the 2nd cycle (cylinder 5). Continuous fuel increase in fueling for the following cylinders 3, 6, 2 and 4 resulted in the engine crossing the idling speed. Engine speed overshoot continued till 960 rpm which was followed by reduced fueling in cylinder 1 as evident from the decreased injection pulse signal from the ECU. The very low injection duration as commanded by the ECU resulted in a very small rise in pressure in cylinder. The engine speed increased from 620 rpm from the start of the cycle to 960 rpm by the end of the cycle.

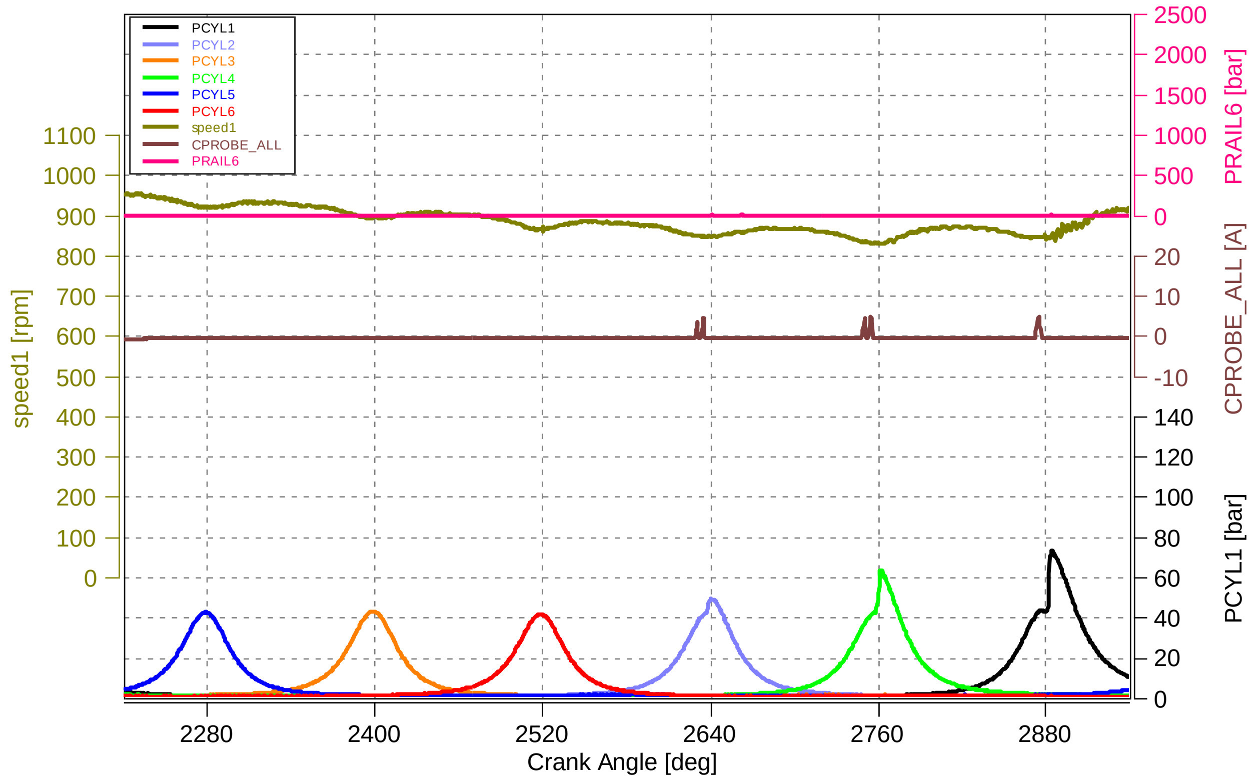

Figure 4.41 – Cold starting of JP8 at 77F-3rd cycle

Figure 4.41 represents the engine speed as well as pressure traces for the third cycle of JP8 at 77F. The three initial injections were cut off by the ECU inorder to control the engine speed at the idling speed. The ECU tried to switch the strategy from single injection to pilot and main injection for two injections (cylinders 2 and 4) because of the speed oscillation it switched to single injection again at the end of the third cycle. Engine speed decreased from 960 rpm at the start of the third cycle to 920 rpm at the end of the cycle. It is interesting to note that as soon as the speed reached 850 rpm fuel injection started in this case, while with ULSD 77F experiment the speed in which fueling restarted was 800 rpm and not 850 rpm. This trend in fueling continued for the first five cycles.

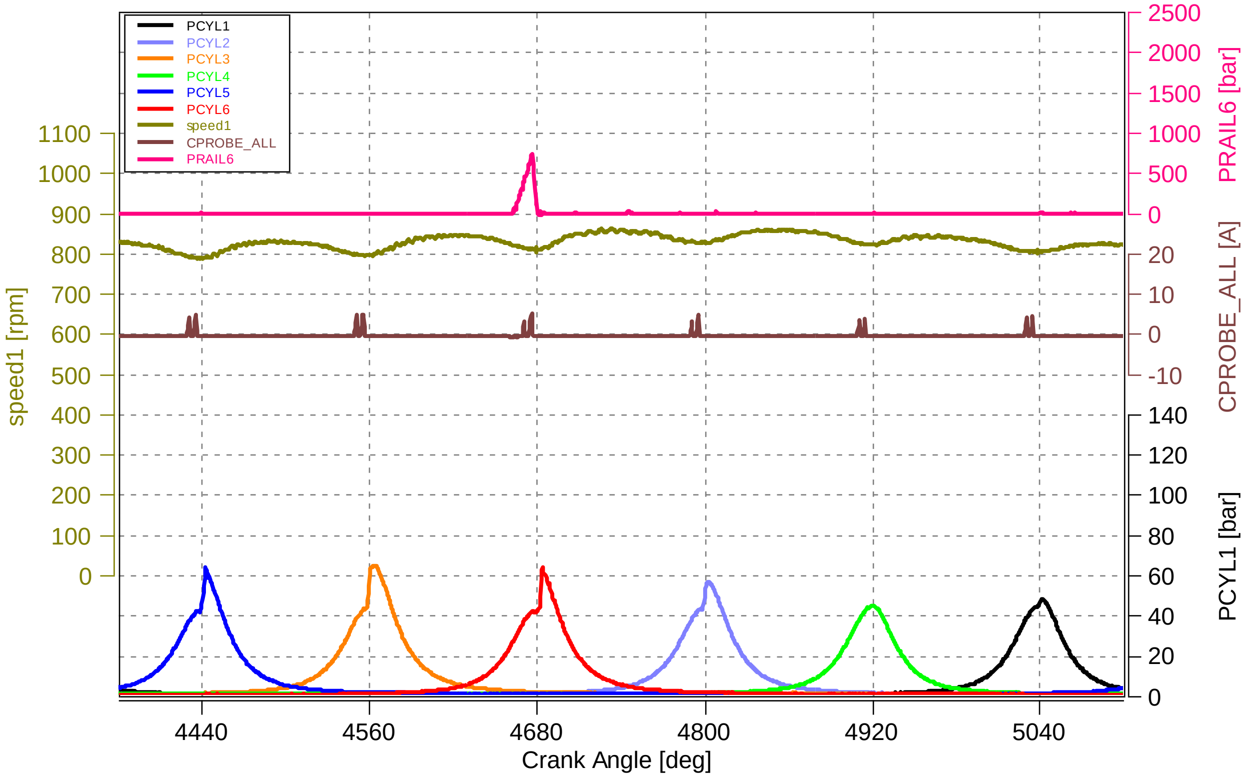

Figure 4.42 – Cold starting of JP8 at 77F-6th cycle

Figure 4.42 represents the engine speed as well as pressure traces for the sixth cycle of JP8 at 77F. After initial 5 cycles, the engine speed finally stabilized at it idling speed and the fuel injection strategy switched to pilot + main injection which continued till the engine was shut off after recording first 400 cycles of data.

4.7.1 Conclusions – JP8 77F

- Engine successfully started at JP8 77F
- Engine idling speed was 142 which was the same as the ULSD 77F experiment
- Engine reached the idling speed in its 2nd cycle without any misfires.
- Engine speed oscillations after reaching the idling speed was higher than the ULSD 77F case which can be attributed to the unchanged calibration between ULSD and JP8 fuels to adjust the variations in physical and chemical properties.
- Engine speed was overshoot till it reached 960 rpm which is a lower value than the ULSD 77F case in which the maximum speed was 1150 rpm
- Engine speed stabilized to the idling speed in its 6th cycle and fueling strategy shifted from single to double injection

4.8 Cold Start – JP8 35 F

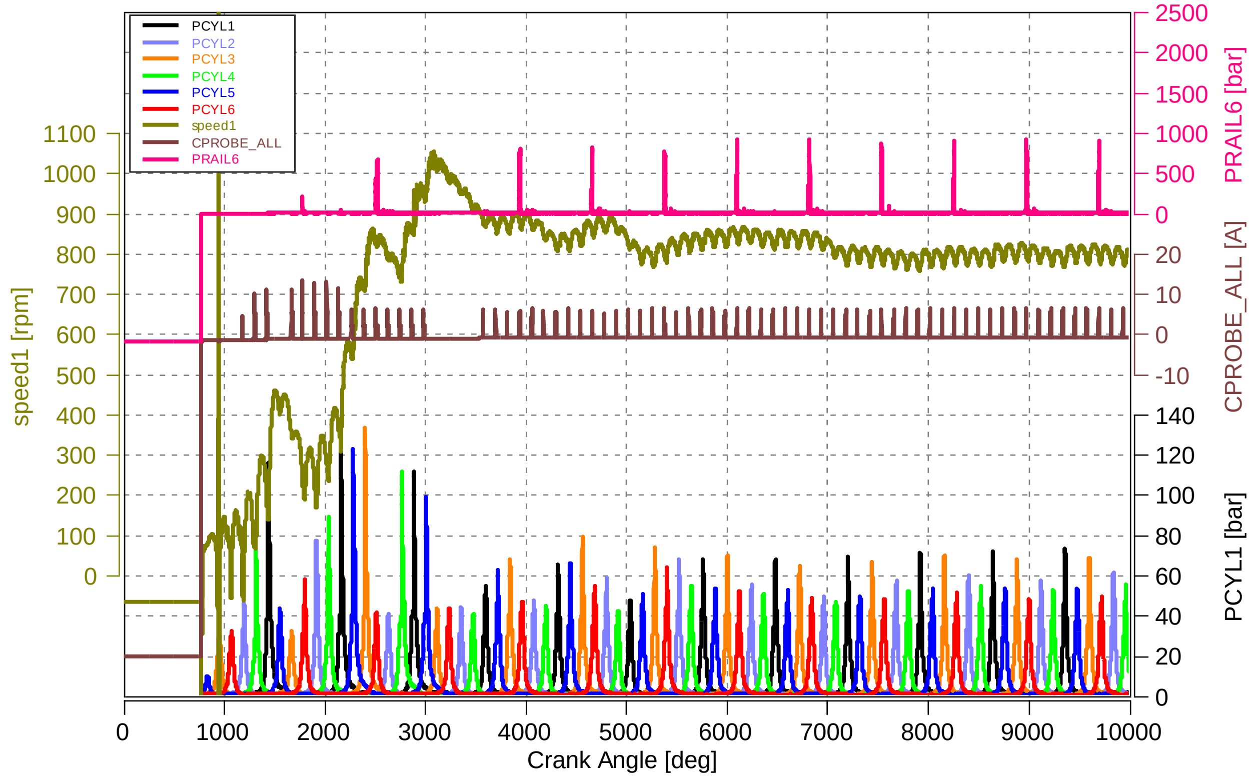

Figure 4.43 – Cold starting of JP8 at 35F

Figure 4.43 represents the cold start data of first 13 cycles using the JP8 fuel at 35F. Following the cranking stage the engine speed was increased followed by a prompt fuel injection cycles which led to the engine speed overshoot until 1050 rpm which was followed by fuel injection cut off by the governor which reduced the speed to 900 rpm which was followed by continuous fuel injections which led to the gradual stabilization of the engine speed at its idling speed.

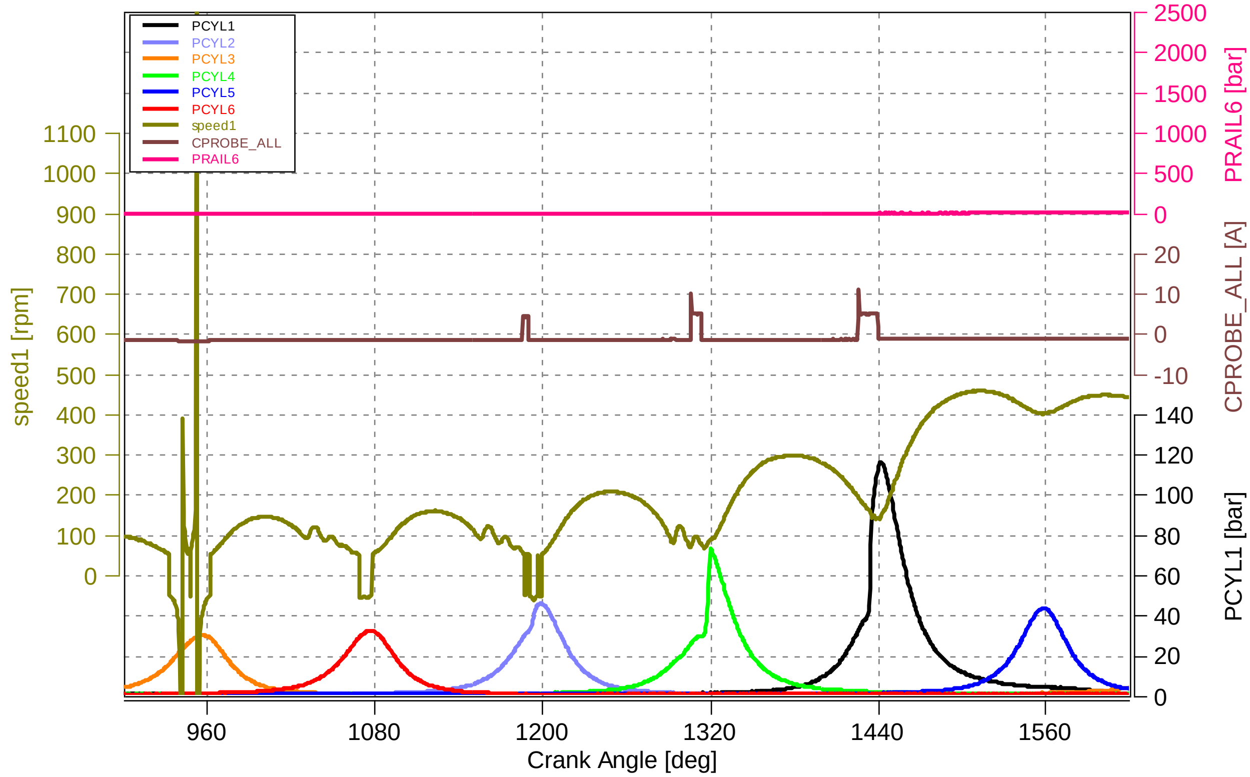

Figure 4.44 – Cold starting of JP8 at 37F-1st cycle

Figure 4.44 represents the engine speed as well as pressure traces for the first cycle of JP8 at 35F. The average engine cranking speed was 123 rpm as observed in ULSD 35F experiment. It is interesting to note that the first fueling starts two TDCs, which were three TDCs for ULSD fuel at the similar temperature. One of the possible explanations for this phenomena might be the less density of the JP8 fuel at lower temperatures as well as low viscosity than the ULSD at lower temperatures. First fuel injection started after two TDCs in cylinder 2, which was followed by gradual increase in fueling which resulted in the engine speed increase from cranking speed to close to 500 rpm. The following fuel injection was cut off for cylinder 5, further fuel injection pressure data is required to find the exact root cause for fuel injection cutoff. In general the fuel injection has to be continued till the engine reaches the idling speed. Engine speed increased from the cranking speed at the start of the cycle to 460 rpm at the end of the first cycle.

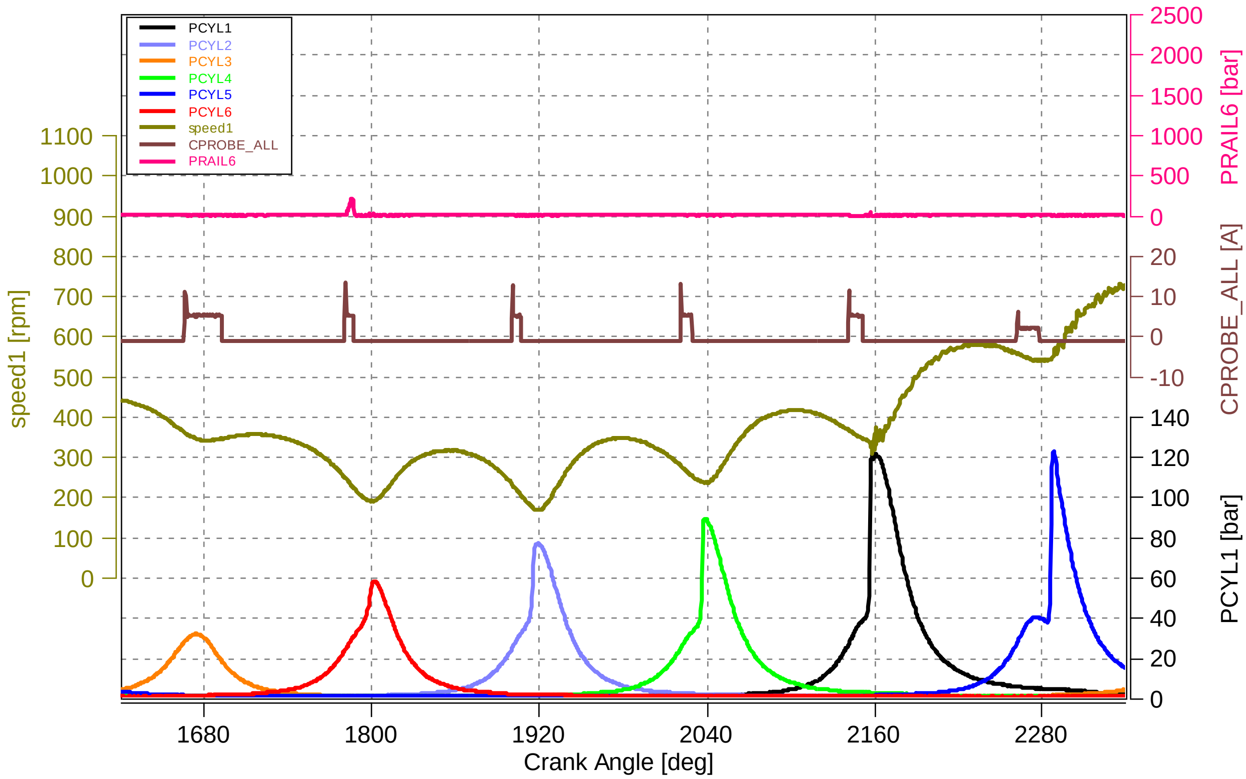

Figure 4.45 – Cold starting of JP8 at 35F-2nd cycle

Figure 4.45 represents the engine speed as well as pressure traces for the second cycle of JP8 at 35F. The first cylinder (cylinder 3) misfired despite a reasonable injection pulse width. The following cylinders 6, 2, 4, 1 and 5 continuously fired which resulted in increasing the engine speed from 450 rpm at the start of the second cycle to 720 rpm by the end of the cycle.

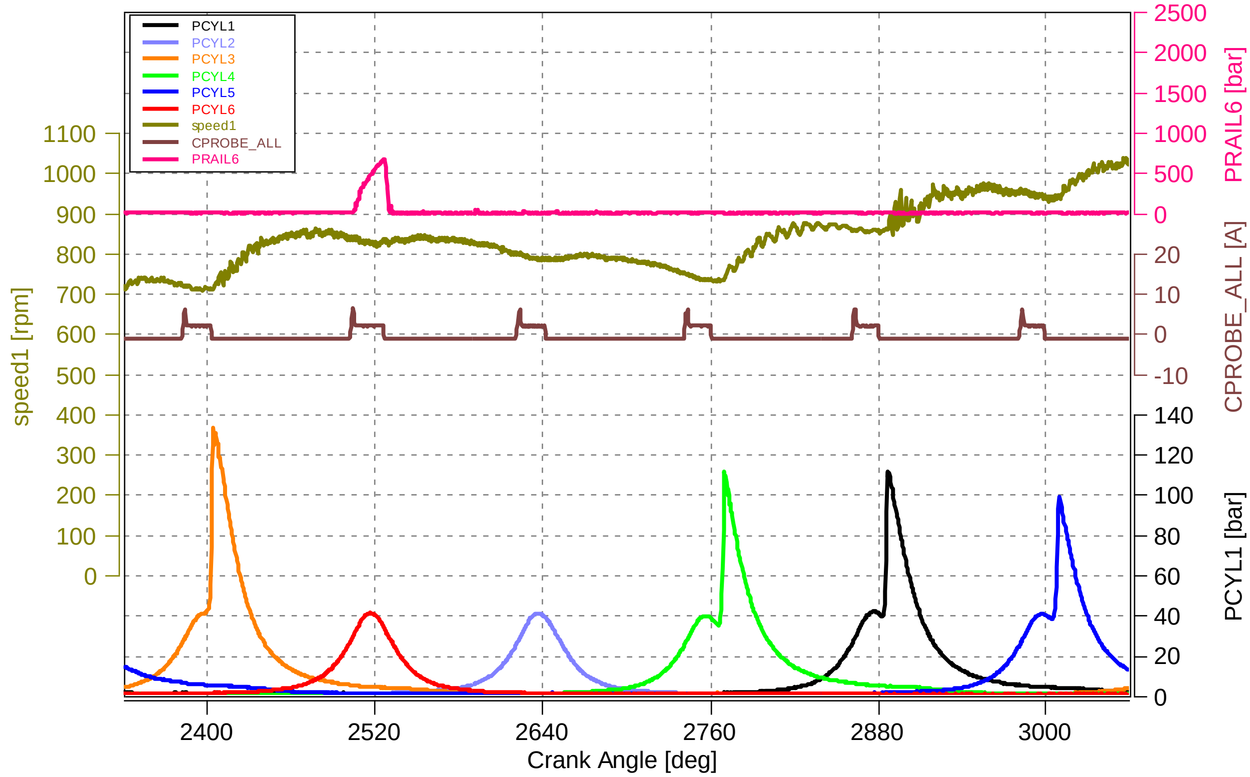

Figure 4.46 – Cold starting of JP8 at 35F-3rd cycle

Figure 4.46 represents the engine speed as well as pressure traces for the third cycle of JP8 at 35F. It is interesting to observe that the cylinders 6 and 2 misfired, despite having a peak fuel rail pressure of over 600 bar as evident from the figure 4.46 In general if the injection timing was kept constant increase in engine speed results in increased ignition delay, but for the cylinders 4 and 1 increase in engine speed with constant injection timing resulted in shorter ignition delay. The reason could be because of the increased engine speed compression pressure will be higher which resulted in decreasing the ignition delay.

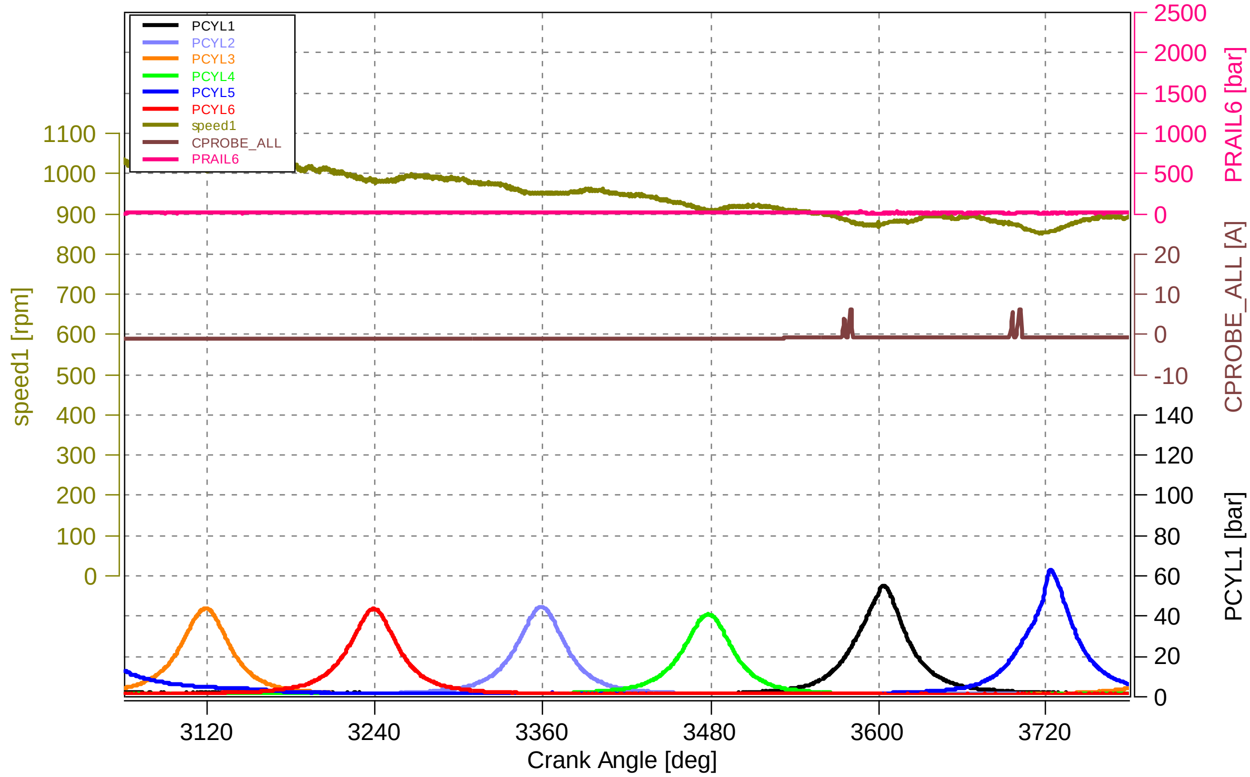

Figure 4.47 – Cold starting of JP8 at 35F-4th cycle

Figure 4.47 represents the engine speed as well as pressure traces for the fourth cycle of JP8 at 35F. Since the engine speed was higher than the idling speed the fuel injection was cut off for four cylinders 3, 6, 2 and 4 by the idle governor. The fuel injection resumed for cylinder 1 in pilot + main injection mode. The engine speed decreased from 1060 rpm at the start of the cycle to 900 rpm at the end of the cycle. The engine speed oscillation along with the change in fuel injection strategy from single to main + pilot continued for seven cycles.

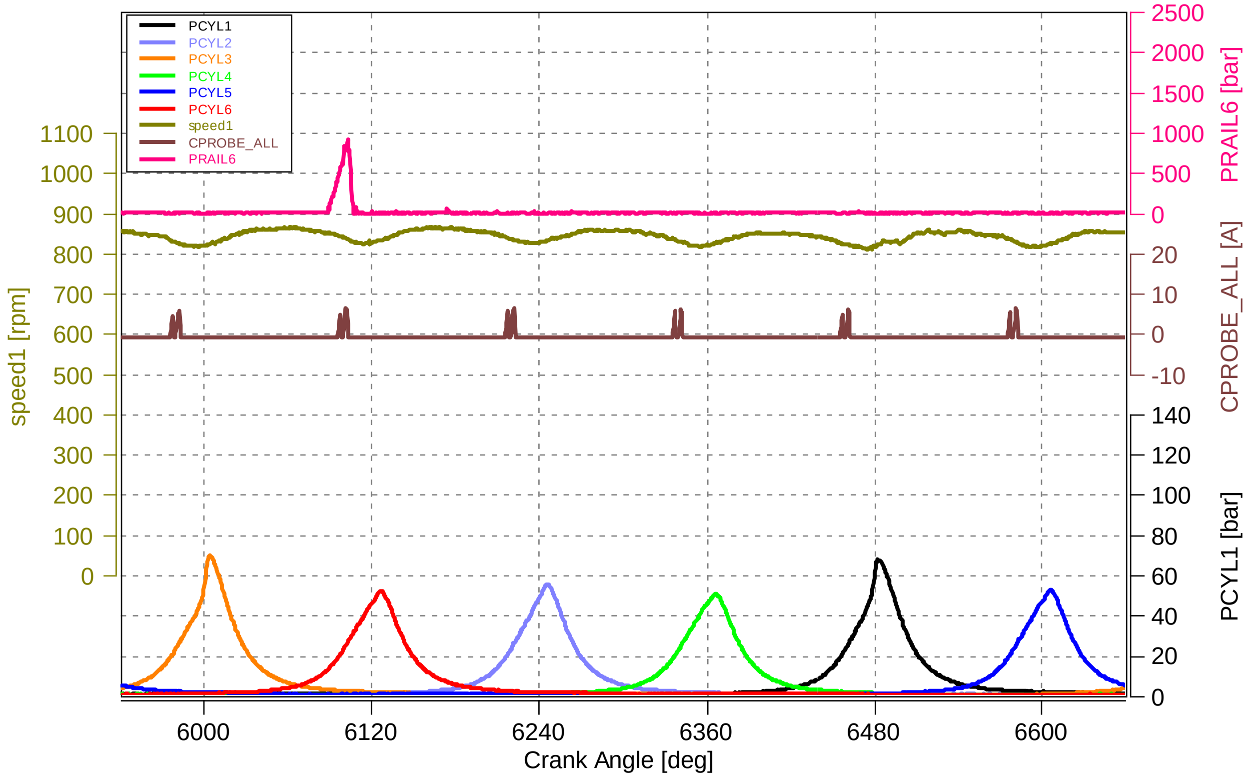

Figure 4.48 – Cold starting of JP8 at 35F-8th cycle

Figure 4.48 represents the engine speed as well as pressure traces for the eighth cycle of JP8 at 35F. The engine speed oscillations finally stabilized at 8th cycle in JP8 35F experiment with the pilot + main injection strategy which was continued till the engine was stopped after recording the 400 cycles of data.

4.8.1 Conclusions – JP8 35F

- Engine successfully started at an ambient temperature of 35F using JP8 fuel
- Engine took longer time to stabilize around the idling speed in comparison with JP8 77F experiment as a result of the low ambient temperature which resulted in increased blowby and heat losses
- The average cranking speed was reduced to 123 rpm
- Maximum engine speed overshoot occurred at 1050 rpm which is higher than the JP8 77F experiment
- Engine speed stabilized after seven cycles and the injection strategy switched to pilot + main injection.

4.9 Cold Start – JP8 25 F

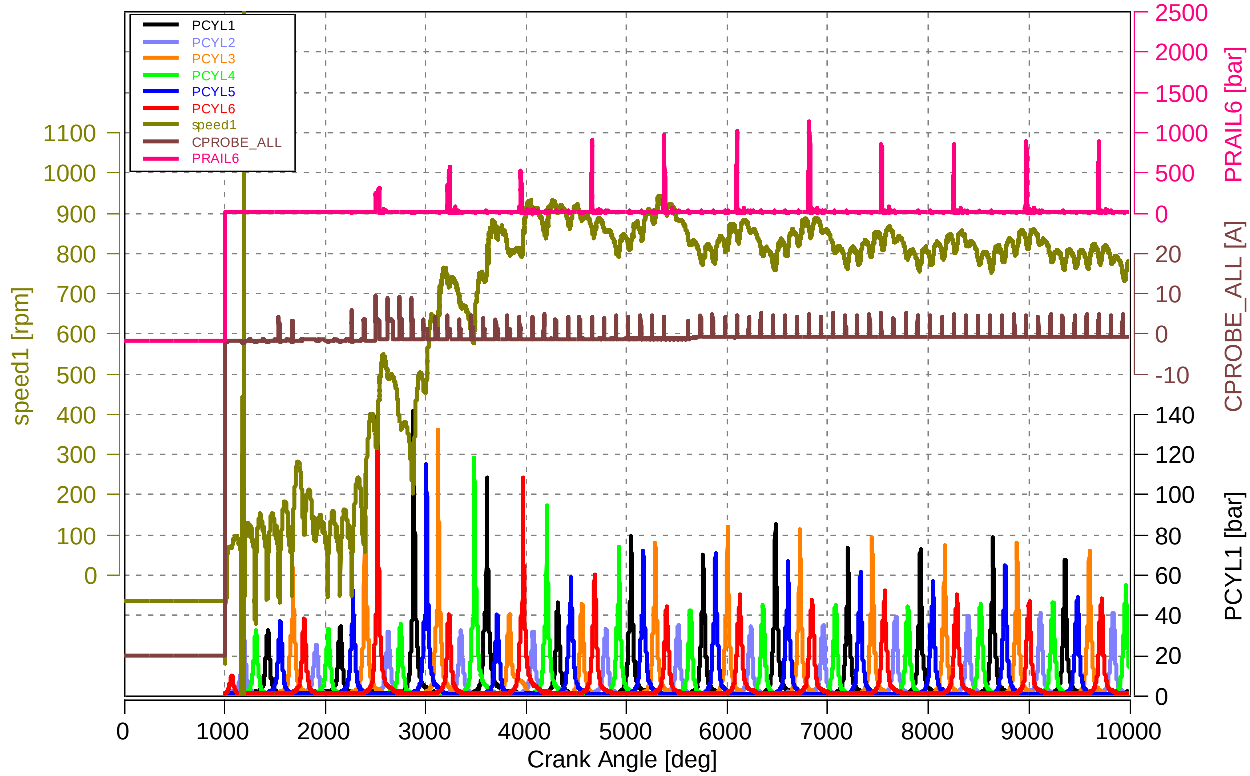

Figure 4.49 – Cold starting of JP8 at 25F

Figure 4.49 represents the cold start data of first 13 cycles using the JP8 fuel at 25F. The first fuel injection started after three TDCs. The engine successfully started at JP8 25 F. Fuel injection was cut off after two initial injections even before reaching the idling speed. Fueling resumed in the middle of the second cycle in cylinder 5. The continuous increase in fueling in the following cycles resulted in the prompt engine speed increase upto the cranking speed in the fourth cycle. Even after reaching the idling speed, engine speed was not stable and oscillated between 800 and 900 rpm initially which was gradually reduced as the engine was warmed up because of the continuous combustion process. Finally the engine speed stabilized at 65th cycle.

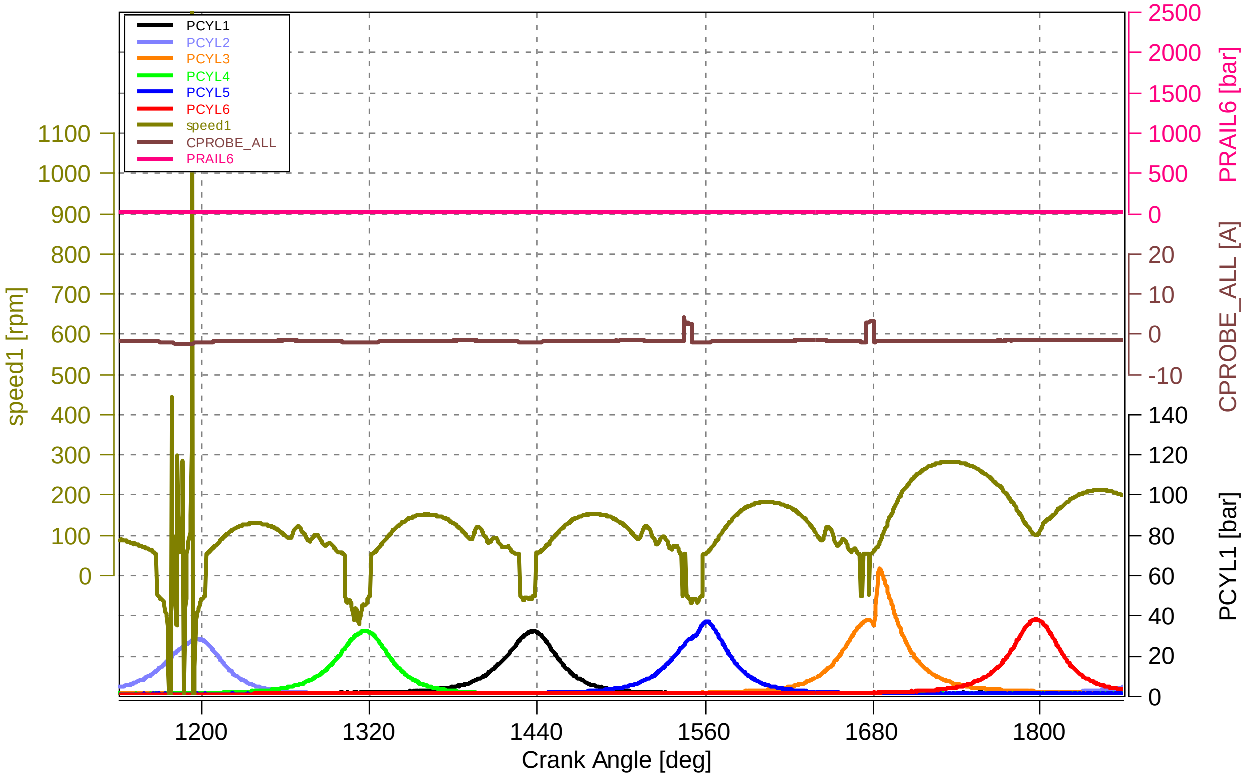

Figure 4.50 – Cold starting of JP8 at 25F-1st cycle

Figure 4.50 represents the engine speed as well as pressure traces for the first cycle of JP8 at 25F. First fuel injection event happened in cylinder 5 after three TDCs at a cranking speed of 112 rpm, which was followed by another fuel injection in the following cylinder (cylinder 3). The fuel injection was suddenly cut off as indicated by the absence of ECU injection signal in the figure. ECU calibration needs to be examined in order to find out the cause of the issue. The pressure rise due to the first injection (cylinder 3) appears to be low, which could be because of the low injection pressure/injection quantity which could not be verified because of the absence of instrumentation to measure the injection quantity / injection pressure.

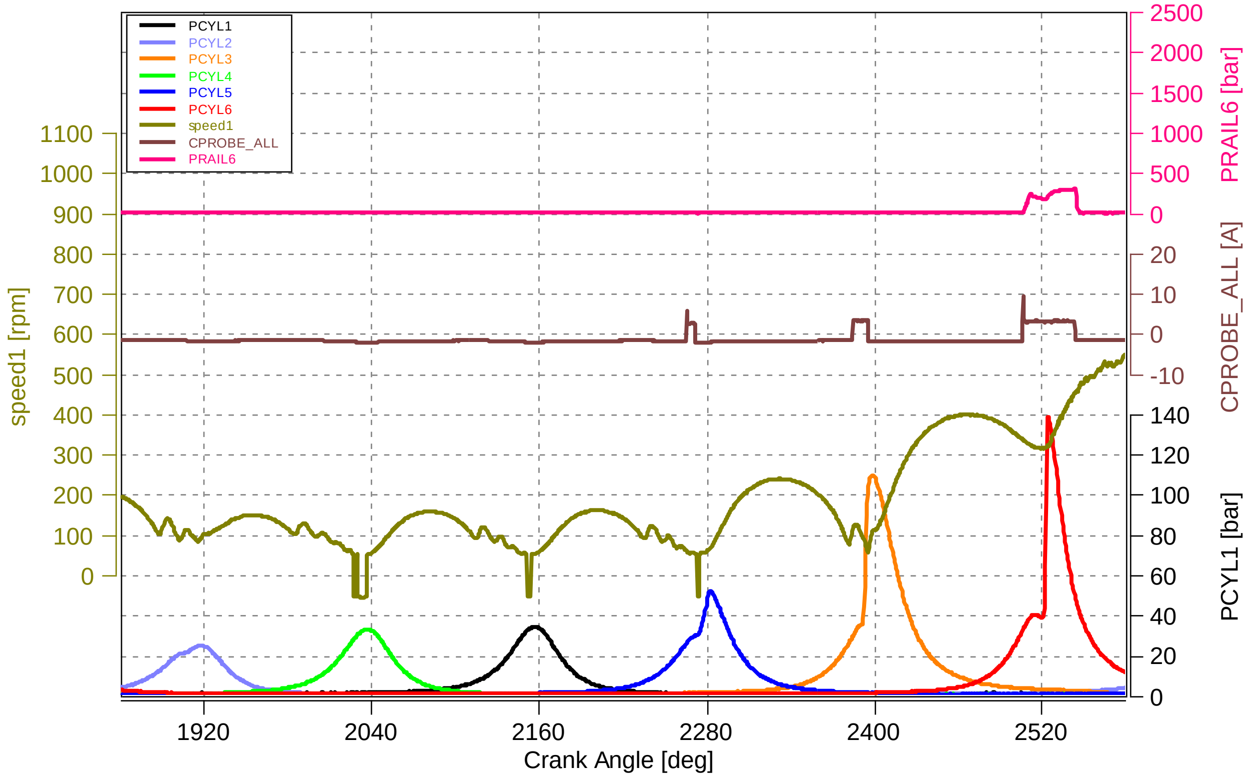

Figure 4.51– Cold starting of JP8 at 25F-2nd cycle

Figure 4.51 represents the engine speed as well as pressure traces for the second cycle of JP8 at 25F. After four cycles without any fuel injection starting from the first cycle, fuel injection started in the cylinder 5 which was followed by gradual increase in fueling pulse width, increased fueling resulted in prompt engine speed acceleration which increased the engine speed from the cranking speed at the start of the cycle to close to 550 rpm at the end of the cycle. It has to be noted that the engine speed did not reach the idling speed in 2nd cycle.

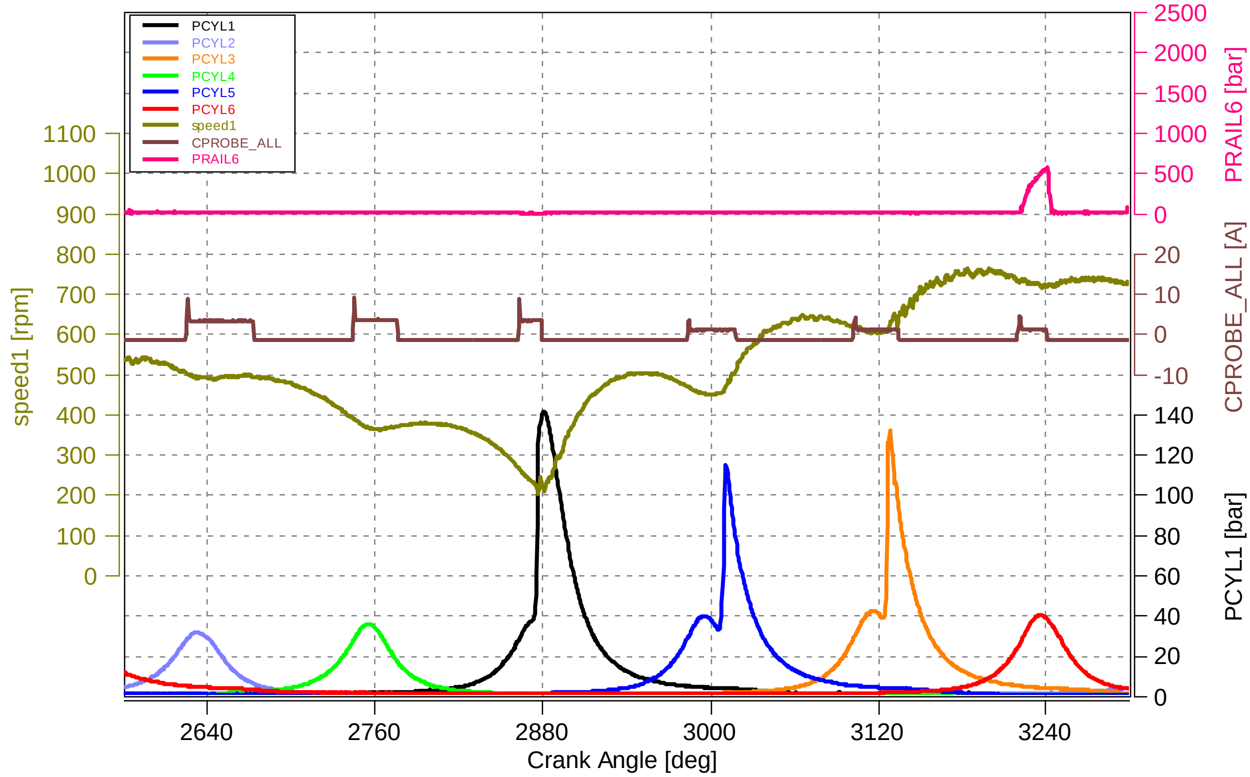

Figure 4.52 – Cold starting of JP8 at 25F-3rd cycle

Figure 4.52 represents the engine speed as well as pressure traces for the third cycle of JP8 at 25F. Due to the absence of injection pressure trace it is difficult to conclude whether there was a misfire or there was no fuel injection in cylinders 2 and 4. Rapid fueling in the cylinders 1, 5 and 3 resulted in engine speed acceleration upto 760 rpm. The cylinder 6 misfired since there was enough pressure on the fuel line and fuel injection signal was given by the ECU before the TDC.

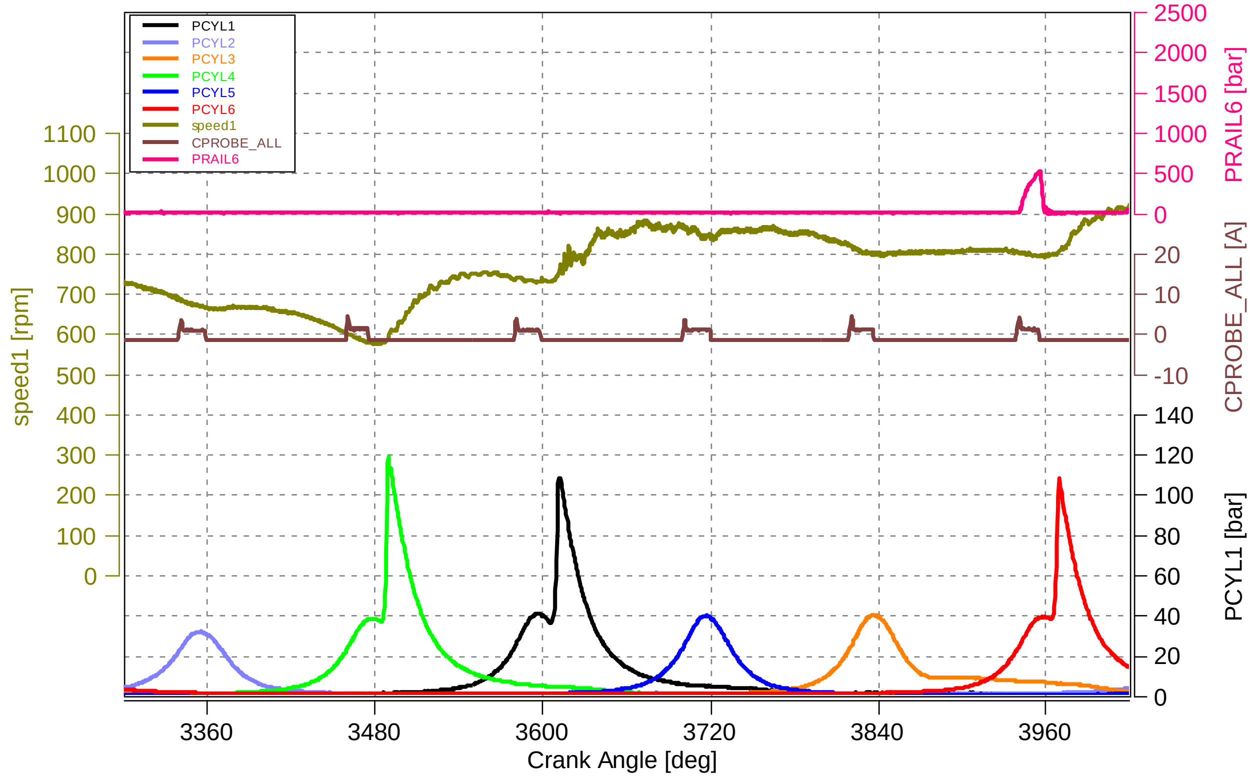

Figure 4.53 – Cold starting of JP8 at 25F-4th cycle

Figure 4.53 represents the engine speed as well as pressure traces for the fourth cycle of JP8 at 25F. The engine speed reached the idling speed of 800 rpm in the fourth cycle as illustrated in the figure. A total of three cylinders misfired in the third cycle. Even though the injection pulse width is varied a little bit throughout the cycle, injection timing was kept constant for all the cylinders in the third cycle, which could be the cause of the misfire since increase in engine speed requires more time near the TDC for successful autoignition. Autoignition might fail because of the inadequate time period near the TDC. Engine speed increased from 730 at the start of the cycle to 900 rpm at the end of the cycle. The engine speed oscillation along with the change in fueling strategy from single to pilot and vice versa continued for 65 cycles.

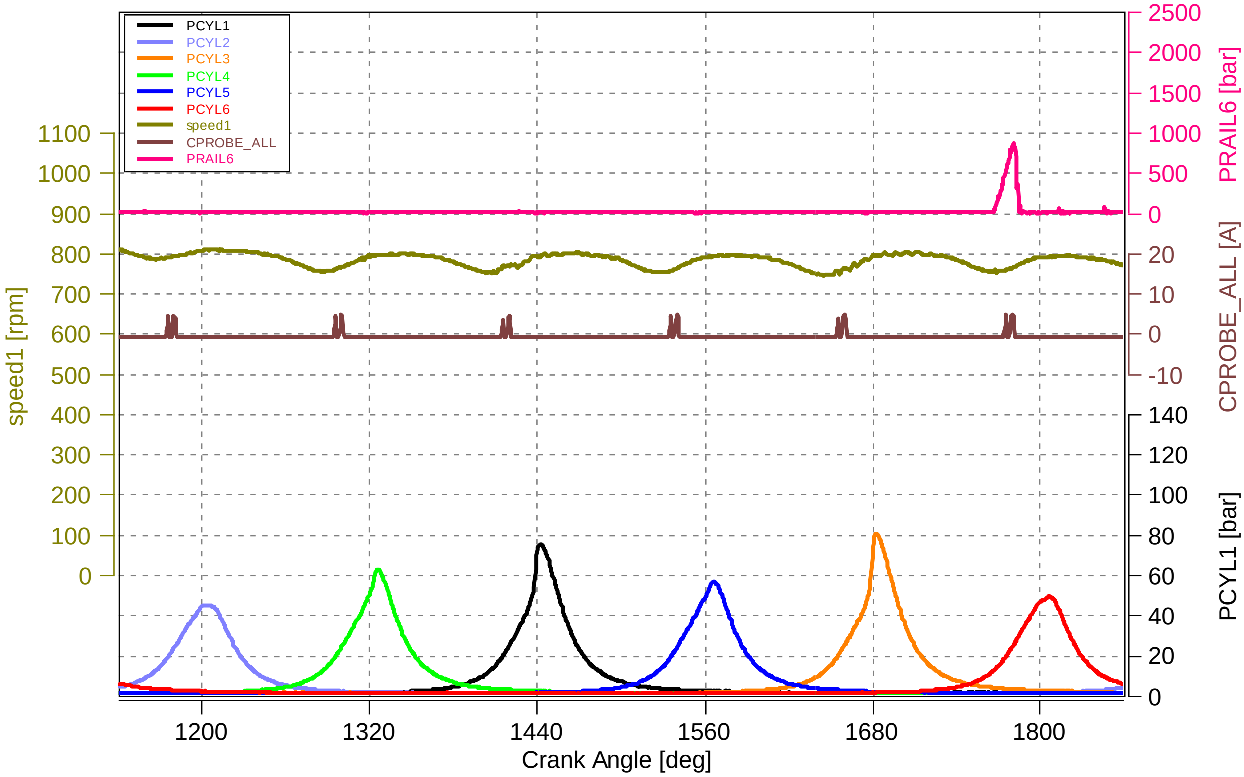

Figure 4.54 – Cold starting of JP8 at 25F-65th cycle

Figure 4.54 represents the engine speed as well as pressure traces for the 65th cycle of JP8 at 25F. The engine speed finally stabilized at the idling speed along with the fuel injection strategy shift from single injection to main + pilot injection in 65th cycle.

4.9.1 Conclusions – JP8 25F

- Engine successfully started using JP8 at 25F
- Average cranking speed of the engine was 112 rpm
- A total of three cylinders misfired in the fourth cycle. It was observed that the injection timing was kept constant for all the cylinders in that cycle with increase in engine speed which could be the cause of the misfire. It is recommended to advance the injection timing with increase in engine speed.
- Engine speed oscillation continued for 64 cycles as a result of continued misfire after firing. Engine speed stabilized after 64 cycles and the injection strategy switched to pilot + main injection in the 65th cycle.

4.10 Cold Start – JP8 16 F

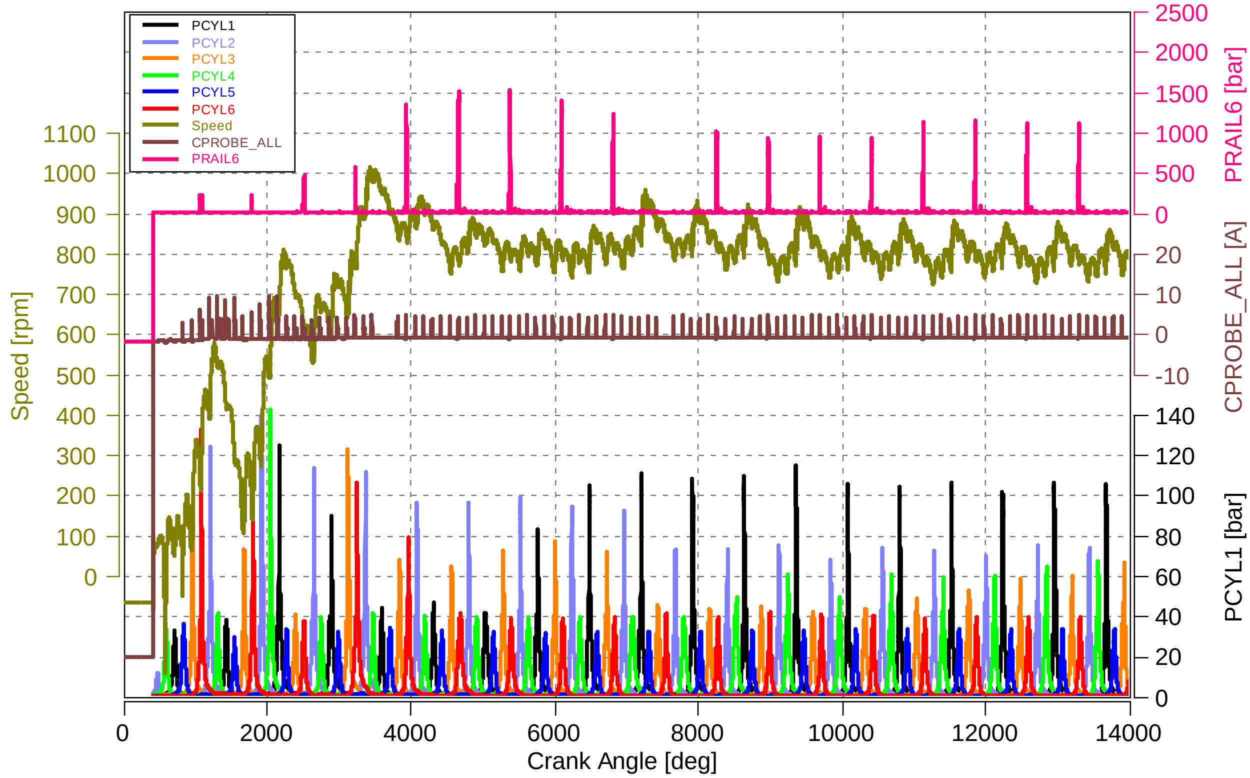

Figure 4.55 – Cold starting of JP8 at 16F

Figure 4.55 represents the cold start data of first 13 cycles using the JP8 fuel at 16F. The engine promptly accelerated towards the idling speed, which had a few misfires in cycle 2, hence the speed dropped after reaching a peak speed of 600 rpm. Following the misfires the fueling was gradually increased which resulted in the engine reaching the idling speed of 800 rpm. The engine speed continuously oscillated for a total of 184 cycles before completely stabilizing to the idling speed.

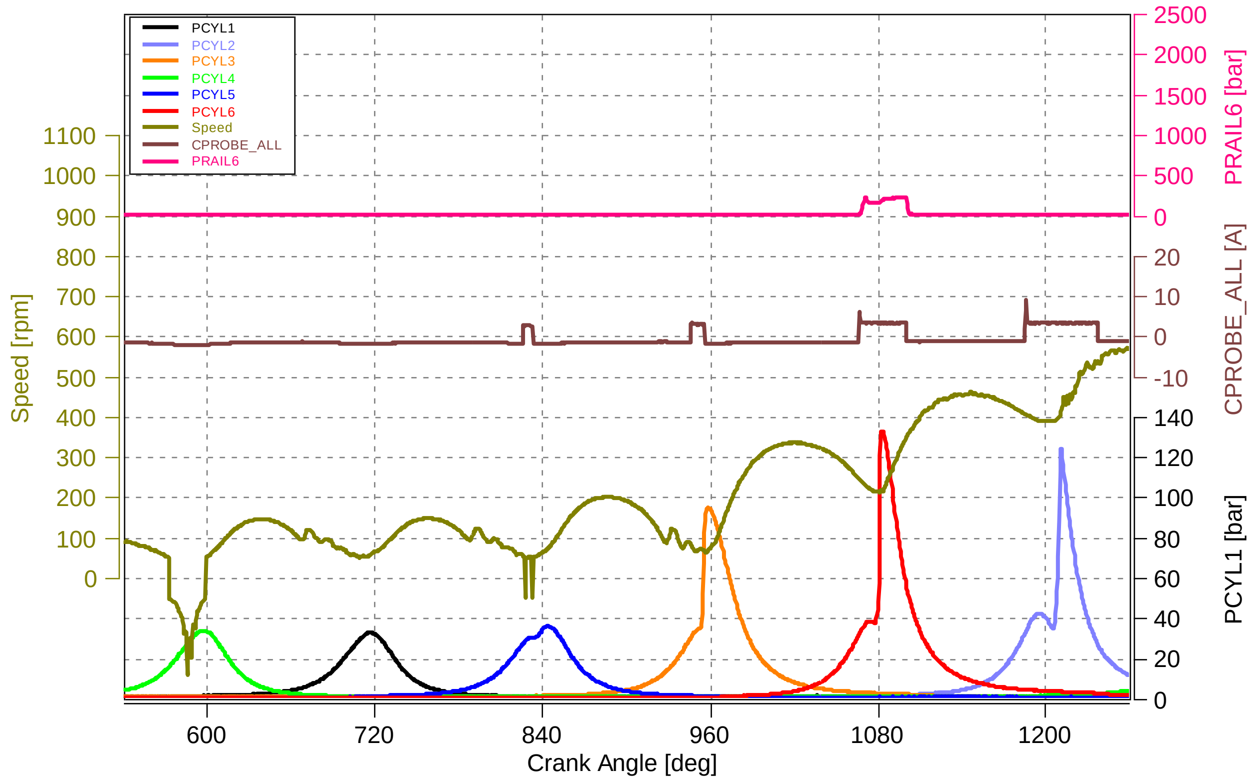

Figure 4.56 – Cold starting of JP8 at 25F-1st cycle

Figure 4.56 represents the engine speed as well as pressure traces for the first cycle of JP8 at 16F. Unlike the JP8 25F experiment the first injection started early in the first cycle after two TDCs in cylinder 5. The fuel injection pulse width was gradually increased as observed in the figure, which resulted in the increased fuel injected into the combustion chamber. Thus the engine resulted in prompt acceleration from the cranking speed at the start of the cycle to close to 600 rpm at the end of the first cycle. It is interesting to observe that all the cylinders fired where there was a fuel injection even at low temperatures.

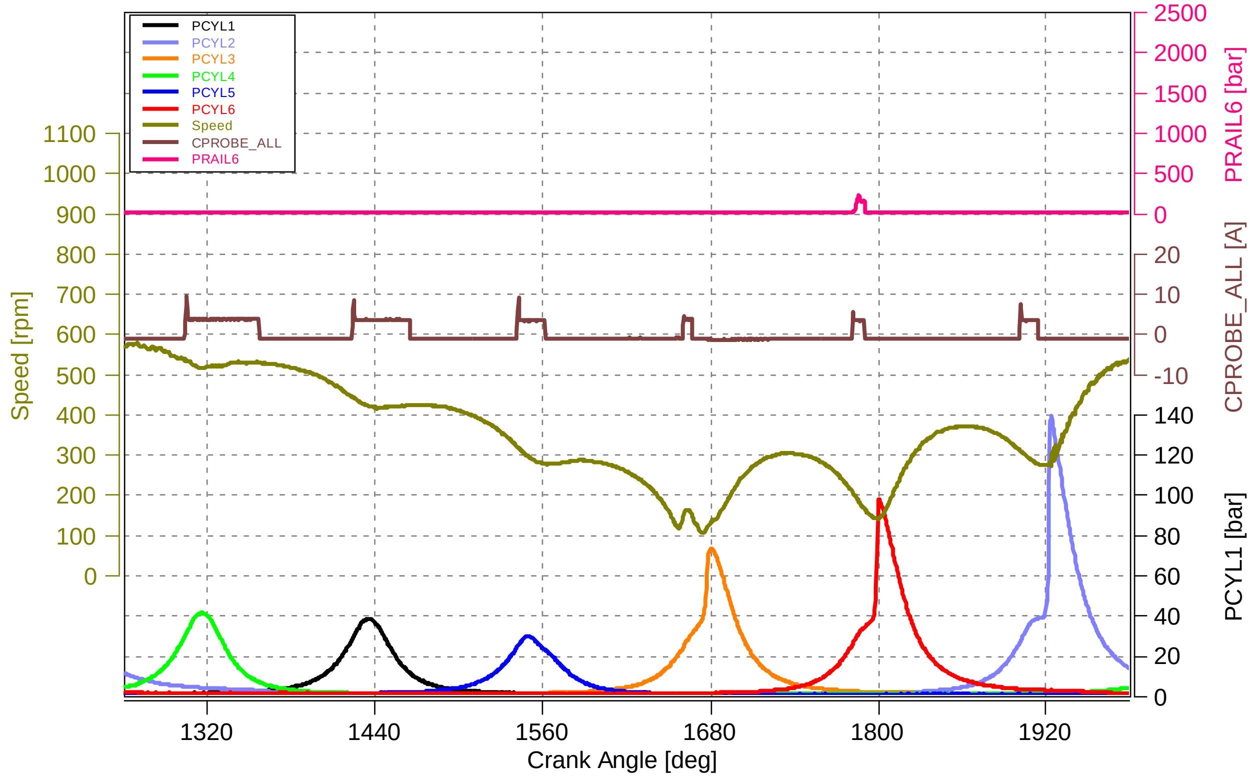

Figure 4.57 – Cold starting of JP8 at 16F-2nd cycle

Figure 4.57 represents the engine speed as well as pressure traces for the second cycle of JP8 at 16F. It is interesting to observe that despite longer injection pulse widths, cylinders 4, 1 and 5 resulted in misfire. It is also interesting to note that the peak compression pressure of the cylinder 5 was only 29 bars, which was a very low value. It is unclear as of this moment whether it is because of blowby and it requires further investigation. The injection pulse width was shortened for cylinder 3, which was gradually increased as the engine speed accelerated.

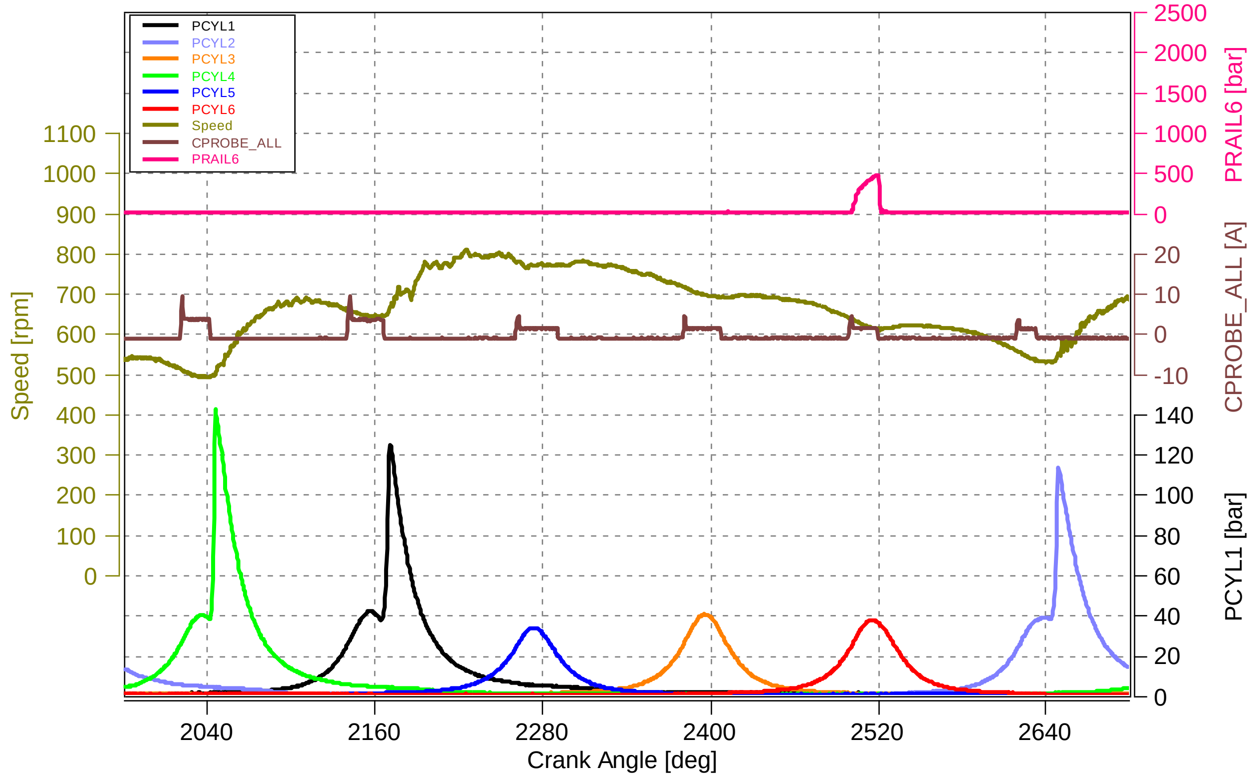

Figure 4.58 – Cold starting of JP8 at 16F-3rd cycle

Figure 4.58 represents the engine speed as well as pressure traces for the third cycle of JP8 at 16F. Continuous engine acceleration as a result of the continuous increase in fueling resulted in the engine reaching the idling speed in the 3rd cycle. After the cylinder 1, three cylinders misfired. Even though the injection timing was advanced with increase in speed, it resulted in misfire. It is interesting to observe the compression pressure of cylinder 5 close to 33 bar, while the compression pressures of other cylinders are close to 40 bar. Engine speed increased from 530 rpm at the start of the cycle to 700 rpm at the end of the third cycle.

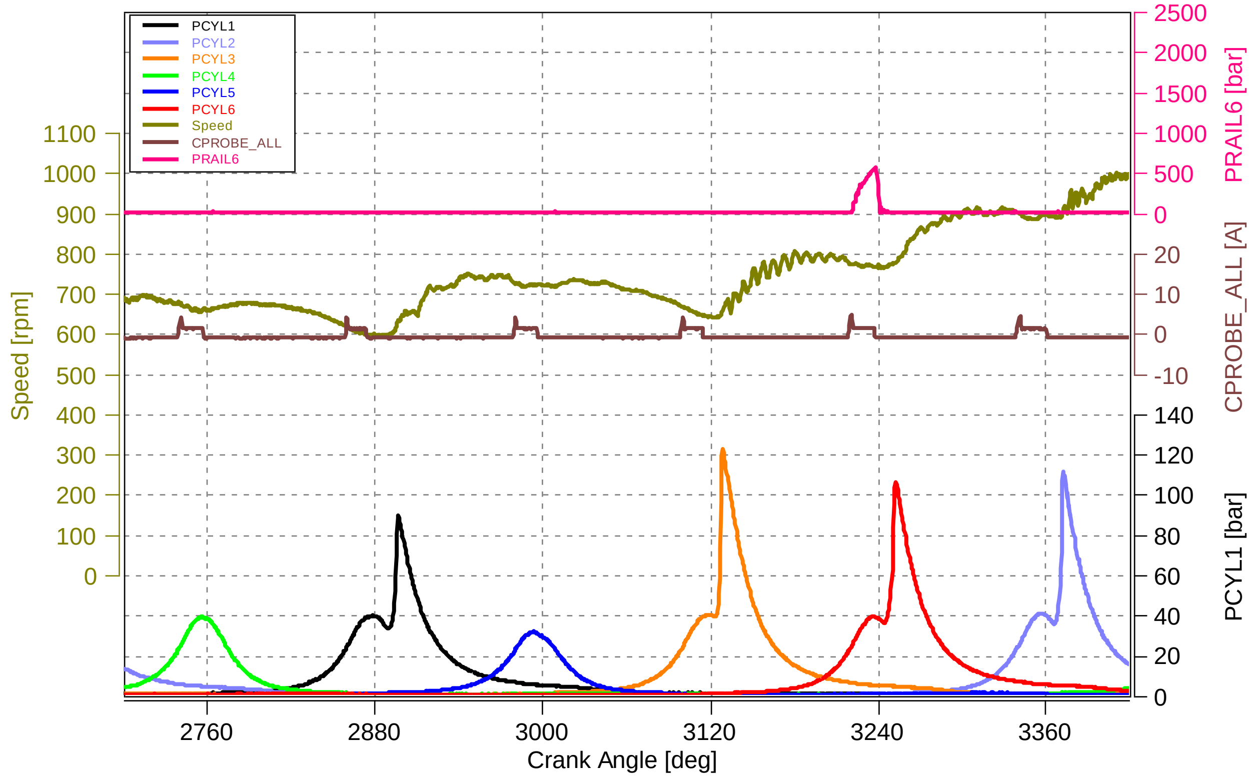

Figure 4.59 – Cold starting of JP8 at 16F-4th cycle

Figure 4.59 represents the engine speed as well as pressure traces for the fourth cycle of JP8 at 16F. As observed in the figure the engine speed overshoot resulted in increase in engine speed from 700 rpm at the start of the cycle to 1000 rpm at the end of the 4th cycle. Cylinder 4 misfired at the beginning of the cycle. Cylinder 5 resulted in combustion but the energy released was very minor which can be observed from the instantaneous engine speed. The instantaneous engine speed after the TDC of cylinder 5 showed a slight increase instead of decrease, which indicates that a small amount of fuel energy was released.

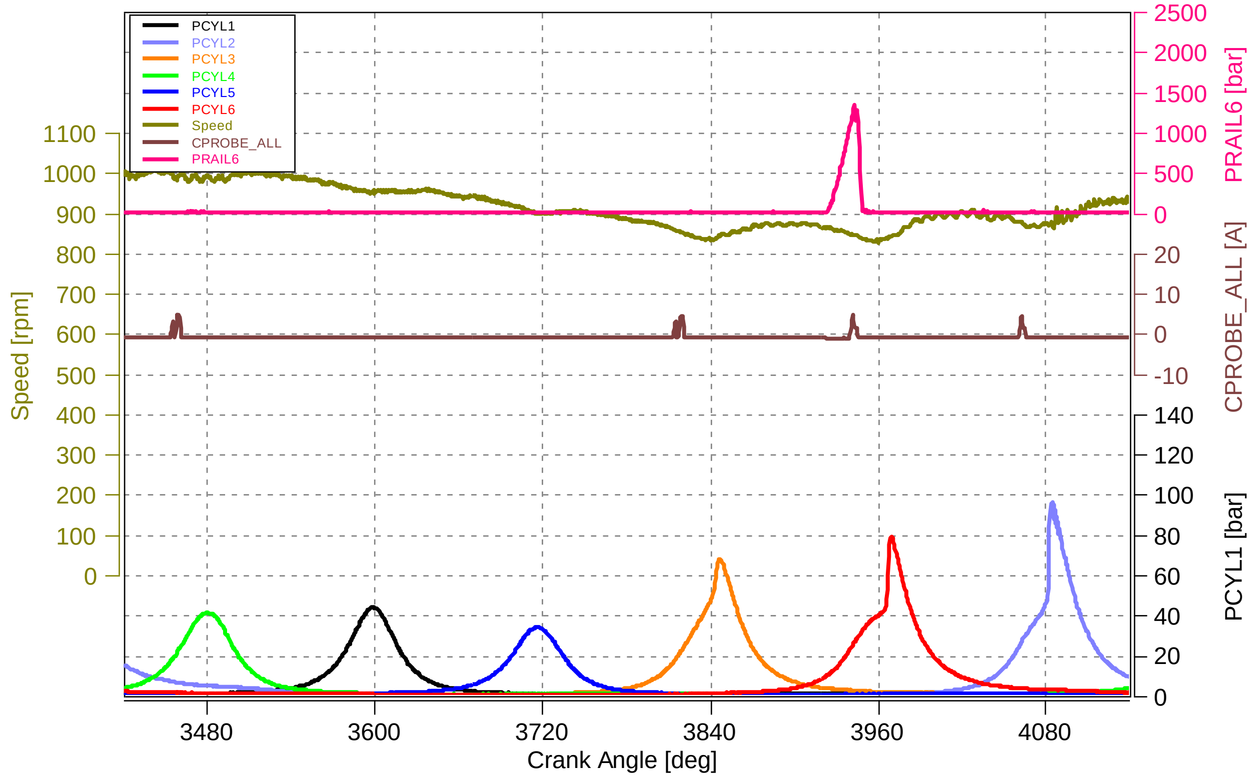

Figure 4.60 – Cold starting of JP8 at 16F-5th cycle

Figure 4.60 represents the engine speed as well as pressure traces for the fifth cycle of JP8 at 16F. The fueling was cut off by the governor for two cylinders 1 and 5 in the fifth cycle. This reduced the engine speed close to 850 rpm. Engine speed at the start of the cycle was 1000 rpm which was reduced to 930 rpm at the end of the cycle as a result of fuel injection cut off. The engine speed continued to oscillate for 184 cycles before stabilizing at the idling speed.

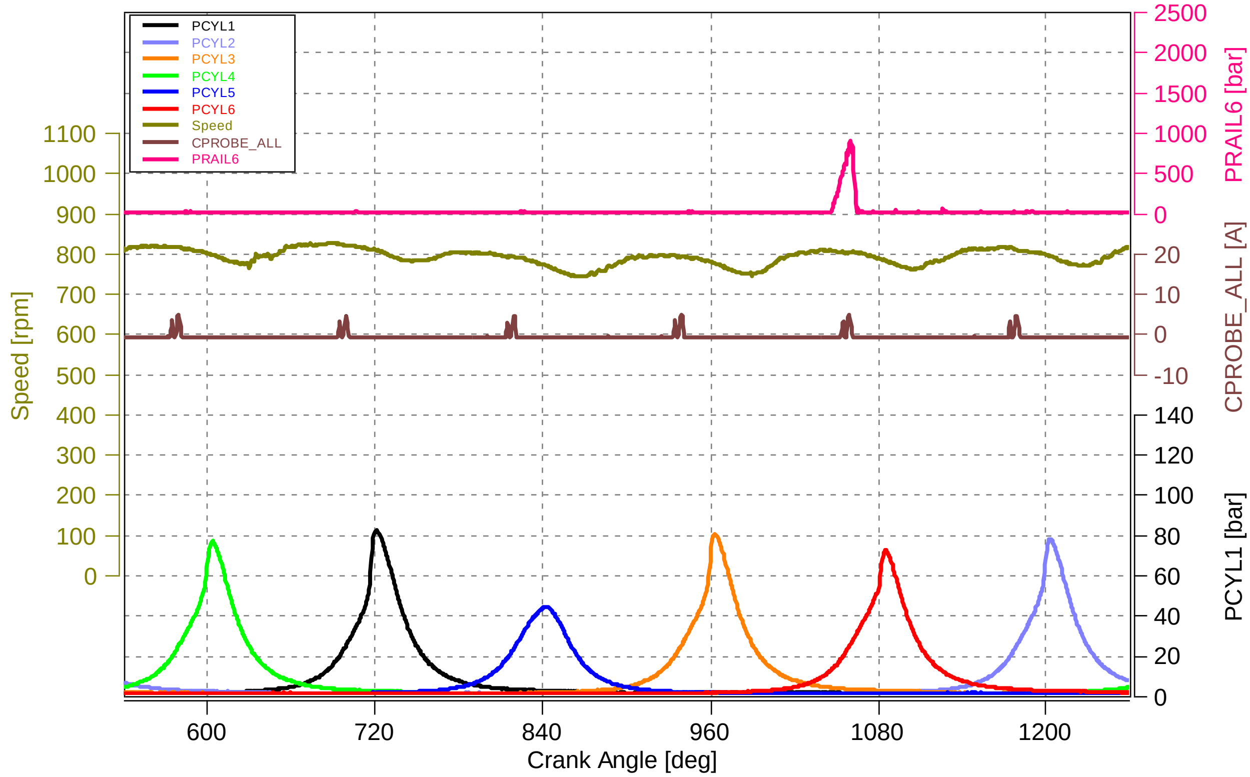

Figure 4.61 – Cold starting of JP8 at 16F-185th cycle

Figure 4.61 represents the engine speed as well as pressure traces for the 185th cycle of JP8 at 16F.Even though the cylinder 5 resulted in partial combustion, the engine speed finally stabilized at the constant idling speed along with the fuel injection strategy shift from single injection to main + pilot injection in 185th cycle.

4.10.1 Conclusions – JP8 16F

- Engine successfully started at an ambient temperature of 16F using the JP8 fuel
- The engine average cranking speed was reduced to 98 rpm
- Engine reached the idling speed in 4^{th} cycle. A total of 7 cycles misfired before the engine reached the idling speed of 800 rpm.
- In the third cycle misfire occurred even though the injection timing was advanced with increase in engine speed, misfire occurred which requires further investigation into the fuel injection system
- Engine speed oscillations continued for 184 cycles as a result of continued misfire after firing phenomenon. Finally engine speed stabilized after 184 cycles and the injection strategy switched to pilot + main injection in the 185^{th} cycle

4.11 Cold Start – JP8 10 F

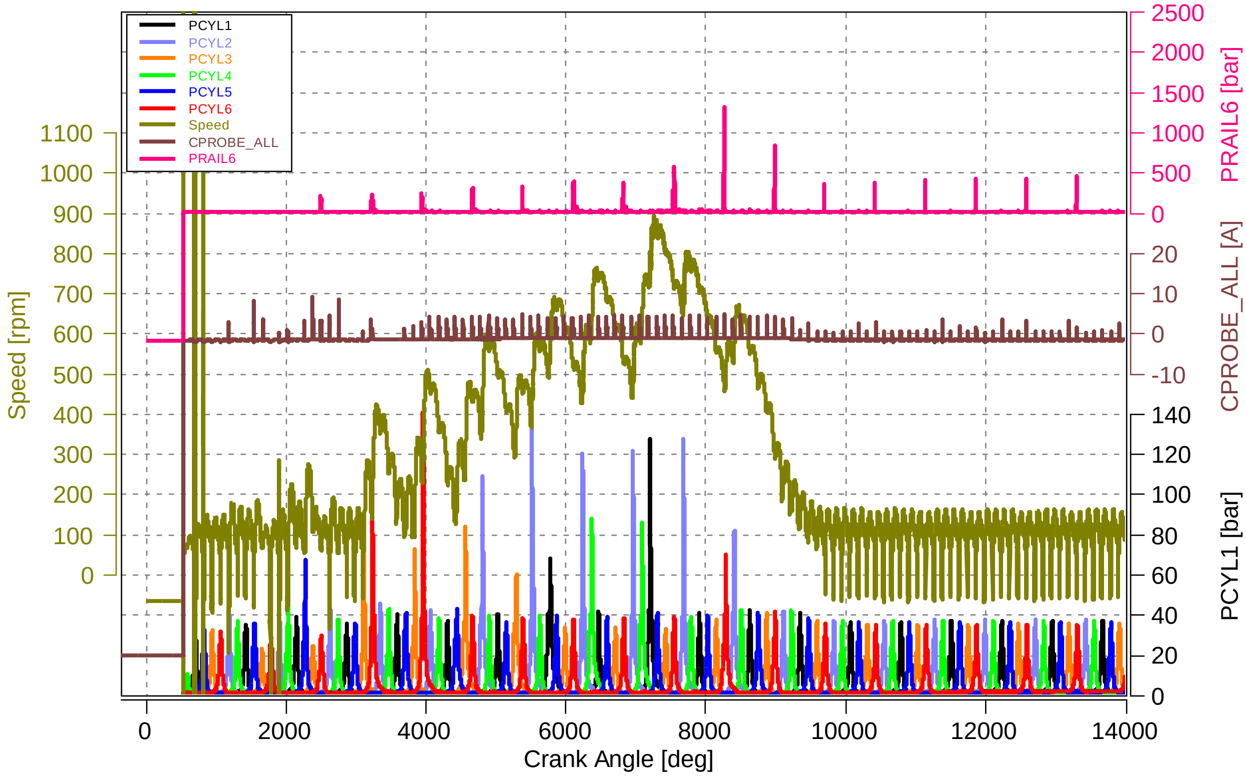

Figure 4.62– Cold starting of JP8 at 10F

Figure 4.62 represents the cold start data of first 13 cycles using the JP8 fuel at an ambient temperature of 10F. Lower ambient temperature resulted in higher heat losses, as well as blowby losses which reduced the compression temperature inside the cylinder. This resulted in numerous misfires and partial combustion as illustrated in the figure 4.62. Finally the engine reached idling speed in 11th cycle, which was followed by the inadequate fueling strategy, which resulted in combustion failure. This returned the engine speed to initial cranking speed.

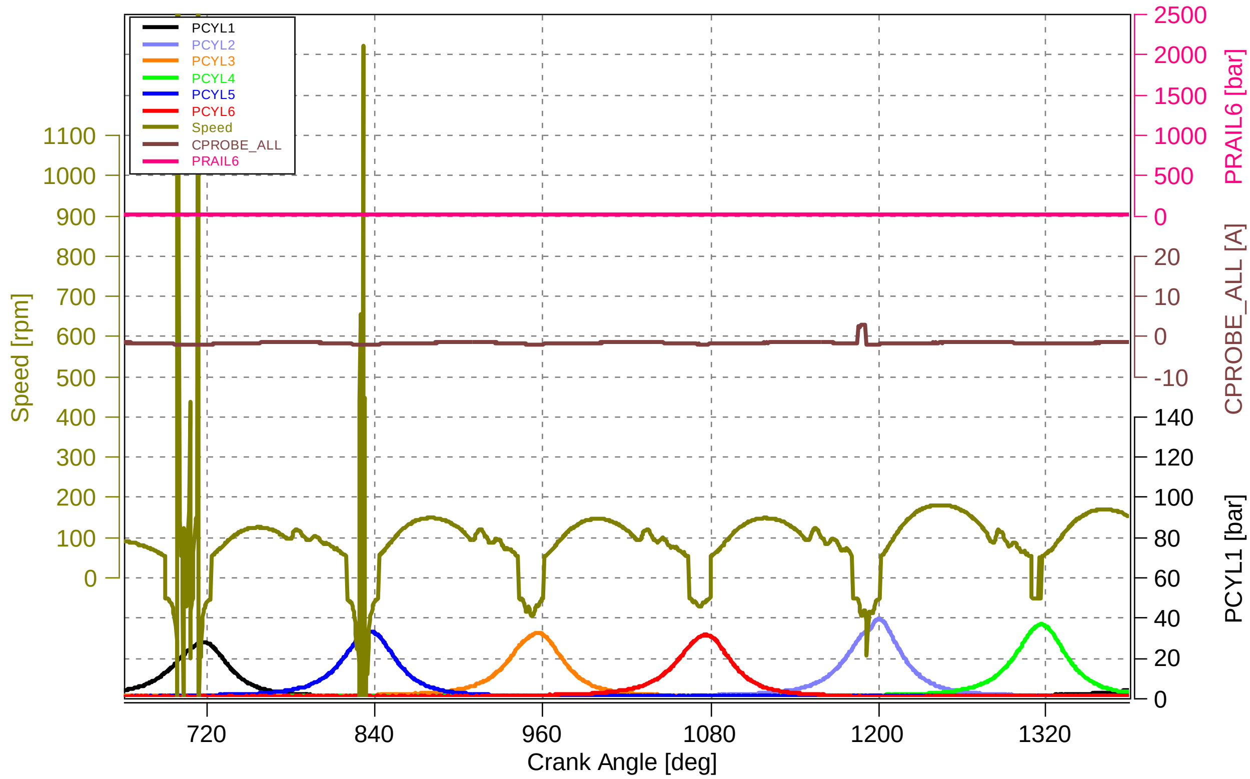

Figure 4.63 – Cold starting of JP8 at 10F-1st cycle

Figure 4.63 represents the engine speed as well as pressure traces for the 1st cycle of JP8 10F experiment. The first fuel injection signal was sent by the ECU after four TDCs and in cylinder 2, which resulted in releasing low amount of fuel energy as reflected by the occurrence of peak cylinder pressure after the TDC as well as increase in instantaneous engine speed after the TDC of cylinder 2. The average peak cranking pressure was 26 bars and the average cranking speed for the first cycle was 95 rpm. After the first injection, fuel injection was cut off for the following cylinder 4.

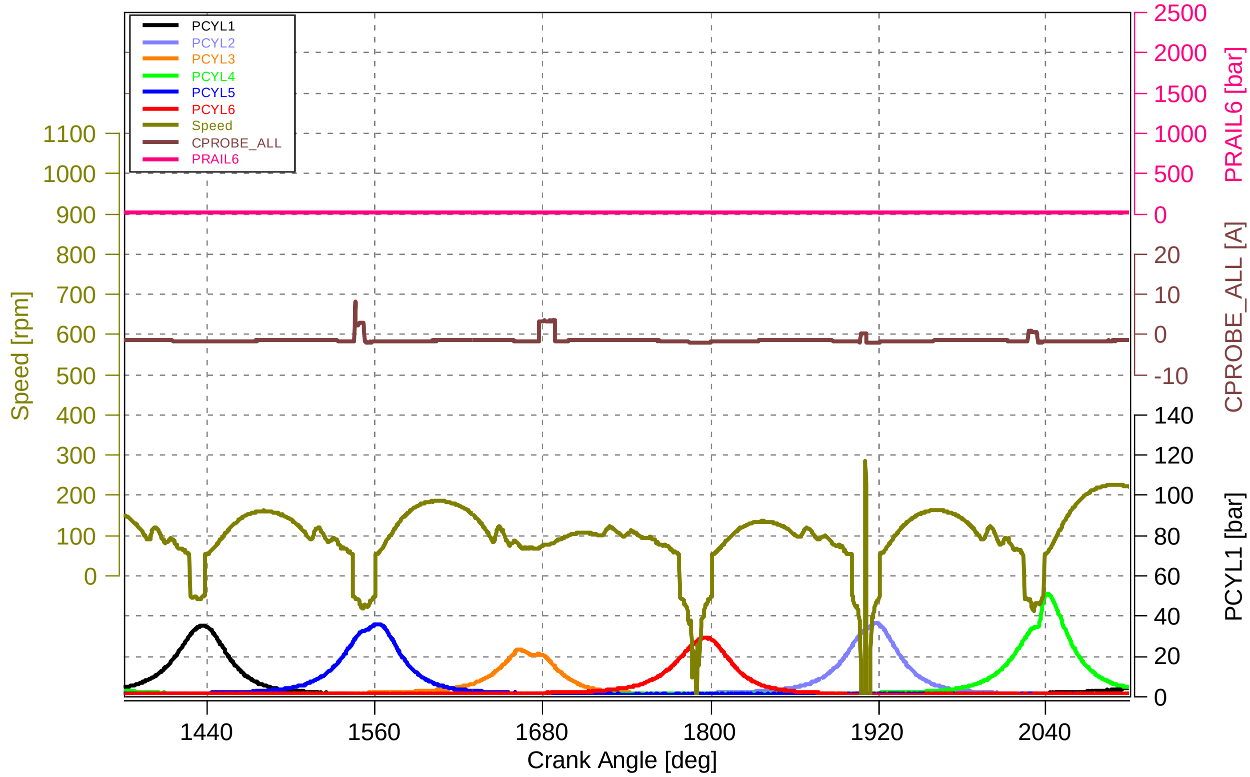

Figure 4.64 – Cold starting of JP8 at 10F-2nd cycle

Figure 4.64 represents the engine speed as well as pressure traces for the 2nd cycle of JP8 10F experiment. A total of four injection signals were provided by the ECU during the 2nd cycle. The amplitude of the current signals sent by the ECU for cylinders 2 and 4 are comparatively less than the fuel injection signal amplitude of cylinders 5 and 6.Cylinders 5, 2 and 4 resulted in a small release of fuel energy as observed form the instantaneous speed higher after the TDC. Engine speed at the start of the cycle was 150 rpm which was increased to 215 rpm at the end of the cycle.

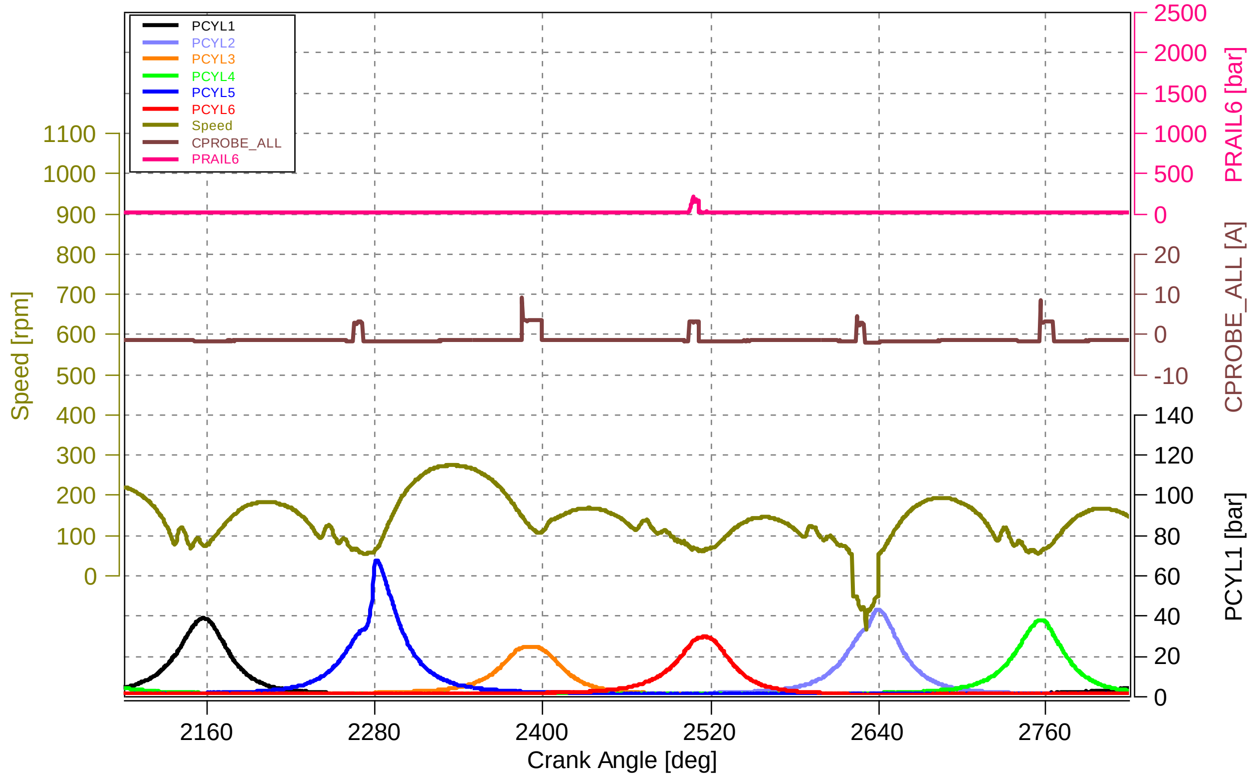

Figure 4.65 – Cold starting of JP8 at 10F-3rd cycle

Figure 4.65 represents the engine speed as well as pressure traces for the 3rd cycle of JP8 10F experiment. As observed in the earlier cycles, third cycle consists of firings and misfiring thorough the entire cycle. There was no fuel injection in cylinder 1 and the cylinders 3, 6 and 4 misfired. This firing after misfiring pattern continued till the end of this experiment.

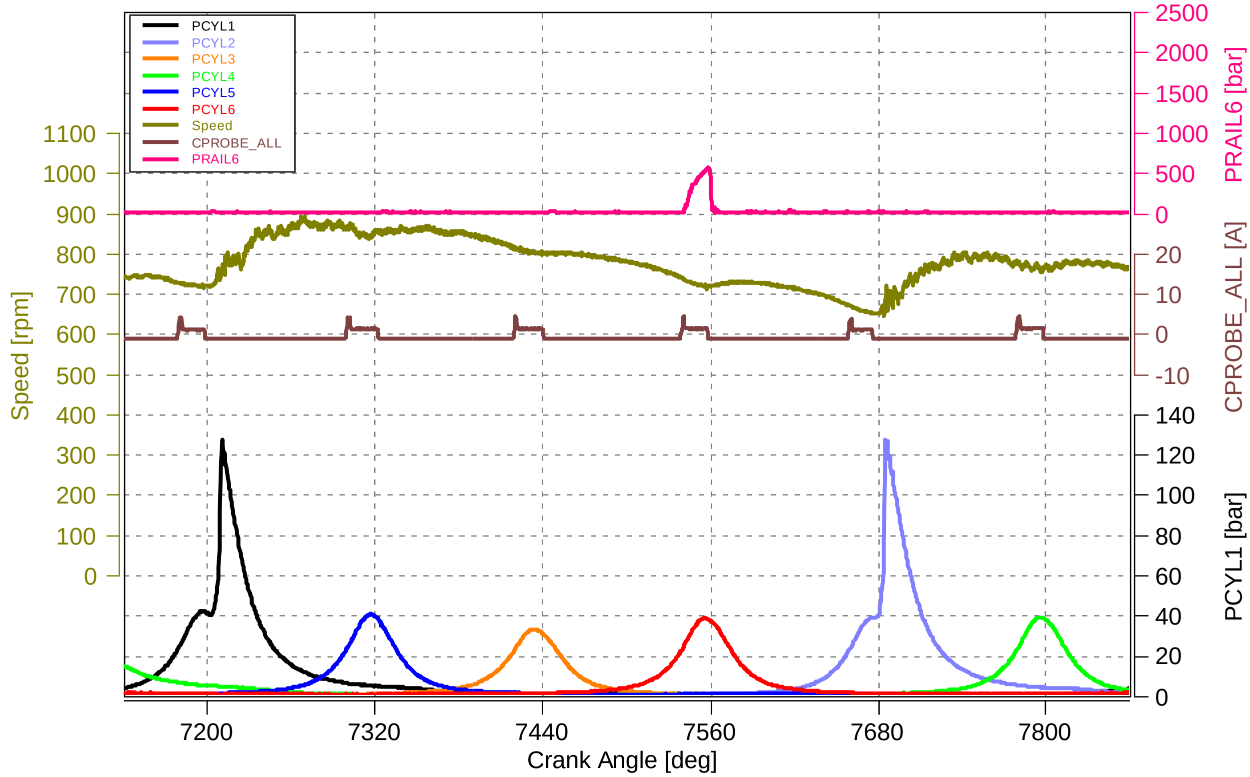

Figure 4.66 – Cold starting of JP8 at 10F-11th cycle

Figure 4.66 represents the engine speed as well as pressure traces for the 11th cycle of JP8 10F experiment. It took 10 cycles to reach the idling speed of 800 rpm at 10F, because of the reduced oxidation reactions and increased heat losses at very low ambient temperatures along with the misfires. Cylinders 5, 3 and 6 resulted in a misfire, which could be attributed to the fact that the injection timing was kept constant with increase in engine speed, which should have been advanced. Engine speed at the end of the cycle was 775 rpm.

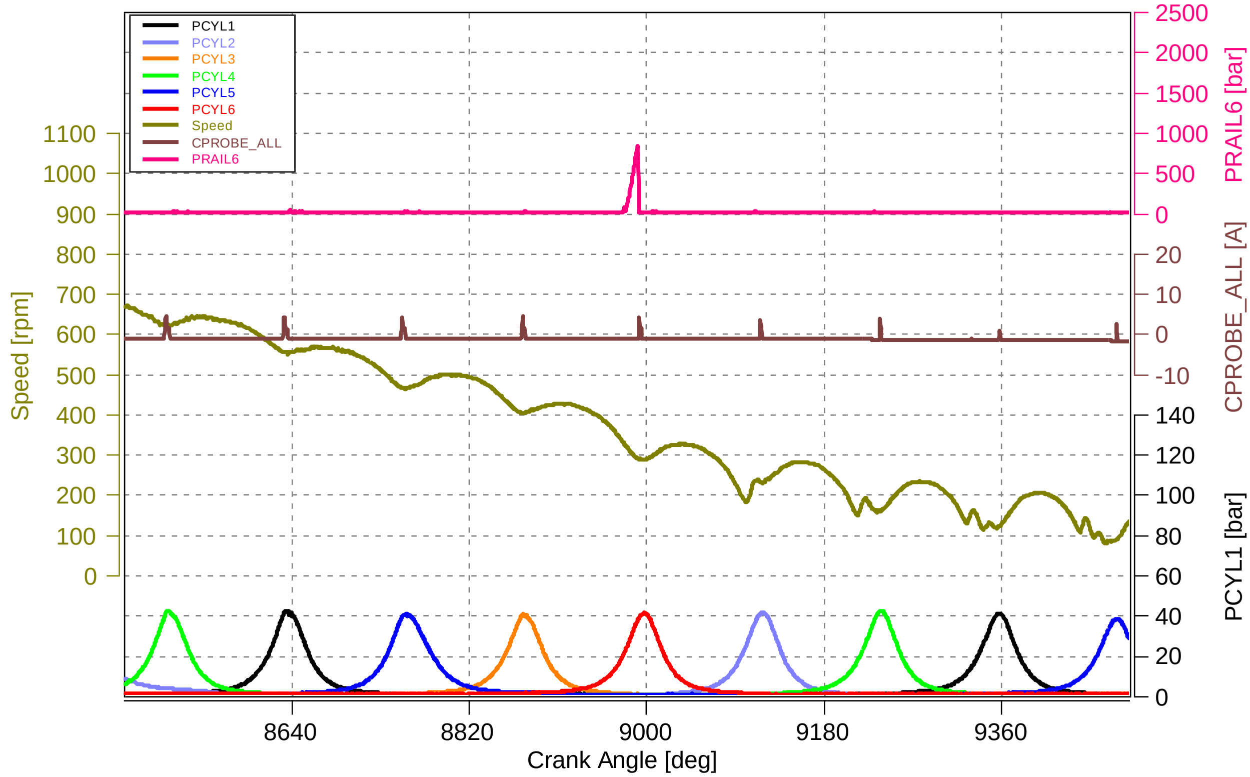

Figure 4.67 – Engine speed drop because of the inadequate fueling strategy

As evident form the figure ECU fuel injection signals were too low as observed in ULSD 10F experiment. Under certain cases the fuel injection signal was issued by the ECU after the pressure in the rail was dropped. This resulted in very little to no fuel being injected hence resulted in no combustion starting from the 12th cycle. Since the engine failed to start beyond this point hence the experiment was concluded that JP8 cold starting failed at 10F.

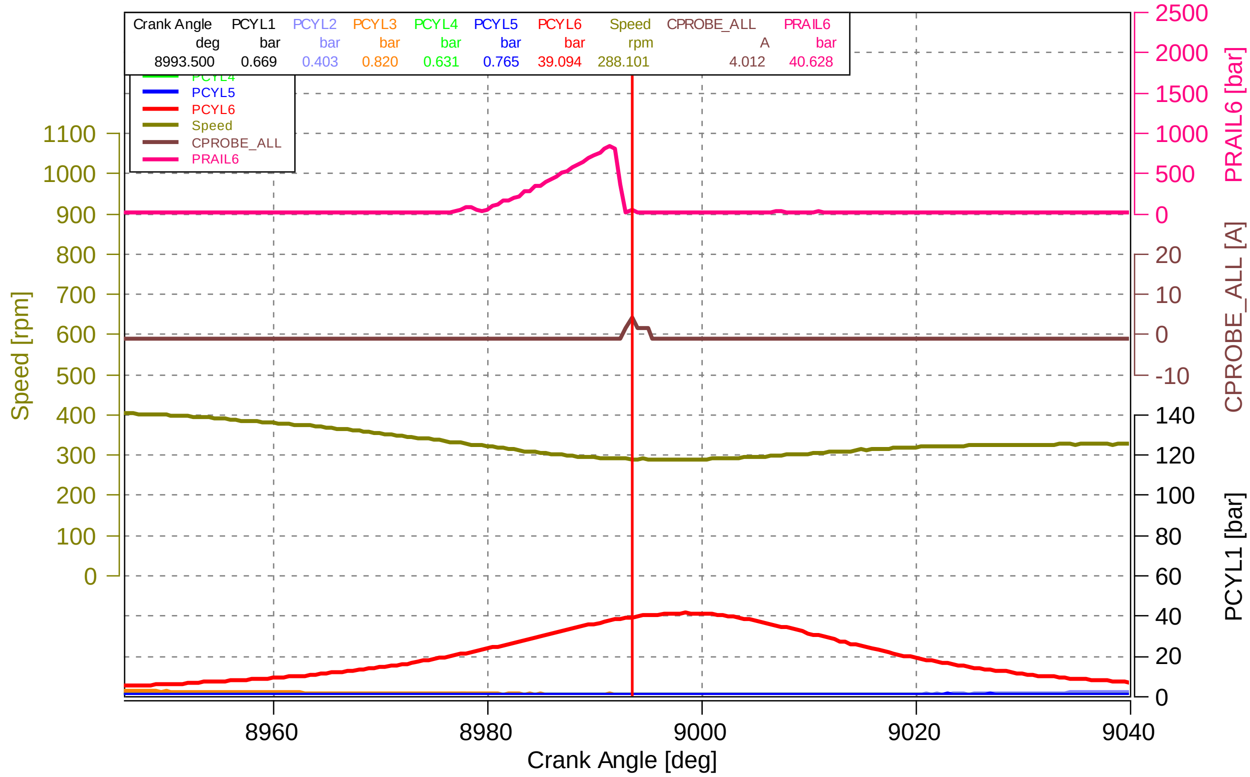

Figure 4.68 – Engine speed drop because of the inadequate fueling strategy

As illustrated in the figure 4.68 fuel injection signal was issued by the ECU after the pressure in the fuel line was dropped which resulted in the out of synchronization fuel injection.

4.11.1 Conclusions – JP8 10F

- Engine started successfully and reached the idling speed but did not continue the idling speed because of the inadequate fueling strategy
- Average cranking speed of the engine was reduced to 95 rpm
- A lot of partial combustion cycles (Cycles with very low pressure rise due to combustion) were observed as a result of the very low ambient temperatures along with the high heat losses from the combustion chamber.
- ECU Fuel injection signal duration was reduced to a minimal value because of the inadequate fueling strategy, which resulted in the absence of fueling hence the engine failed to maintain the idling speed and continuous combustion which resulted in the engine speed reduction upto cranking.
- When fuel injection was stopped, the peak compression pressure in the cylinders reached about 40 bar, the same value at which engine started under room temperature. Engine start could occur if enough fuel would have been injected

4.12 Cold Start – JP8 5 F

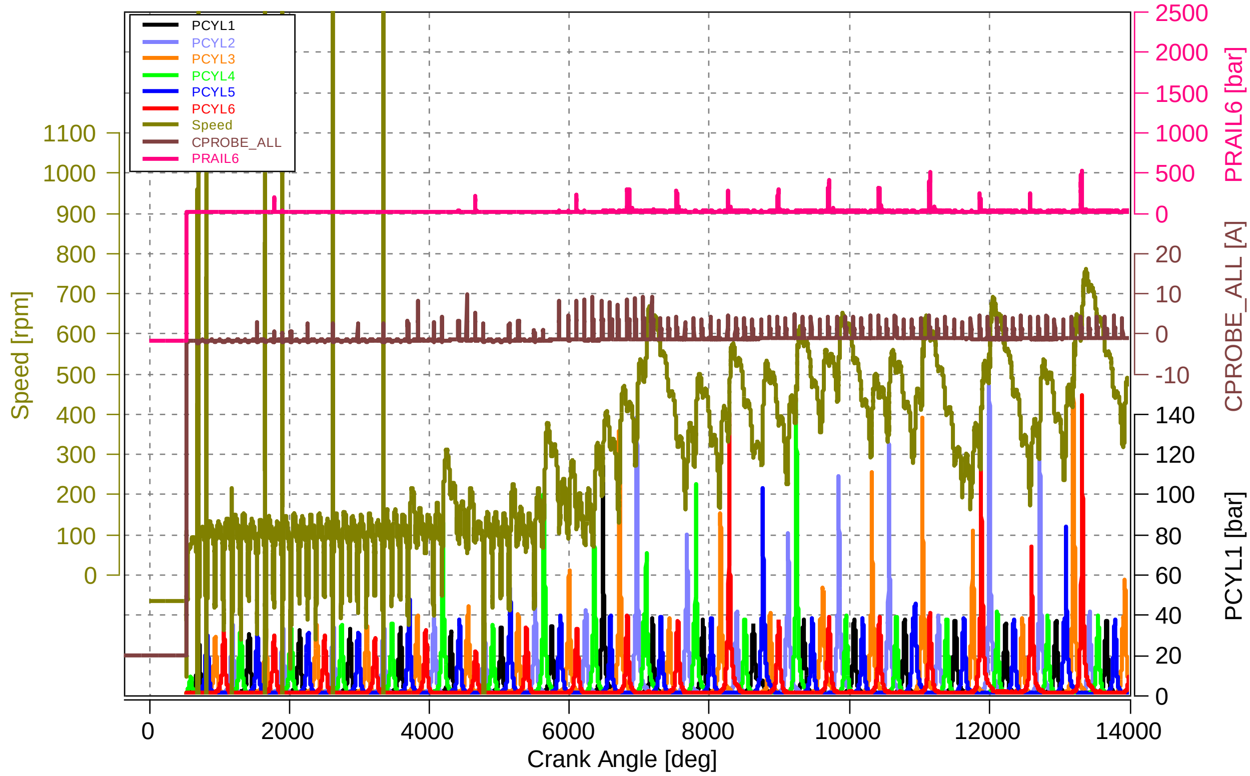

Figure 4.69 – Cold starting of JP8 at 5F

Figure 4.69 represents the cold start data of first 13 cycles using the JP8 fuel at an ambient temperature of 5F. As evident from the picture, the cranking time is very high than the earlier experiments with JP8 and ULSD because of the very low ambient temperature. Engine cranking continued until 8th cycle with a few firings in the in between cycles but not substantial enough to increase the engine speed to the idling speed. Engine firings increased from the 9th cycle but the engine was unable to reach the idling speed even after the first 13 cycles. The phenomena of firing after misfiring continued till the end of the thirteenth cycle.

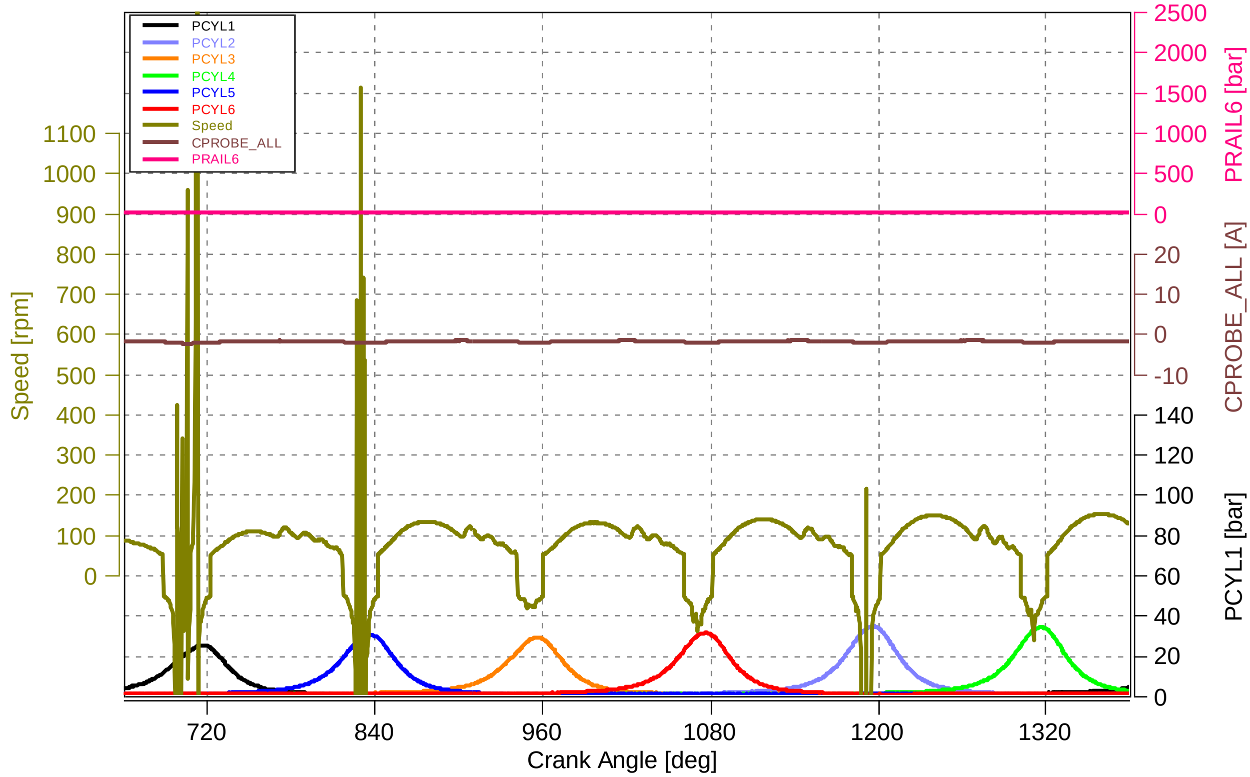

Figure 4.70 – Cold starting of JP8 at 5F-1st cycle

Figure 4.70 represents the engine speed as well as pressure traces for the 1st cycle of JP8 5F experiment. Throughout the entire first cycle the engine was cranking without any fuel injection at the average cranking speed of 94 rpm. The cranking speed was lower when compared with the JP8 5F experiment (95 rpm). It can be observed that the cranking in cylinder pressure gradually increases from cycle 1 which has a peak pressure of 25 bar until cylinder 4 which has a peak pressure of 32 bar.

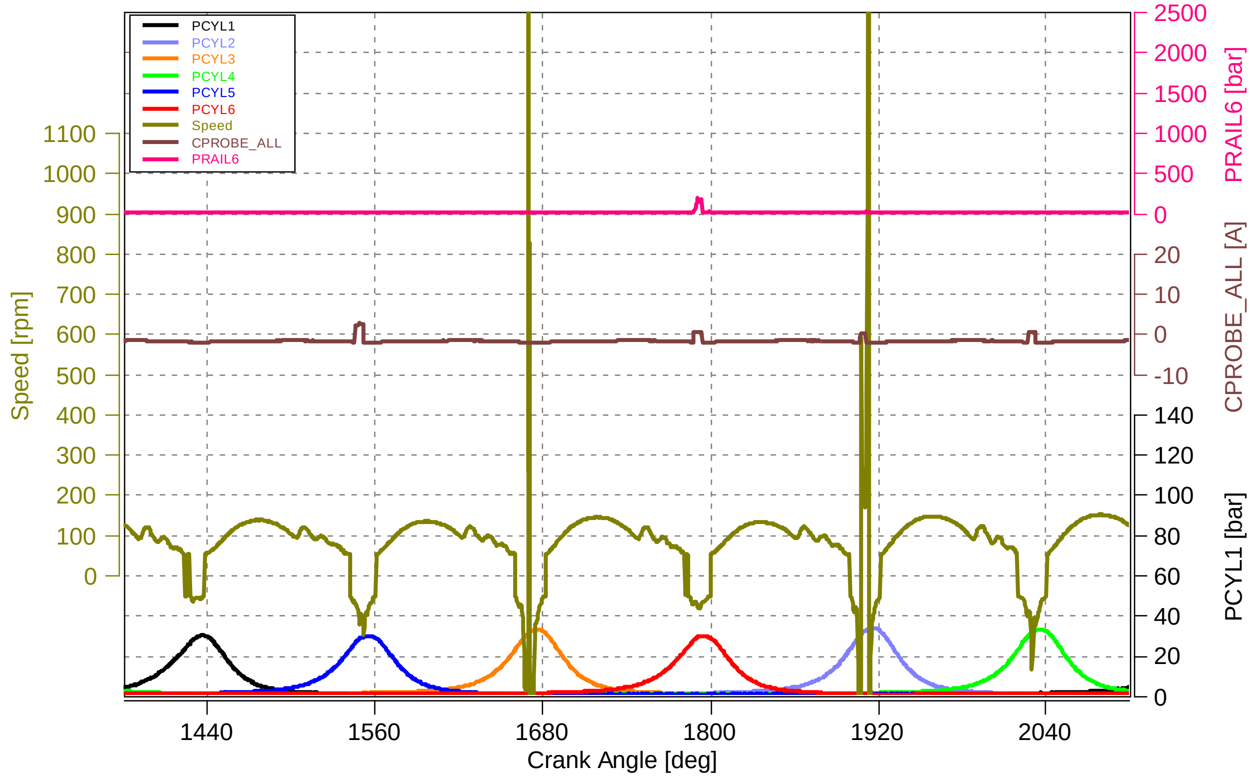

Figure 4.71 – Cold starting of JP8 at 5F-2nd cycle

Figure 4.71 represents the engine speed as well as pressure traces for the 2nd cycle of JP8 5F experiment. A total of three injection events happened in the 2nd cycle but all of them resulted in a misfire. The rail pressure in the fuel line was very low as observed in the picture. It cannot be accurately determined if that pressure rise in the fuel rail was sufficient enough to initiate a proper combustion. Throughout the 2nd cycle the engine continued in cranking speed.

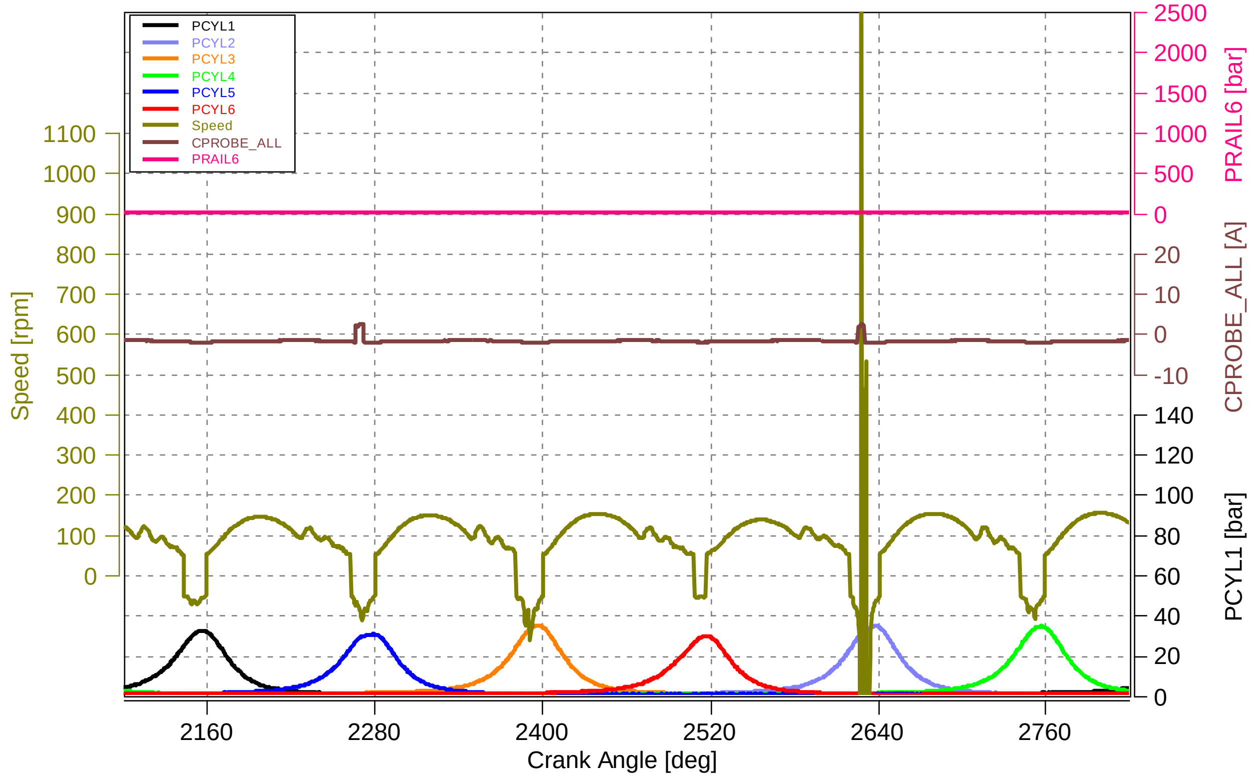

Figure 4.72 – Cold starting of JP8 at 5F-3rd cycle

Figure 4.72 represents the engine speed as well as pressure traces for the 3rd cycle of JP8 5F experiment. Only one injection signal was sent by the ECU in 3rd cycle for cylinder 5 which resulted in a misfire. No fuel was injected for the rest of the cylinders and the engine continued cranking.

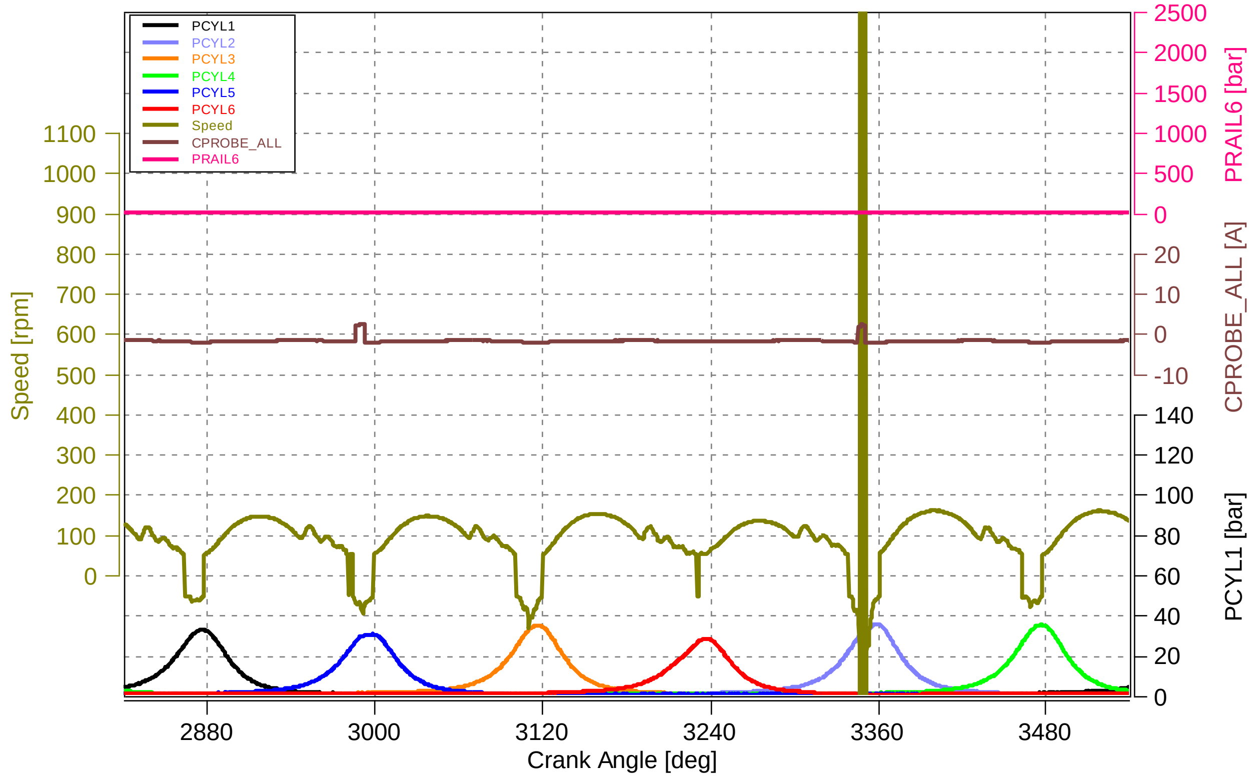

Figure 4.73 – Cold starting of JP8 at 5F- 4th cycle

Figure 4.73 represents the engine speed as well as pressure traces for the 4^{th} cycle of JP8 5F experiment. As observed in the 3^{rd} cycle there was only one injection signal in the fourth cycle as well. It is unclear as of this moment whether this is a error in the ECU calibration or the fuel system. The firing followed by misfiring phenomena continued for 6 cycles without any substantial increase in engine speed.

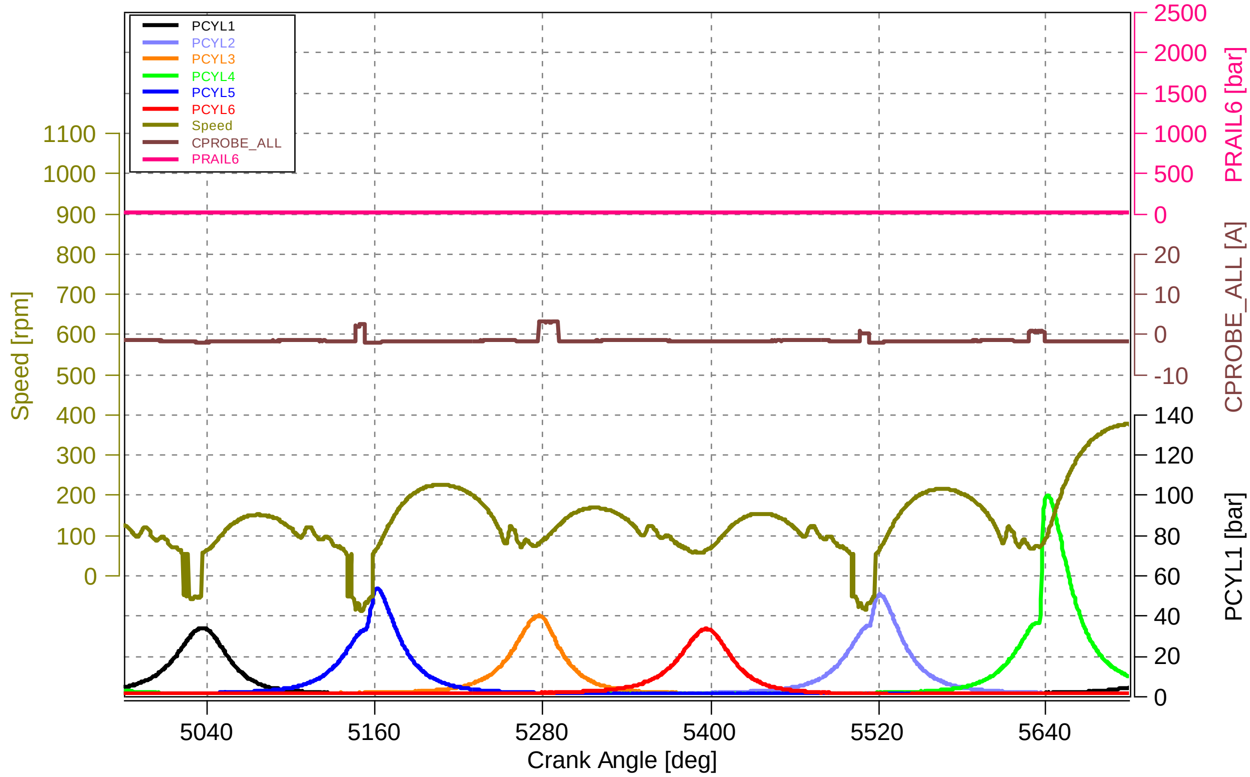

Figure 4.74 – Cold starting of JP8 at 5F- 7th cycle

Figure 4.74 represents the engine speed as well as pressure traces for the 7th cycle of JP8 5F experiment. The same issue of missing the fuel injection for certain cylinders while injecting fuel for the rest of the cylinders occurred in the 7th cycle but the engine speed increased to 400 rpm at the end of the cycle.

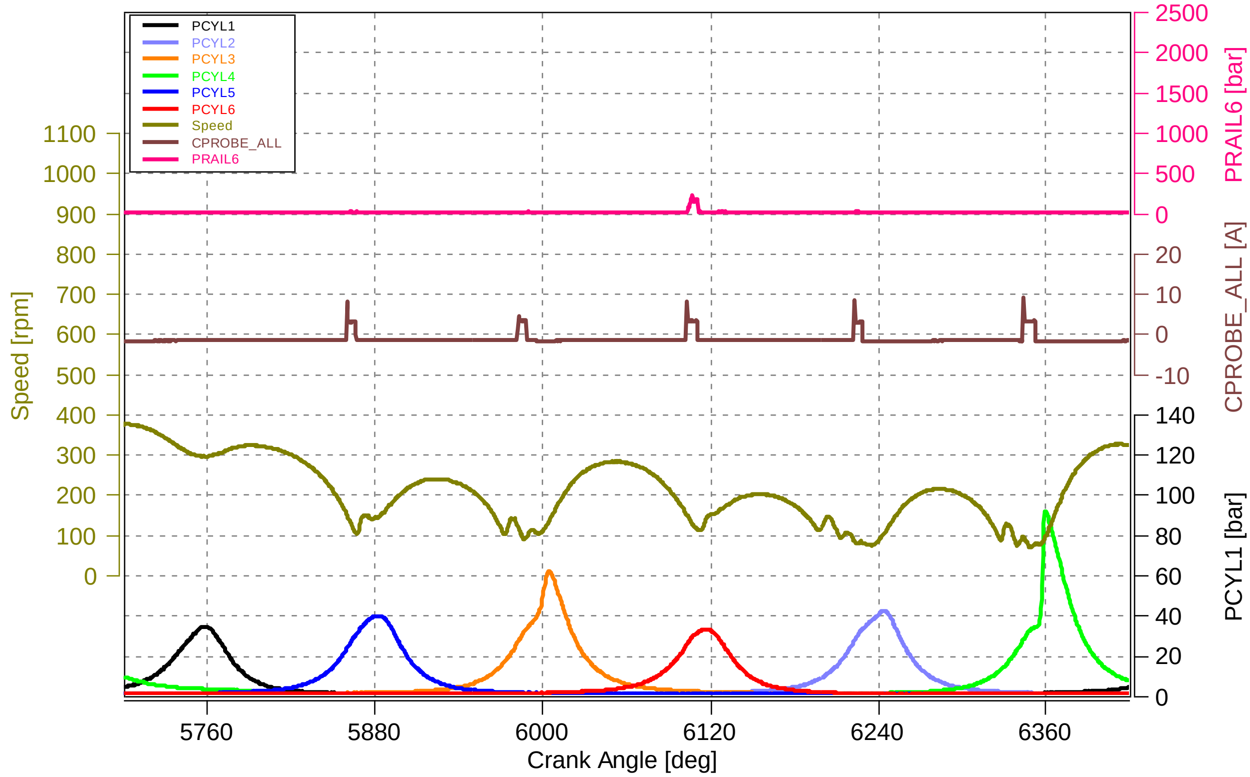

Figure 4.75 – Cold starting of JP8 at 5F- 8th cycle

Figure 4.75 represents the engine speed as well as pressure traces for the 8th cycle of JP8 5F experiment. In the 8th cycle no fuel was injected in cylinder 1. With the exception of cylinder 6 all the rest of the cylinders fired. Despite the firings the engine speed was well below 400 rpm.

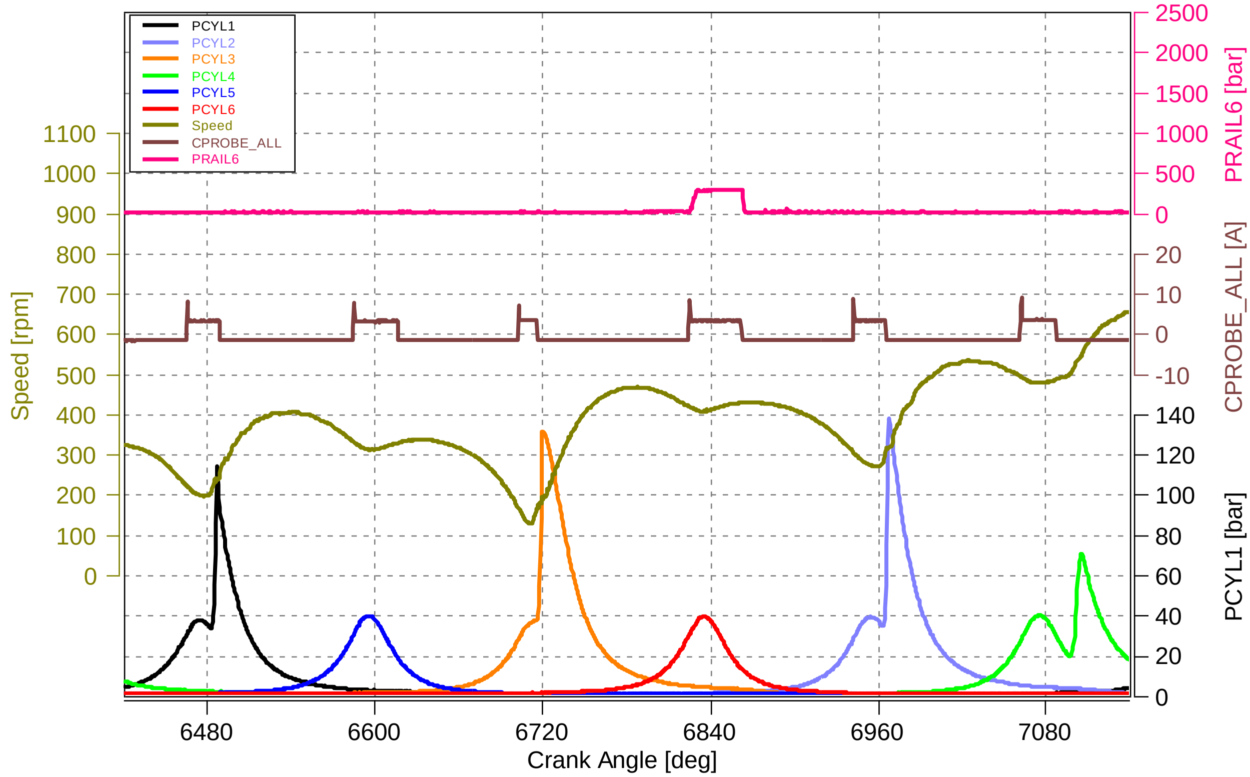

Figure 4.76 – Cold starting of JP8 at 5F- 9th cycle

Figure 4.76 represents the engine speed as well as pressure traces for the 9th cycle of JP8 5F experiment. Form the 9th cycle the injection pulse width as well as the rail pressure started to increase and resulted in steep pressure rise rates as observed in the figure for cylinders 1, 3 and 2. This trend of firing after misfiring continued till the end of 13 cycles. It was decided to stop the experiment at this stage to prevent any damage to the starter motor as well as the battery.

4.12.1 Conclusions – JP8 5F

- Engine did not achieve a stable cold start at the ambient temperature of 5F using JP8 fuel
- The average cranking speed was reduced to 94 rpm as a result of increased heat and blowby losses.
- Engine failed to reach the idling speed of 800 rpm during the duration of testing.

4.13 Cold Start – JP8 0 F

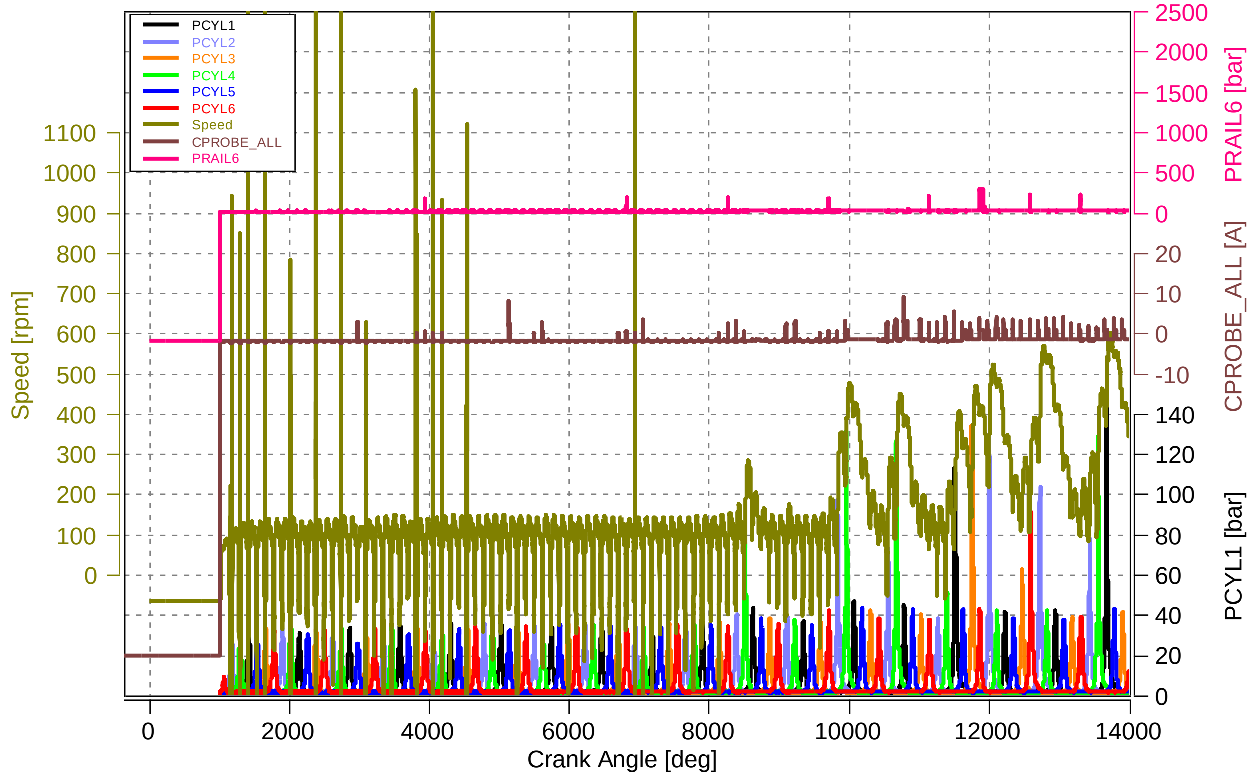

Figure 4.77 – Cold starting of JP8 at 0F- cycles 0 - 20

Figure 4.77 represents the cold start data of first 13 cycles using the JP8 fuel at an ambient temperature of 0F. As illustrated in the figure 4.77, engine was cranked continuously for first 13 cycles with very few combustion cycles which didn't result in increased engine speed. It's also evident that the pressure buildup in the fuel rail failed during the majority of the first 10 cycles because of the controller error (PRAIL6 - in Fig 4.77). After the first 19 cycles of firing after misfiring, engine never reached the idling speed.

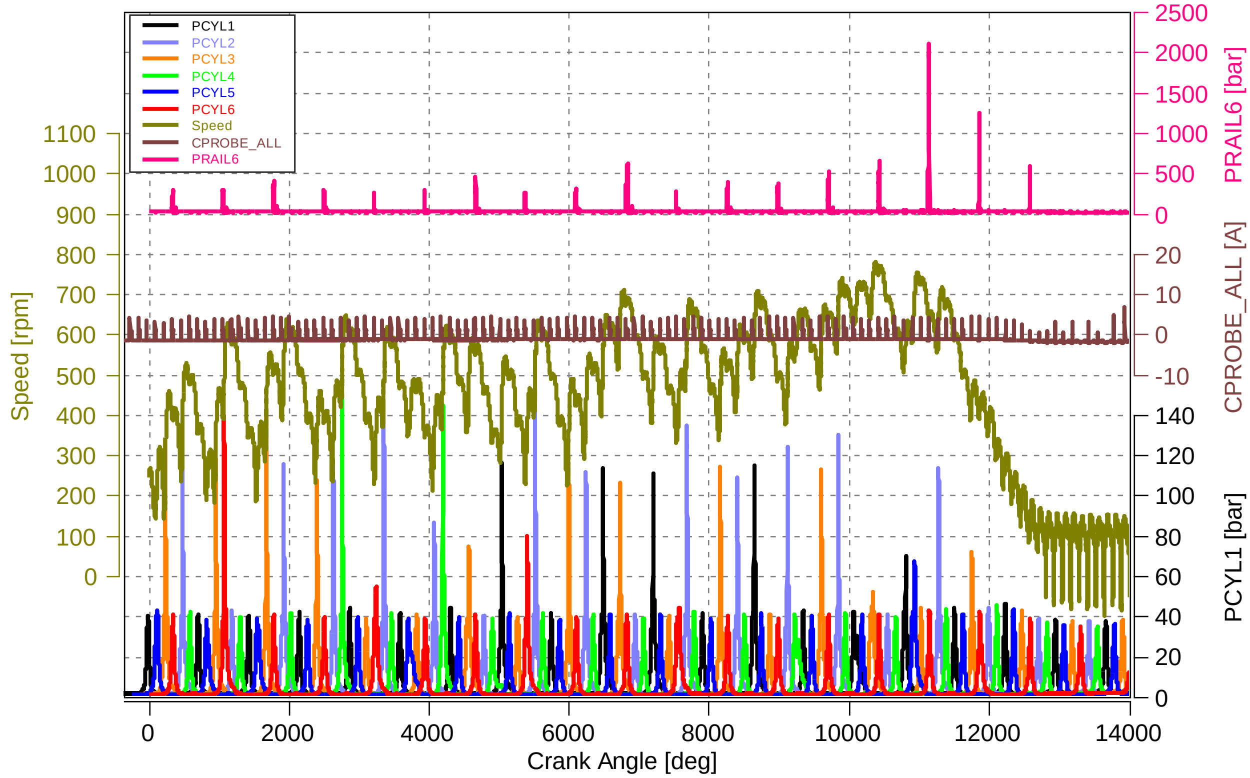

Figure 4.78 – Cold starting of JP8 at 0F- cycles 20 - 40

Figure 4.78 represents the cycles 20 - 40. It is evident that on the 34th cycle the engine was close to idle speed, immediately after the fuel injection was cut off as a result of the engine controller malfunction which resulted in engine speed decline upto the idle speed.

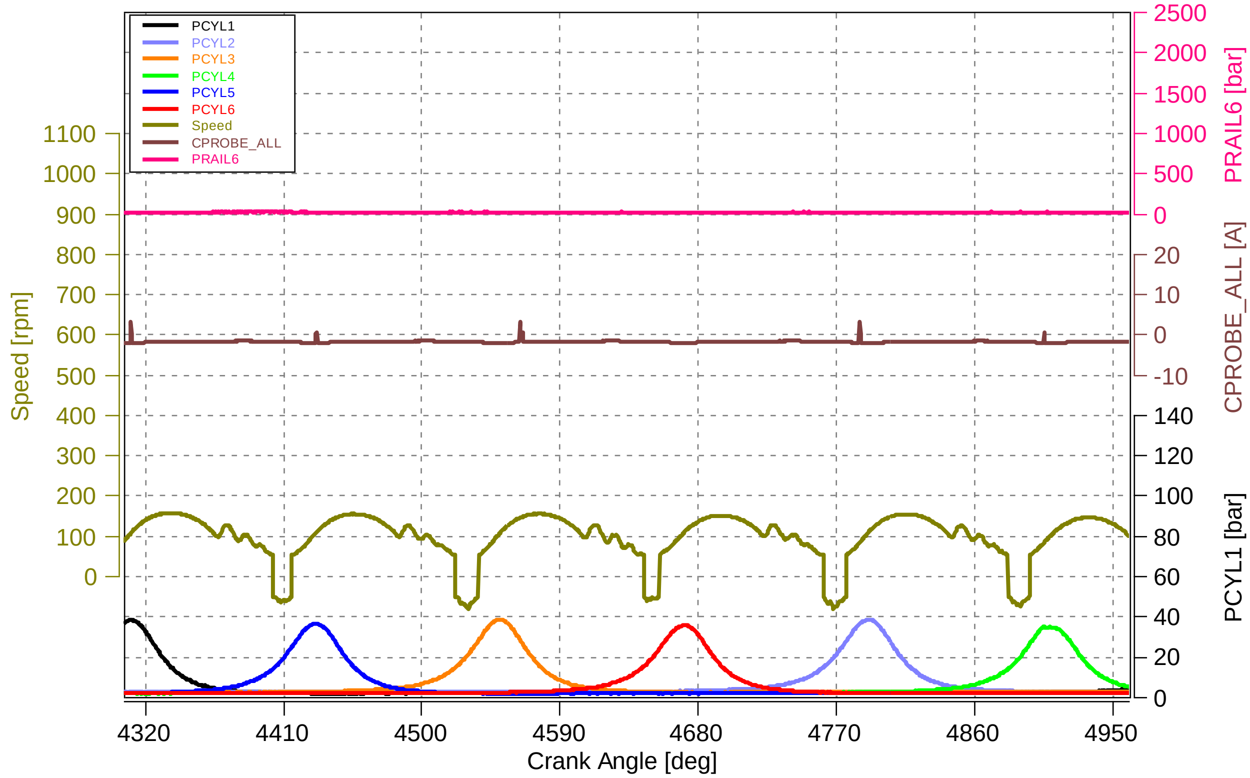

Figure 4.79 – 35th Cycle with no fuel injection

Figure 4.79 represents 35th cycle with practically no fuel injection, which resulted in engine speed drop upto the cranking speed and resulted in the failure of cold start.

4.13.1 Conclusions – JP8 0F

- Engine did not result in successful cold start at 0F
- Engine tried to accelerate up to the cranking speed but because of the repeated fuel injection cut off, cranking speed could not be attained.
- Engine cranking speed was reduced to 90 rpm.

CHAPTER 5

COLD START DATA ANALYSIS

5.1 JP8 and ULSD Fuel Property Comparison

Mercedes MBE 926 engine tested in this work was run on both ULSD and JP8 fuels. The engine was calibrated by the manufacturer to run only in ULSD fuel, addition of JP8 fuel resulted in a few variations in the combustion characteristics which will be discussed in the following sections.

The major differences between the JP8 and ULSD fuels are viscosity, cetane number, density and energy content. As we know the viscosity and the density are strong function of the fuel temperature. Higher the temperature, lower the density and lower the viscosity, which is true for both the fuels tested. Density of fuel obtained through the laboratory analysis was only available at a temperature of 15^{0}C for both fuels. The linear model correlation obtained from the literature [3] was used to calculate the density of ULSD fuel at various temperatures, as shown below,

$$D = 0.8527 - \left((6.41 * 10^{-4}) * (T)\right)$$

Where,

D = Density in Kg/m^3

T = Temperature in ^{0}C

JP8 fuel composition and blends has significant variation in North America and properties of the exact blend used for this study couldn't be found in the literature, hence the slope of the JP8 fuel density was calculated from the literature [4] and by using the measured value at 15^0C, density at lower temperatures were calculated by assuming the linear relationship

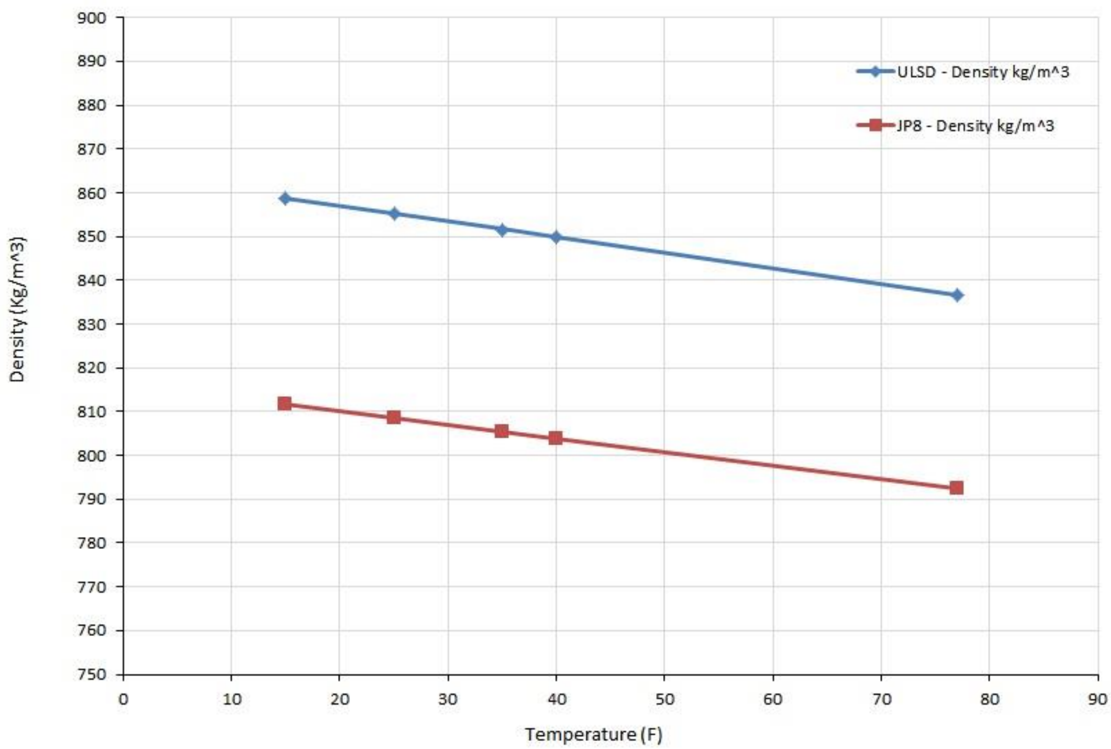

Figure 5.1 – Effect of temperature on fuel densities – JP8 and ULSD

Calculated density values for ULSD and JP8 are shown in figure 5.1. The fueling system in diesel engine works in the principle of volume metering rather than mass. To be elaborate, engine ECU extracts the total of quantity of fuel to be injected per cycle based on the input from the sensors from the lookup table and it converts the mass into corresponding volume by using the density value embedded by the manufacturer in the ECU.

Table 5.1 – Effect of density and temperature change on JP8 energy difference

Temperature	Temperature	ULSD - Density	JP8 - Density	ULSD - Energy Content	JP8 - Energy Content	% Difference in Energy - JP8 per unit volume
F	C	kg/m^3	kg/m^3	Mj/kg	Mj/kg	%
77.000	25.000	837	792	41.200	43.200	0.689
40.000	4.444	850	804			0.820
35.000	1.667	852	805			0.837
25.000	-3.889	855	808			0.872
15.000	-9.444	859	812			0.906

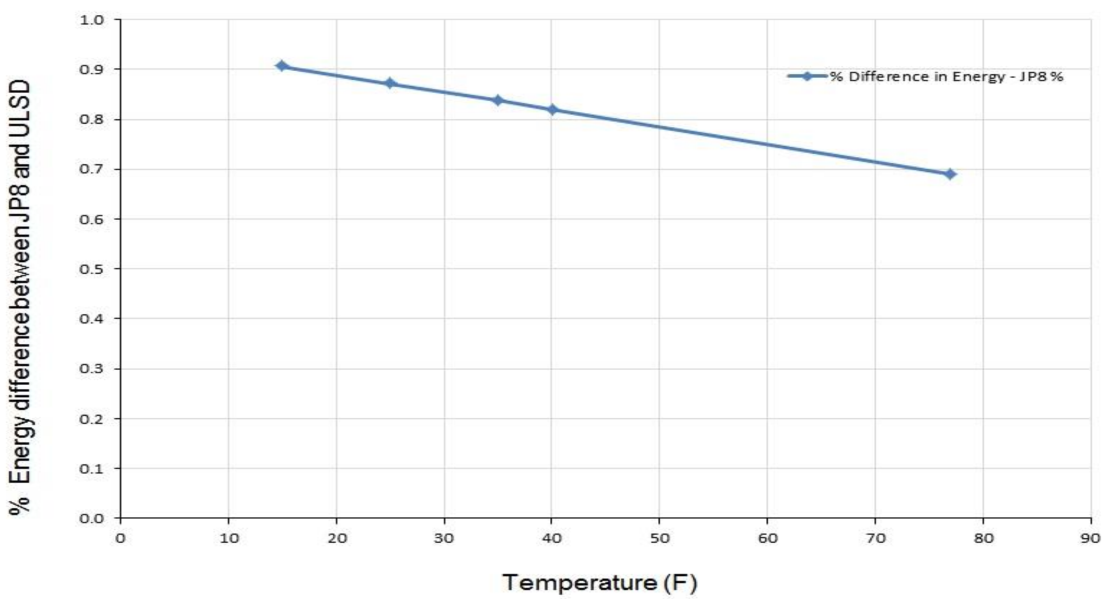

Figure 5.2 – Effect of temperature on energy content between JP8 and ULSD

Since there is difference in density between JP8 and ULSD, each fuel injection consisted of less jp8 fuel (mass) injected than corresponding ULSD, because JP8 has a lesser density than ULSD. This effect might be partially compensated because of the higher energy content on mass basis in JP8 and higher cetane number. Table 5.1 shows the calculated density values of both JP8 and ULSD for various temperatures as well as the energy differences between the two fuels on volumetric basis. Formula used to calculate the energy difference is shown below.

$$Energy\ difference = \frac{(\boldsymbol{\rho}_{ulsd} * HV_{ulsd}) - (\boldsymbol{\rho}_{jp8} * HV_{jp8})}{\boldsymbol{\rho}_{ulsd} * HV_{ulsd}} * 100$$

Where

$\boldsymbol{\rho}_{ulsd}$ = density of ULSD fuel

$\boldsymbol{\rho}_{jp8}$ = density of JP8 fuel

HV_{ulsd} = heating value of ULSD fuel

HV_{jp8} = heating value of JP8 fuel

Even though the energy difference per unit volume doesn't look very significant, it is interesting to note that the difference increases with decrease in temperature. This energy difference between ULSD and JP8 might be responsible for varied combustion characteristics during the cold start.

5.2 Effect of Ambient Temperature on Cranking Speed

In order to identify the effect of ambient temperature on cranking speed, a dynamometer was required which was not available during the time of this investigation, hence engine speed traces in which no fuel was injected during the initial cranking cycles were collected and then averaged. Figure 5.3 shows the effect of ambient temperature on the cranking speed on this engine. It has to be noted that the cranking speed is a strong function of engine oil viscosity, higher the viscosity higher the frictional losses, hence more energy (torque) supplied by the engine starter motor will be wasted in order to overcome these high frictional losses. It is interesting to note that as the ambient temperature decreases, the average cranking speed also decreases.

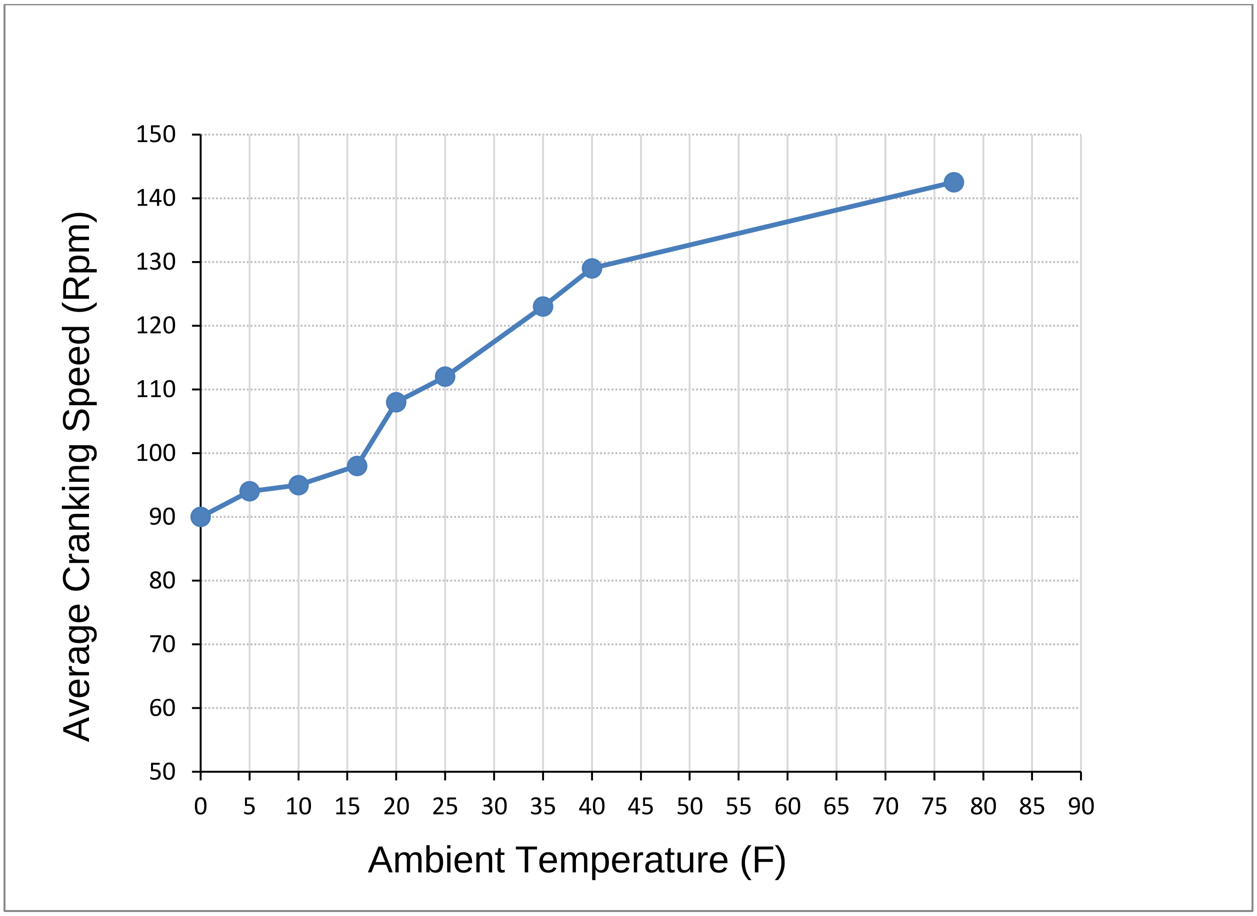

Figure 5.3 – Effect of Ambient Temperature on Cranking Speed

As mentioned in the engine setup section in chapter 2, for all these experiments the battery was fully charged before sealing the cold room for the cold start experiment. The main reasons for the reduced cranking speeds at low ambient temperatures are as follows

- Increased oil viscosity at low ambient temperatures which resulted in higher friction losses
- Lower the ambient temperature, the lower the battery discharge capacity, which resulted in reduced starter motor torque
- Increased heat losses to the engine coolant and surroundings

5.3 Effect of Cranking Speed on Motoring Pressure

At the time of this investigation dynamometer which is required for motoring the engine was not available, hence in order to obtain the cranking pressures; pressure traces were sampled form the initial cranking cycles where there is no fuel injection. Figure 5.4 represents the motoring pressure trace of the first cylinder during the cold start. The pressure traces shown in figure 5.4 is not necessarily from the same cylinder because the engine stops at different cylinder positions after each run. Figures 5.4 and 5.5 clearly indicate the cranking pressures of the first cylinder as recorded by the indicom data acquisition system at various ambient temperatures. Lower the ambient temperature; lower the compression pressure, which has a significant effect on the fuel auto ignition and combustion characteristics.

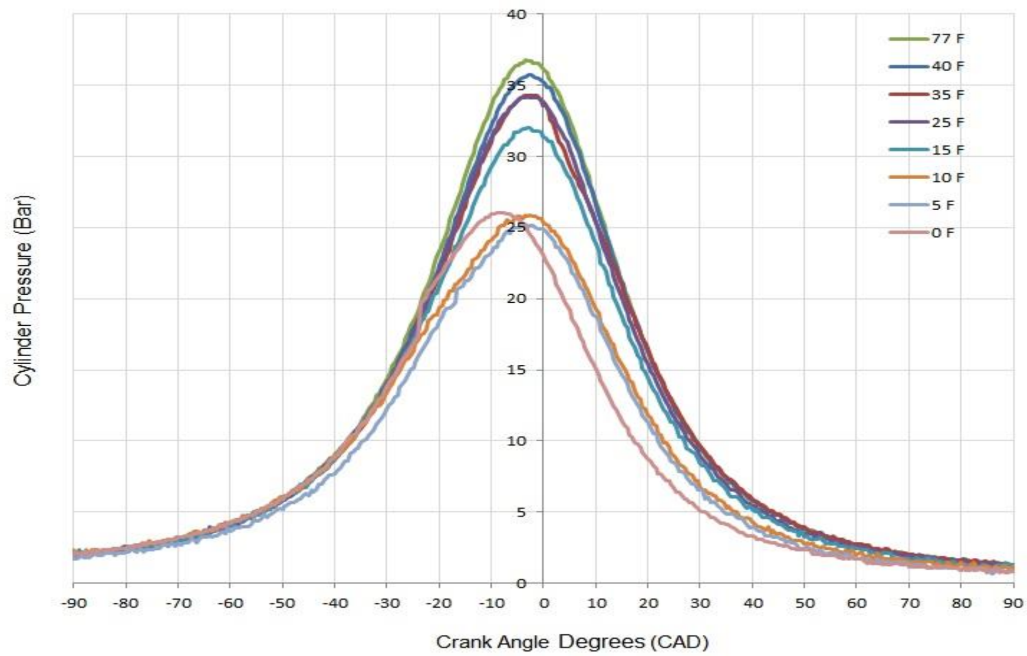

Figure 5.4 – Effect of Ambient Temperature on Motoring Pressure

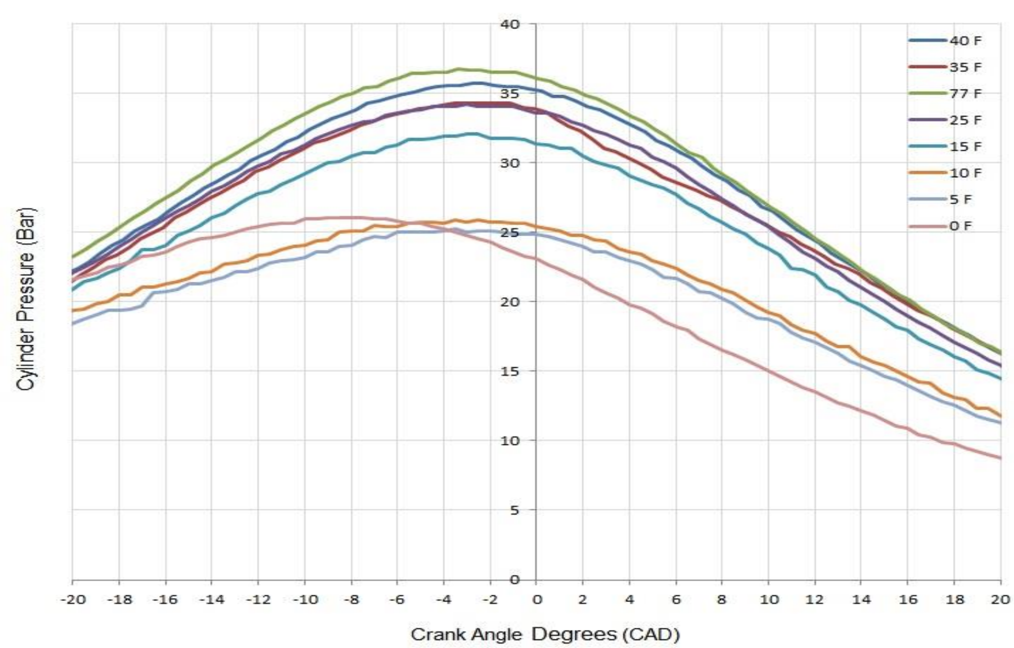

Figure 5.5 – Effect of Ambient Temperature on Motoring Pressure – Elaborated

From the figures 5.4 and 5.5 it is clear that lower the ambient temperature, lower will be the compression pressure. Another important reason for the reduced cranking pressure is the lower cranking speeds. Cylinder pressures and temperatures are strong functions of engine cranking speed, higher the cranking speed, higher the in cylinder pressure and temperature. It has to be noted that the peak cylinder pressures for all the ambient temperatures described in the figures 5.4 and 5.5 occur before the top dead center. Engine peak cylinder pressure during motoring always occurs before the top dead center because of the blowby losses as discussed in the literature review.

At room temperature maximum cranking pressure was 37 bars which gradually decrease with decrease in ambient temperature. The difference between the cranking pressures of 15F and 10F appears to be significant (6 bar) as a result of increased blowby losses and significantly reduced average cranking speed to 86 rpm. The remaining pressure traces for lower temperatures are close to 26 bars, but the location of the peak cylinder pressure occurs very early at 0F in comparison with other pressure traces, which indicates the significance of increased blowby and heat losses at very low ambient temperatures.

5.4 Effect of Ambient Temperature on Engine Speed of ULSD and JP8

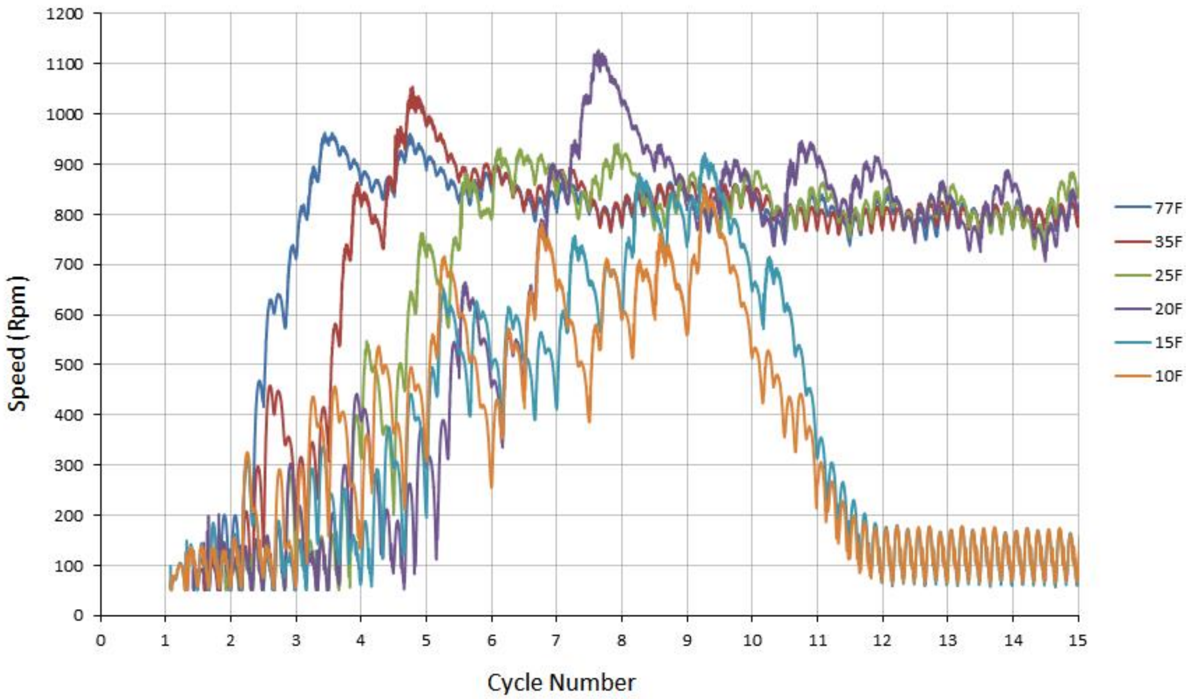

Figure 5.6 - Effect of Ambient Temperature on Instantaneous Speed - JP8

Figure 5.6 represents the effect of ambient temperature on the engine speed trend for the JP8 and ULSD fuels respectively. As the ambient temperature was lowered starting from 77F it took longer time (number of cycles) to accelerate as well as to reach the engine idling speed of 800 rpm. The interval at which the engine reaches idle speed increases with decrease in ambient temperature. The ambient temperature experiments 15 and 10F resulted in starting failure because of the inadequate fueling strategy in the engine controller.

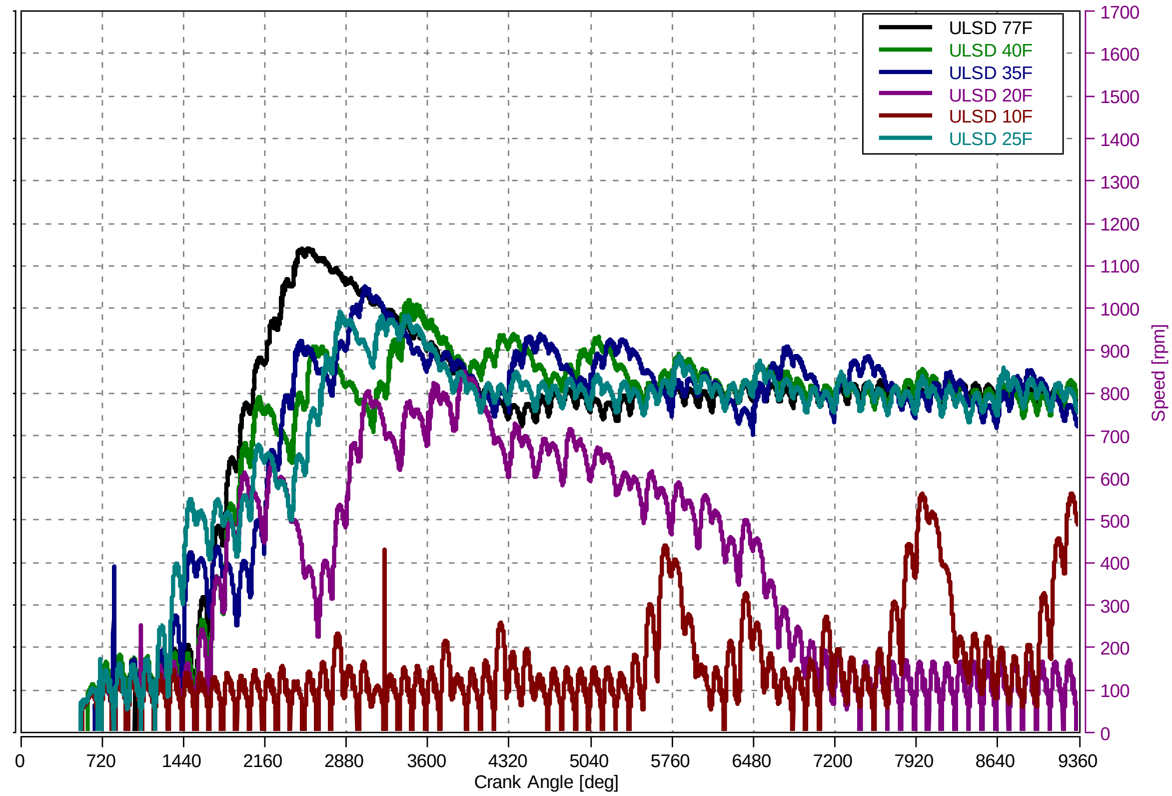

Figure 5.7 - Effect of Ambient Temperature on Instantaneous Speed - ULSD

Figure 5.7 represents the effect of ambient temperature on the engine speed trace for the ULSD fuel at various ambient temperatures. As illustrated in the figure 5.7 the lower the ambient temperature the longer it takes to accelerate and reach the engine idling speed. During the ambient temperatures of 10F and 20F the engine failed to start as illustrated in the figure. The reason as explained in chapter 4 was found to be the failure in the engine controller as a result of inadequate fueling strategy.

CHAPTER 6

CONCLUSIONS AND FUTURE WORK

6.1 Conclusions

The following are the brief conclusions made from this study,

1. The lower the ambient temperature , the longer it takes for the engine speed to stabilize at idling speed
2. Engine Control Unit (ECU) used in MBE 926 engine is identified to have the following issues
    a. Fuel injection was cutoff for several cycles during the initial engine acceleration in between cycles before reaching idling speed.
    b. Injection timing was kept constant for a few cycles with increase in engine speed
    c. Premature fuel injection cut off, even before reaching the idling speed at low ambient temperatures
    d. Fuel injection signal was out of phase with the pressure rise in the fuel line
3. Lower the ambient temperature, lower will be the engine cranking speed. Main reasons are higher engine friction as a result of increased oil viscosity at low ambient temperatures. Another reason is the reduced current discharge rate from the battery at low ambient temperatures

4. Lower the ambient temperature lower will be the cylinder compression pressure. Main factors are the increased blowby losses along with the increased heat losses as a result of reduced engine cranking speed and coolant temperatures at low ambient temperatures
5. Peak cylinder pressure of the engine during motoring (cranking without fuel injection) always occurs before the TDC and never exactly at TDC because of the pressure loss because of blowby
6. It was observed in the experiments that one of the main cause of misfire is that increasing speed results in less time for the piston around the TDC , which doesn't leave enough time for the fuel to mix fully with the air auto ignite.
7. JP8 has less energy content on a volumetric basis and more energy content on a mass basis. Since the fuel metering system always operates on volumetric basis, each injection of JP8 contained less energy per unit mass than the corresponding quantity of ULSD fuel injection
8. It was observed form the experiments that, the engine speed following the fuel injection cutoff after crossing the idling speed wasn't completely stable for both ULSD and JP8, except the ULSD 77F condition. It can be concluded that the engine was not properly calibrated to maintain the idling speed at low temperatures even while using the ULSD fuel which was certified to be used by the manufacturer
9. Engine took longer time to stabilize in the idling speed while using ULSD fuel.

6.2 Future Work

The following are the recommended future work as observed from the conclusions made from this study.

- Develop an electronic controller to override the stock engine ECU and control the parameters such as injection timing and injection pressure in fuel injectors
- Test and tune the controller for starting at room temperature as well as low ambient temperatures
- Develop simulation model for cold starting at low temperatures
- Develop new injection strategies for cold starting at low temperatures and test them on the engine

REFERENCES

1. Henein, N.A., " Diesel Cold Starting: A Phenomenological Model", ASME Energy-Sources Technology Conference, Paper No. 93-ICE-24, 1993
2. Ceausu, R.V, “Improving Turbocharged Diesel Engine Transient Response”, Ph.D. dissertation, Wayne State University - 2006
3. Scheider, J.C., “Fuel Composition And Quality Sensing For Diesel Engines”, M.S Thesis, University of Illinois - 2011
4. Coordinating Research Council, “Aviation Fuel Properties” , 1983
5. Han, Z., “ Diesel Engine Cold Start Combustion Instability And Control Strategy”, Ph.D dissertation, Wayne State University - 2000
6. Kobayashi, A., Akira Kurashima, Shin Endo, “Analysis Of Cold Start Combustion In A Direct Injection Diesel Engine”, SAE paper 840106, 1984
7. Zahdeh, A.R., “Diesel Engine Startability And White Smoke Formation Under Cold Temperature Conditions”, Ph.D Dissertation, Wayne State University, 1990
8. Lyn, W.T., E.Valdmanis,”The Effects Of Physical Factors On Ignition Delay”, SAE paper 950466, 1995
9. Yassine, M.K., Tagamori, M.K, Henein, N.A., Bryzik ,W.,”White Smoke Emissions Under Cold Starting Of Diesel Engines”, SAE paper 960249, 1996
10. Rafik, N.Rofail., “Opposing Effects Of Recirculated Gases During Cranking On Cold Start Of Diesel Engines”, Ph.D. Dissertation, Wayne State University – 2011
11. Clerc, J.C., “Cetane Number Requirements Of Light Duty Diesel Engines At Low Temperatures”, SAE 860529, 1986

12. Austen, W. and Lyn, W., "Some Investigations On Cold Starting Phenomena In Diesel Engines" Proceedings of the Institution of Mechanical Engineers: Automobile Division 1959

13. Biddulph, T. W., W.T. Lyn, “Unaided Starting of Diesel Engines”, SAE paper 680103, 1963

14. Delphi, “Smart Injector for 2007 DDC MBE 900 and 4000” – Presentation.

15. Hara, H., Itoh, Y., Bryzik, W and Henein N, A., “Effect of Cetane Number with and without Additive on Cold Startability and White Smoke Emissions in a Diesel Engine”, SAE Paper 1999-01-1476, 1999

16. Liu, Z. and Karim, G. A., "An Examination of the Role of Residual Gases in the Combustion Processes of Motored Engines Fueled with Gaseous Fuels", SAE 961081, 1996.

17. Mocanu, F., “Multi-fuel operation of modern engines; on board fuel identification” Ph.D. Dissertation, Wayne State University – 2012

18. Singh, B., “Effect Of Alternative Fuels On Aftertreatment Device” , MS Thesis, Wayne State University - 2010

19. Roy, M. M. and Tsunemoto, H., “Effect of Injection Pressure and Split Injection on Exhaust Odor and Engine Noise in DI Diesel Engines”, SAE 2002-01-2874, 2002.

20. Henein, N. A., "Starting of Diesel Engines: Uncontrolled Fuel Injection Problems," SAE 860253, 1986.

21. Bielaczyc, P., Merkisz, J. and Pielecha, J., "A Method of Reducing the Exhaust Emissions from DI Diesel Engines by the Introduction of a Fuel cut Off System During Cold Start". SAE 2001-01-3283, 2001.

22. Lindl, B. and Schmitz, H. G., “Cold Start Equipment for Diesel Direct Injection Engines” SAE Paper 1999-01-1244, 1999.

23. Girotra, M., Henein, N. A., Zhong, L. and Bryzik, W., "Split Injection strategy for Prompt Cold Starting and Low White Smoke Emissions, " ASME ICE 2005 Spring Technical Conference, ICES2005-1100, 2005.

24. Zahdeh, A., Henein, N., and Bryzik, W., "Diesel Cold Starting: Actual Cycle Analysis Under Border-Line Conditions," SAE Technical Paper 900441, 1990

25. Bryzik, W., Henein, N. A., "Fundamental Cold Start Phenomena Within Advanced Military Diesel Engines," 19th Army Science Conference, Orlando, Florida, 20-23 June 1994

26. Xiao G.F., Qiao X.Q., “improvement of startability of direct-injection diesel engines by oxygen-enriched intake air” , Proceedings of the Institution of Mechanical Engineers, Part D: Journal of Automobile Engineering, 2007

27. Nakamura, T and Phatak, R, "Cold Startability of Open-Chamber Direct-Injection Diesel Engines-Part I: Measurement Technique and Effects of Compression Ratio," SAE Technical Paper 831335, 1983

28. Manuel, A., Gonzalez, D., Borman, G., and Reitz, R., "A Study of Diesel Cold Starting using both Cycle Analysis and Multidimensional Calculations," SAE Technical Paper 910180, 1991

29. Andree A., Pachernegg S. J., “Ignition conditions in diesel engines”, Society of Automotive Engineers paper 690253, 1969

30. J. A. Bolt and N. A. Henein., “The Effect of Some Engine Variables on Ignition Delay and Other Combustion Phenomena in a Diesel Engine”, Proceedings of the Institution of Mechanical Engineers, Conference Proceedings 1969.

ABSTRACT

Characteristics of Cold Start of a Diesel Engine using JP8 and ULSD Fuels

by

MADHUSHANKAR PALANISAMY

August 2013

Advisor: Dr. Dinu Taraza

Major: Mechanical Engineering

Degree: Master of Science

This study involves the cold start testing of ULSD and JP8 fuels on the 6 cylinder 7.2 liter turbocharged diesel engine at various ambient temperatures as low as 0^{o}F for JP8 fuel and 10^{o}F for ULSD fuel. Cycle by cycle analysis of the cold start transient data, along with the effects of variation in ambient temperature on the engine cranking speed and in cylinder motoring pressure were analyzed and presented. It was found that the reduction in ambient temperature resulted in prolonged cranking periods along with the longer time taken to reach idling speed as well as increased combustion instability. This phenomenon was observed for both ULSD and JP8 fuels at low ambient temperatures.

The engine ECU fueling strategy was studied at ambient temperatures as low as 0^{o}F and found to be inadequate to result in prompt engine start. Several challenges with the engine controller such as fuel injection cut off, out of phase injection signal between the ECU and the fuel line pressure buildup were also identified.

AUTOBIOGRAPHICAL STATEMENT

I, Madhushankar Palanisamy was born on June 10th 1989 in Coimbatore, India. I obtained my Bachelor's degree in Production Engineering from Government College of Technology, Coimbatore on April 2010. During my undergraduate period, I developed a keen interest in the Internal Combustion Engines and decided to pursue my Masters in Mechanical Engineering with Internal Combustion Engines specialization.

I came to the USA in fall 2010 where I started my master's program in mechanical engineering at Wayne State University. During my master's program, I had the opportunity to work at the Center for Automotive Research (CAR) at Wayne State University under the leadership of Dr. Dinu Taraza, where I did research work on cold starting on various fuels in a turbocharged diesel engine. My work at CAR included conducting transient experiments on a Mercedes MBE 926 6 cylinder 7.2 liter turbocharged diesel engine with JP-8 and ULSD fuels.

A valuable diesel engine research experience gained at Wayne State University helped me land a fulltime employment with AVL Powertrain Engineering Inc, Plymouth in September 2012.

.